

Recruitment Characteristics of Juvenile Striped Bass (*Morone saxatilis*) Across Recovery
Periods, Year Classes, and Subestuaries in the Chesapeake Bay

A Thesis

Presented to

The Faculty of the School of Marine Science

The College of William & Mary

In Partial Fulfillment

of the Requirements for the Degree of

Master of Science

by

Olivia M. Phillips

January 2020

APPROVAL PAGE

This thesis is submitted in partial fulfillment of
the requirements for the degree of
Master of Science

Olivia M. Phillips

Approved by the Committee, December 2019

Mary C. Fabrizio, Ph.D
Committee Chair / Advisor

Mark J. Brush, Ph.D

Robert J. Latour, Ph.D

David H. Secor, Ph.D
University of Maryland
Cambridge, Maryland

I dedicate this thesis to my grandparents who have always supported me no matter the goal. To my Mammie and Pappie, Constance and Roland Boileau, for teaching me that there is so much more to this life than work. And to my Grandma and Grandad, Isabel and Michael Phillips, for instilling in me a love and respect for the natural world.

TABLE OF CONTENTS

ACKNOWLEDGMENTS	vi
LIST OF TABLES	viii
LIST OF FIGURES	x
AUTHOR’S NOTE.....	xvi
ABSTRACT.....	xvii
INTRODUCTION	2
Literature cited.....	5
CHAPTER 1: Mortality rates and hatch-date distributions for 32 year classes of juvenile striped bass: Implications for recruitment	7
ABSTRACT.....	8
INTRODUCTION	9
METHODS	15
Fish sampling & otolith preparation	15
Consistency of age determinations	16
Daily age estimation	17
Age-length keys	18
Instantaneous daily mortality rates (<i>Z</i>)	21
Hatch-date distributions	24
Relationship between hatch-date distributions & abundance of juvenile striped bass.....	26
Comparison of hatch-date distributions for 32 year classes	28
RESULTS	30
Consistency of age determinations	30
Age-length keys	30
Instantaneous daily mortality rates (<i>Z</i>)	31
Relationship between hatch-date distributions & abundance of juvenile striped bass.....	32
Comparison of hatch-date distributions for 32 year classes	33
DISCUSSION	36
Instantaneous daily mortality rates	36
Hatch-date distributions and relative abundance of juvenile striped bass.....	39
Conclusions and recommendations.....	46
LITERATURE CITED	48

CHAPTER 2: Growth, body condition, and recruitment potential of juvenile striped bass in a declining population in the Chesapeake Bay	76
ABSTRACT.....	77
INTRODUCTION	79
METHODS	86
Fish sampling & otolith preparation	86
Consistency of age determinations	87
Environmental factors.....	87
Daily growth rate of juvenile striped bass	89
Body condition of juvenile striped bass.....	91
Recruitment potential of juvenile striped bass.....	93
RESULTS	97
Daily growth rates of juvenile striped bass.....	97
Body condition of juvenile striped bass.....	99
Recruitment potential of juvenile striped bass.....	100
DISCUSSION	102
LITERATURE CITED	114
 CONCLUSIONS.....	 153
Literature cited.....	158
 APPENDIX A.....	 159
APPENDIX B.....	161
 VITA.....	 162

ACKNOWLEDGMENTS

Many people were instrumental in making this thesis possible, but I would first like to thank my advisor, Mary Fabrizio, for her support and guidance over the years. Thank you for giving me the opportunity to learn from you. I would also like to thank my committee members, Mark Brush, Rob Latour, and Dave Secor for providing me with their expertise, and for their genuine enthusiasm for my project. I am especially grateful to Mark for explaining temperature interpolations to me; to Rob for helping me develop my weight-specific exponential growth model; and to Dave for inviting me to learn about otoliths and processing methods, from members of his lab group, before I had even asked him to join my committee. I thank John Graves, who moderated both my qualifying exam and my thesis defense, for his support, but especially for insisting that I finish this thesis before he retires.

I am deeply indebted to all those who served on the VIMS seine survey crew from 1986 to today for providing me with the data and juvenile striped bass necessary to complete this project. In particular, I am forever grateful to Max Grezlik, Haley Burleson, and Brittnee Barris for naming me “Chief”, ensuring I didn’t take myself too seriously, and making my summers on the seine survey so memorable. Thank you, Wendy Lowery, for your constant encouragement and for sharing your wisdom and experience with me. The Fabrizio lab would be lost without you. I would especially like to thank Chris Davis for his example in leadership, and for maintaining our friendship, even after he left VIMS and I got caught up in this thesis. I am incredibly appreciative of Jillian Swinford, who not only worked with me on the seine survey, but also spent long hours in the age and growth lab with or without me, polishing teeny-tiny juvenile striped bass otoliths. The countless hours (and blood, sweat, and tears) Jillian contributed to my thesis project will never be forgotten. I also want to thank Brian Gallagher for teaching me how to process otoliths when he was finishing up his own thesis, for troubleshooting issues with aging techniques, for helping me with my age verification, and for generally sharing in the misery that is otolith work. Overall, the members of the Fabrizio lab (Jack Buchanan, Corey Corrick, Emily Loose, Ben Marcek, Vaskar Nepal, Shannon Smith, Troy Tuckey), past and present, were especially valued resources during my time at VIMS. Thank you for providing me with feedback on ideas and presentations, for sharing your R code or data analysis experience, and for your overall support as a lab group.

I would like to acknowledge my funding sources: the Virginia Marine Resources Commission, the Saltwater Recreational Fund, and the Sportfish Restoration Fund. As well as the VIMS Office of Academic Studies, especially for the award from the student equipment trust fund, which allowed me to buy a necessary microscope camera used to image and age my otoliths. I also want to thank the International Women’s Fishing Association for the scholarship they awarded me.

I am grateful to the VIMS graduate student body for providing me with a sense of community. My favorite part about the graduate students at VIMS is that we all support one another in our professional endeavors, and are more than willing to lend a hand or

some R code! No one quite understands the challenges of graduate school like graduate students. That said, I would like to thank Dan Crear for helping me when I was especially frustrated with my data analysis; Bruce Pfirrmann who helped me with field work and served as my boat captain on more than one occasion; Chase Long for teaching me to use the imaging software that made aging otoliths so much easier; and Kelley Uligh for telling me that I wasn't alone and for reassuring me that I was on the right track, despite some challenges. I would like to thank my roommate of three years, Julie Krask, for helping me unwind with a shared bottle of wine and some Gilmore Girls or Friends. And, speaking of wine, I am absolutely certain that I would have given up on this thesis a long time ago if not for my wine nights with Serina Wittingham and Gail Schwieterman – thank you both for your constant encouragement, for calling me out when I needed it, and for just listening.

Last and most importantly, I thank my family for their constant support, encouragement, and love. They never faltered when I told them I no longer wanted to pursue veterinary school, but rather wanted to attend graduate school for fisheries science. I am grateful to my mother, Joanne Phillips, for showing me what a strong woman looks like, for reminding me that I am worthy, and for insisting that I demand what I deserve. My father, Andrew Phillips, is my rock, my center, my pillar. Thank you, dad, for being a place of comfort, for reminding me that I make you proud, and for always listening. You made me feel like my thesis was important even when I lost sight of that. To my little brother, Thomas Phillips, your journey to where you are today has been incredibly inspiring to watch. Thank you for being the person I look up to, and for showing me to keep following my dreams, especially when they feel most out of reach. I am especially thankful for my partner in this life, my love, Ben Siegal, for building a home with me, and for taking me away from the VIMS bubble. Thank you for reminding me that I am defined by more than just this thesis, and that I am worthy of truly amazing things. Somehow you kept me grounded and also raised me up all at the same time. Lastly, I need to express some serious gratitude for my dog, Sir. Walter “Raleigh” for maintaining my sanity throughout this process. Raleigh came into my life exactly when I needed him, incidentally, he is almost exactly the same age as this thesis. He finds joy in the smallest things, which brings so much light and pawitivity into my life.

I'm sure there are people I have not acknowledged here, by name, but know that I appreciate your contribution. Thank you for getting me here.

LIST OF TABLES

CHAPTER 1

Table 1. Attributes of the hatch-date distribution of 32 year classes of juvenile striped bass in the James and Rappahannock subestuaries of the Chesapeake Bay. Hatch-date distributions were developed from daily ages that were estimated using subestuary-specific age-length keys. Truncated hatch duration was calculated by removing the earliest and latest 1% of hatch dates, and rounded to the nearest day. Unless otherwise noted, all attributes were calculated using calendar days..... 58

Table 2. Paired *t*-test statistics comparing mean otolith increment counts of each of the six pairs of reading combinations for striped bass otoliths. Each reading included increment counts from 40 striped bass otoliths subsampled across three year classes (2011, 2016, and 2017) within the James and Rappahannock subestuaries. Pairs exhibiting significant differences ($p < 0.05$) are highlighted with bold text..... 60

Table 3. Estimated daily instantaneous mortality rates for the month of July and their 95% confidence intervals (CI) for 32 year classes (1986-2017) of juvenile striped bass in the James and Rappahannock subestuaries of the Chesapeake Bay. For ease of interpretation, discrete mortality rate, or the proportion of the population that is lost through mortality, was calculated with $1 - e^{-Z}$ and the monthly *Z* (for July) was calculated using daily *Z* estimates..... 61

Table 4. Spearman's rank correlation (ρ) which measured the relationship between rankings of the attributes of the hatch-date distributions and rankings of the relative abundance of juvenile striped bass from 32 year classes in the James and Rappahannock subestuaries of the Chesapeake Bay. There were no significant correlations between attributes and relative abundance..... 63

CHAPTER 2

Table 1. Models considered to describe daily growth of three year classes (2011, 2016, and 2017) of juvenile striped bass in the James and Rappahannock subestuaries of the Chesapeake Bay ($N = 450$). AIC and Δ AIC are presented for the final model (shaded), the model with the lowest AIC (bold) and alternate models. Symbols in the model are: the model intercept (β_0), partial regression coefficients (β_{1-5}) for year class (*Year*), subestuary (*Subestuary*), chlorophyll-*a* (*Chla*_{30 day lag} or *Chla*_{60 day lag}), temperature (*Temp*_{30 day lag} or *Temp*_{60 day lag}), and freshwater flow (*Flow*_{30 day lag} or *Flow*_{60 day lag}). The asterisk (*)

in the model notation indicates the inclusion of subestuary, chlorophyll-a, and the interaction between subestuary and chlorophyll-a in the model..... 125

Table 2. Tolerance values for effects in the ANCOVA model of mean daily growth rate as a function of year class (2011, 2016, and 2017), subestuary (James or Rappahannock), 60-day lagged chlorophyll-a (covariate), and 30-day lagged temperature. Tolerance values for the effect of “Year: 2011” and “Subestuary: James” were not calculated because these effects are included in the intercept of the ANCOVA. Tolerance values less than 0.1 indicate collinearity among variables. To address collinearity, chlorophyll-a data were centered by subtracting the mean chlorophyll-a, which yielded new tolerance values less than 0.1. 127

Table 3. Models considered to describe body condition (Fulton’s K) of nine year classes (2009-2017) of juvenile striped bass in the James and Rappahannock subestuaries of the Chesapeake Bay. AIC and Δ AIC are presented for each model; the model with the lowest AIC is indicated in bold. Symbols in the model are: the model intercept (β_0), partial regression coefficients (β_{1-5}) for year class (*Year*), subestuary (*Subestuary*), chlorophyll-a (*Chla_{30 day lag}* or *Chla_{60 day lag}*), temperature (*Temp_{30 day lag}* or *Temp_{60 day lag}*), and freshwater flow (*Flow_{30 day lag}* or *Flow_{60 day lag}*)..... 128

Table 4. Tolerance effects for variables in the ANCOVA model of mean body condition (Fulton’s K) as a function of year class (2009-2017), subestuary (James or Rappahannock), and 30-day lagged chlorophyll-a, temperature, and flow (covariates). Tolerance values for the “Year: 2009” and “Subestuary: James” effects were not calculated because these effects are included in the intercept of the ANCOVA. Tolerance values less than 0.1 indicate collinearity among variables. There is no collinearity present among these variables... 130

Table 5. Residual sum-of-squares (RSS), Akaike’s Information Criterion (AIC), and Δ AIC for models M_{1-10} fitted to juvenile striped bass weight-at-age data collected from the 2011, 2016, and 2017 year classes within the James and Rappahannock subestuaries of the Chesapeake Bay. 131

Table 6. Estimates and 95% confidence intervals (in parentheses) of weight-specific instantaneous growth rates (G), daily instantaneous mortality rates (Z), and recruitment potential (G:Z) for juvenile striped bass from the James and Rappahannock subestuaries. The juvenile recruitment index values were provided by the VIMS seine survey (Gallagher *et al.* 2018)..... 132

LIST OF FIGURES

CHAPTER 1

- Figure 1.** VIMS seine survey sites from which 32 year classes of juvenile striped bass (1986-2017) were sampled from the James and Rappahannock subestuaries of the Chesapeake Bay. 64
- Figure 2.** Temperature stations monitored by the Chesapeake Bay Program in tidal fresh (TF) regions of the James and Rappahannock subestuaries. Daily temperature values were linearly-interpolated from approximately biweekly monitoring data collected at each site, and were used to estimate mean temperature during hatch and during the yolk-sac larval stage..... 65
- Figure 3.** Estimated daily instantaneous total mortality rate (Z , day^{-1}) of juvenile striped bass in July from 1986 to 2017 in the James and Rappahannock subestuaries of the Chesapeake Bay. Gray bars represent 95% confidence intervals. The lower confidence interval for the 2012 year class was negative, and thus truncated at zero. 66
- Figure 4.** The abundance (A) and percent of the total population (B) of juvenile striped bass within a 15-day cohort assuming no differential mortality between older and younger cohorts (black line) and assuming a loss of 1% per day (gray line; Secor *et al.* 1995). A greater proportional abundance of older cohorts of juvenile striped bass is expected in the mortality-adjusted distribution (gray line) than in the non-adjustment distribution (black line) if the differential mortality between older and younger cohorts is high..... 67
- Figure 5.** Hatch-date distribution of juvenile striped bass from the James and Rappahannock subestuaries of the Chesapeake Bay. Hatch dates range between calendar days 78 and 169 and represent fish sampled from 1986 to 2017. The mean hatch date was 123.00 (SE = 0.14), which is May 3rd. 68
- Figure 6.** Interaction plots for subestuary, period, year, and temperature during hatch for 32 year classes (1986-2017) of juvenile striped bass in the James (JA) and Rappahannock (RA) subestuary of the Chesapeake Bay. There were no notable interactions between subestuary and period (A), temperature during hatch and period (C), year class and subestuary (D), or year and temperature during hatch (E). Panel B suggests a possible interaction between subestuary and temperature during hatching because the lines for the James (JA; black) and Rappahannock (RA; gray) subestuaries intersect; however,

the 95% confidence intervals for low (5.0 - 18.4 °C, N = 3707) and high (18.5 - 29.0 °C, N = 4086) temperature bins overlap, which suggests that the interaction observed may not be strong. The threshold for the temperature bins was based on the observed mean (18.5°C)..... 69

Figure 7. Diagnostic plots from the analysis of covariance where hatch date of 32 year classes of juvenile striped bass within the James and Rappahannock subestuaries of the Chesapeake Bay was a function of period (pre- or post-), year nested within period (pre: 1986-1994; post: 1995-2017), and temperature during hatching was a covariate. The histogram of residuals (A) and Q-Q plot (B) show that the model meets the assumption of normality. For the most part, the values in the fitted versus residuals plot are evenly distributed around zero, and the assumption of homogeneity of variance appears reasonable. To further explore this assumption, box and whisker plots that group hatch dates by year class (E), period (F), and temperature during hatching (G) were used to compare variance among groups. Most year classes exhibited similar variances ranging from 110 to 163, and only four year classes exhibited variance values less than 110 ($\sigma_{1986}^2 = 51.7$, $\sigma_{1988}^2 = 53.7$, $\sigma_{1989}^2 = 56.9$, $\sigma_{1990}^2 = 55.0$). However, year class is nested within period in this model, and variance was similar among the pre- and post- recovery periods ($\sigma_{pre-recovery}^2 = 118$, $\sigma_{post-recovery}^2 = 148$). Temperature during hatching was grouped into low (5.0-18.4 °C, N = 3707) and high (18.5-29.0 °C, N = 4086) temperature groups, and variance appeared similar across the two temperature groups ($\sigma_{low}^2 = 115$, $\sigma_{high}^2 = 88.0$). Considering the similar variances among groups and the normal distribution of the residuals, I concluded that the assumption of homogeneity of variance was reasonably met. The predicted versus observed plot (D) shows an even distribution around the one-to-one line, indicating that this model can be used to make predictions about mean hatch dates. 71

Figure 8. Estimated least-squares mean hatch date (calendar day), adjusted for temperature during hatching, and 95% confidence intervals for 32 year classes of juvenile striped bass in the James and Rappahannock subestuaries of the Chesapeake Bay. These means are from the analysis of covariance in which hatch date was a function of period and year nested within period, and temperature during hatching was the covariate. The solid line is a regression fit to mean hatch date through time, and shows the decline in hatch date through time. The solid line is for display purposes only and is not intended to be a predictive function. 73

Figure 9. A partial regression plot showing the model-based relationship between temperature during hatching and hatch date from the analysis of covariance in which hatch date of juvenile striped bass

in the James and Rappahannock was a function of period and year nested within period, and temperature during hatching was the covariate. The solid line represents the correlation between temperature during hatching and hatch date (calendar day), and the gray dots represent the observed temperature on a given hatch date..... 74

Figure 10. Truncated hatch duration in days (earliest and latest 1% of hatch dates removed) for 32 year classes (1986-2017) of juvenile striped bass in the James and Rappahannock subestuaries of the Chesapeake Bay. Hatch dates were estimated with daily ages estimated from subestuary-specific age-length keys..... 75

CHAPTER 2

Figure 1. Location of VIMS seine survey sites from which juvenile striped bass were collected from the 2009 to 2017 year classes in the James and Rappahannock subestuaries of the Chesapeake Bay 133

Figure 2. Location of temperature stations (TF = tidal fresh zone, RET = riverine-estuarine transition zone, LE = lower estuarine zone) monitored by the Chesapeake Bay Program. Daily temperature values were linearly interpolated from approximately biweekly observations at each site. Daily chlorophyll-a values were also linearly interpolated using approximately biweekly observations collected at each site..... 134

Figure 3. Interaction plots for year, subestuary, 60-day lagged chlorophyll-a, and 30-day lagged temperature for the model of daily growth rates for the 2011, 2016, and 2017 year classes of juvenile striped bass in the James (JA) and Rappahannock (RA) subestuaries of the Chesapeake Bay. Panels A-D show the interaction between the categorical factors (subestuary and year class) and the continuous covariates (60-day lagged chlorophyll-a and 30-day lagged temperature). The points represent the observed chlorophyll-a (A and B) and temperature (C and D) associated with daily growth rates, and the solid lines represent the effect of the covariate on daily growth rate for each categorical variable. For example, in panel A, chlorophyll-a has a positive effect on daily growth rate in the James (black), but a negative effect on daily growth rate of fish in the Rappahannock subestuary (blue). Panel E shows the interaction plot between subestuary and year class. Panel F shows the interaction plot between the two covariates, where 60-day lagged chlorophyll-a is grouped into three bins (0.0-9.4 µg/L, N = 147; 9.5-12.4 µg/L, N = 132; 12.5-21.0 µg/L, N = 150) and 30-day lagged temperature is grouped into two bins (black: 22.0-25.0°C, N = 196; blue: 25.0-30.0°C, N = 233). The vertical bars on the points in panels E and F represent the 95%

confidence interval. Generally, interactions are indicated when lines intersect and, for panels E and F, if lines intersect and confidence intervals do not overlap. There were no appreciable interactions between temperature and subestuary (C), subestuary and year class (E), and chlorophyll-a and temperature (F). Although it appeared that interactions occurred between chlorophyll-a and year class (B) and temperature and year class (D) because the lines for each group intersect, the variability in the observed points is high, which suggests that an interaction cannot be determined. The interaction plot showing subestuary and chlorophyll-a concentrations (A) shows an interaction between subestuary and 60-day lagged chlorophyll-a, such that there is an effect of 60-day lagged chlorophyll-a on daily growth rates of fish in the James, but not in the Rappahannock subestuary..... 135

Figure 4. Diagnostic plots for the analysis of covariance where daily growth rate was a function of year class (2011, 2016, and 2017) and subestuary (James or Rappahannock). 138

Figure 5. Estimated least-squares (LS) mean daily growth rates for 3 year classes of juvenile striped bass in the James (black dots) and the Rappahannock (gray dots) subestuaries. These LS means are derived from an ANCOVA in which daily growth rate is a function of year class and subestuary. The vertical bars indicate the 95% confidence intervals..... 139

Figure 6. Interaction plots for year, subestuary, 30-day lagged chlorophyll-a, 30-day lagged temperature, and 30-day lagged flow for nine year classes (2009-2017) of juvenile striped bass in the James (JA) and Rappahannock (RA) subestuaries of the Chesapeake Bay. The vertical bars represent the 95% confidence interval. An interaction is indicated when the lines in the figures intersect. If the confidence intervals overlap there is not a significant interaction between factors. There is no interaction observed for year and chlorophyll-a concentrations (A), subestuary and chlorophyll-a concentrations (B), year and temperature (C), subestuary and temperature (D), or year and subestuary (F). The interaction plot of temperature and chlorophyll-a (E) depicts an intersection for the lines corresponding to low (7-15.231 µg/L; black) and high (15.323-25 µg/L; gray) concentrations of chlorophyll-a; however, the confidence intervals around the mean response for high and low concentrations of chlorophyll-a overlap for low (22.00-26.31°C) and high (26.32-30.00°C) temperature, which indicated a lack of interaction between the two factors. A similar pattern can be observed in the interaction plots for year and flow (G), subestuary and flow (H), chlorophyll and flow (I), and temperature and flow (J)..... 140

Figure 7. Diagnostic plots for the ANCOVA where body condition (Fulton’s K) was a function of year class (2011, 2016, and 2017), subestuary (James and Rappahannock), 30-day lagged temperature, chlorophyll-a, and flow..... 143

Figure 8. Estimated least-square means for body condition, adjusted for the effects of temperature chlorophyll-a, and flow, for nine year classes of juvenile striped bass in the James (black) and Rappahannock (gray) subestuaries. These least-square means were estimated from the ANCOVA in which body condition (Fulton’s K) was a function of year class, subestuary, 30-day lagged temperature, 30-day lagged chlorophyll-a, and 30-day lagged flow 144

Figure 9. The partial regression plot showing the effect of 30-day lagged temperature, holding all other factors constant, on mean body condition (Fulton’s K) of juvenile striped bass, from the ANCOVA in which body condition is a function of year class, subestuary, and 30-day lagged temperature, chlorophyll-a, and flow. For every one degree increase in temperature, mean body condition increased by 0.021 (95% CI: 0.018 – 0.024) units. The dashed red lines represent the 95% confidence interval..... 145

Figure 10. The partial regression plot showing the effect of 30-day lagged chlorophyll-a, holding all other factors constant, on mean body condition (Fulton’s K) of juvenile striped bass, from the ANCOVA in which body condition is a function of year class, subestuary, and 30-day lagged temperature, chlorophyll-a, and flow. For every one $\mu\text{L/g}$ increase in chlorophyll-a, mean body condition decreased by 0.009 (95% CI: 0.007 – 0.011) units. The dashed red lines represent the 95% confidence interval..... 146

Figure 11. The partial regression plot showing the effect of 30-day lagged flow, holding all other factors constant, on mean body condition (Fulton’s K) of juvenile striped bass, from the ANCOVA in which body condition is a function of year class, subestuary, and 30-day lagged temperature, chlorophyll-a, and flow. For every one m^3/sec increase in flow, mean body condition increased by 0.00010 (95% CI: 0.00005 – 0.00014) units. The dashed red lines represent the 95% confidence interval..... 147

Figure 12. Mean body condition of juvenile striped bass in the James and Rappahannock subestuaries from 2009 to 2017. Body condition (Fulton’s K) was modeled as a function of year, and the estimated breakpoint occurred in 2011. The solid line represents the effect of year on body condition from 2009 to 2012, and the dotted line represents the effect of year on body condition from 2012 to 2017. The red circle represents the breakpoint, or point at which the effect of year

on body condition changes. The gray shading represent the 95% confidence interval..... 148

Figure 13. Diagnostic plots for the exponential growth model where known weights and otolith-derived daily ages of the 2011, 2016, and 2017 year classes of juvenile striped bass within the James and Rappahannock subestuaries were used to estimate weight-specific instantaneous growth rates (G) and weight at hatch (W_0). Panel A showed that the assumption of normality was met and panel B showed that the assumption of homogeneity of variance was reasonable. 149

Figure 14. Observed weight-at-age (dots) and predicted exponential growth curves from model M_{10} for juvenile striped bass from the 2011 (black), 2016 (blue), and 2017 (gray) year classes within the (A) James and (B) Rappahannock subestuaries of the Chesapeake Bay.. 150

Figure 15. The catch curves used to estimate daily Z values for the 2011 (A), 2016 (C), and 2017 (E) year classes in the James subestuary and the 2011 (B), 2016 (D), and 2017 (F) year classes in the Rappahannock subestuary. The points represent log-transformed catch at each daily age. The solid points represent the juvenile striped bass that were fully recruited to the gear. Daily Z values were estimated using the slope of the black line. Z (instantaneous mortality rate) and A (discrete daily mortality rate calculated as $1 - e^{-Z}$) for each year class within each subestuary are indicated on each plot. 151

AUTHOR'S NOTE

This thesis is prepared as two chapters, which are each intended to be submitted as manuscripts for publication. Target journals have not yet been identified.

ABSTRACT

The Atlantic coast striped bass fisheries collapsed in the late 1970's due to recruitment overfishing and poor habitat quality. Recovery of the fisheries in 1995 resulted from protection of mature females, favorable environmental conditions, and several years of strong recruitment. Today, the striped bass stock is overfished. The purpose of this study was to examine recruitment characteristics of juvenile striped bass during the pre- and post-recovery periods through (1) a comparison of mortality and hatch-date distribution between periods, and (2) to examine growth metrics of individuals from the post-recovery year classes. Lengths and otolith-derived daily ages from juvenile striped bass representing three year classes (2011, 2016, and 2017) from the James and Rappahannock subestuaries of the Chesapeake Bay were used to develop subestuary-specific age-length keys. Daily ages of juvenile striped bass from 32 year classes (1986 to 2017) spanning the pre- and post-recovery periods were projected from the age-length keys. Together with count data, the projected daily ages were used to estimate instantaneous daily mortality rates (Z , day^{-1}) for each year class. Although daily Z estimates were relatively constant among the 32 year classes, mean hatch dates shifted earlier today (1996 to 2017) than prior to 1995. Within the post-recovery year classes, daily growth in length and weight was examined along with body condition (Fulton's K). All growth metrics varied by year class and subestuary, but daily growth rates and body condition were inversely related. The results of this study indicate that recruitment dynamics of juvenile striped bass in the Virginia portion of the Chesapeake Bay have changed over time, and within the post-recovery year classes, those changes varied among fish from the James and Rappahannock subestuaries.

Recruitment Characteristics of Juvenile Striped Bass (*Morone saxatilis*) Across Recovery
Periods, Year Classes, and Subestuaries in the Chesapeake Bay

INTRODUCTION

Striped bass, *Morone saxatilis*, are the top recreational species in terms of weight harvested along the Atlantic coast of the United States (NMFS 2018). In the Chesapeake Bay, striped bass support lucrative recreational and commercial fisheries, and provide cultural value as a symbol of the Chesapeake Bay. As such, striped bass fisheries are carefully managed along the Atlantic coast by the Atlantic States Marine Fisheries Commission (ASMFC) and within Virginia, by the Virginia Marine Resources Commission (VMRC) to maintain sustainable fisheries. However, striped bass fisheries in Chesapeake Bay experienced fluctuations during the last 50 years. Most notably, the fisheries collapsed in the early 1970's as a result of recruitment overfishing (i.e., harvesting individuals before they have an opportunity to spawn) and habitat degradation (Richards & Rago 1999). To rebuild the population, managers protected spawners by enacting strict size limits, requiring mandatory monitoring of juvenile recruitment, and eventually imposing complete moratoria on the fisheries in 1985, in Maryland waters, and in 1989, in Virginia waters (ASMFC 2019). Ultimately, the combination of effective management measures, several years of high juvenile abundance, and favorable environmental conditions in nursery areas led to an increase in spawning stock abundance (McGovern & Olney 1996), which resulted in recovery of coast wide fisheries in 1995 (Richards & Rago 1999). Following recovery of the population, the spawning stock biomass increased to a peak in 2010 (ASMFC 2019). Although the spawning stock biomass of striped bass is greater today than it was before 1995, the stock is currently overfished, and overfishing is occurring (ASMFC 2019).

In addition, environmental conditions such as water temperature and freshwater flow have changed in the Chesapeake Bay during the last 50 years (Najjar *et al.* 2000; Preston 2004; Najjar *et al.* 2010; Ding & Elmore 2015; Rice & Jastram 2015), which may affect the probability that young striped bass will survive and recruit to the adult population. For example, water temperatures have increased throughout the Chesapeake Bay, particularly in spawning and nursery areas and during the winter and spring when adults are spawning and young striped bass are present. Increased water temperatures are of concern because temperature affects striped bass at several life stages. For example, temperature can increase survival of young fish because higher water temperatures are associated with more prey availability, but it can also decrease survival because larval and juvenile striped bass can grow and survive only within a certain temperature range. Further, water temperature is a cue for spawning, and earlier warming of estuarine waters may have resulted in earlier spawning migrations in the spring (Peer & Miller 2014). That is, the timing of striped bass spawning affects the time at which young fish encounter favorable environmental conditions for survival, and thus overall recruitment.

Because successful recruitment was a key process that promoted the recovery of striped bass in the past, a study of the characteristics of the juvenile population in recent years may provide insight into how the recovered population responded to population-level and environmental changes. Further, such a study may yield strategies to return the current population to sustainable levels. My research objectives were to compare characteristics of pre-recovery (1986 – 1994) and post-recovery (1995 – 2017) juvenile striped bass populations in terms of hatch-date distributions and survival (Chapter 1); and to evaluate annual and spatial variation in growth rates, body condition, and recruitment

potential of post-recovery juvenile striped bass. In Chapter 1, I developed subestuary-specific age-length keys from otolith-derived ages of juvenile striped bass from the 2011, 2016, and 2017 year classes within the James and Rappahannock subestuaries of the Chesapeake Bay to estimate ages for juvenile striped bass for the year classes encompassing the pre-recovery (1986 to 1994) and post-recovery (1995 to 2017) periods. I also constructed hatch-date distributions and catch-curves for 32 year classes and compared them across the pre-recovery and post-recovery periods, among the 32 year classes, and between the James and Rappahannock subestuaries. In Chapter 2, I estimated daily growth rates and recruitment potential for three year classes associated with high (2011), low (2016), and average (2017) recruitment success. I also estimated and compared body condition of juvenile striped bass among nine year classes (2009 to 2017) and between the James and Rappahannock subestuaries. Results from this research indicate that characteristics of recruitment of juvenile striped bass have changed across and within recovery periods, and that these characteristics of recruitment vary among year classes and subestuaries. Further, at a time when the striped bass population is in decline, this study is particularly useful for scientists and managers who seek information regarding recruitment potential of striped bass to better guide management and return the fishery to sustainable levels.

LITERATURE CITED

- Atlantic States Marine Fisheries Commission (ASMFC). 2019. Summary of the 2019 benchmark stock assessment of Atlantic striped bass. ASMFC, Arlington, Virginia
- Ding H, Elmore AJ. 2015. Spatio-temporal patterns in water surface temperature from Landsat time series data in the Chesapeake Bay, USA. *Remote Sens. Environ.* 168: 335-348
- McGovern JC, Olney JE. 1996. Factors affecting survival of early life stages and subsequent recruitment of striped bass on the Pamunkey River, Virginia. *Can J Fish Aquat Sci.* 53: 1713-1726
- National Marine Fisheries Service (NMFS). 2018. Fisheries of the United States, 2017. NOAA, Silver Spring, Maryland
- Najjar RG, Walker HA, Anderson PJ, Barron EJ, Bord RJ, Gibson JR, Kennedy VS, Knight CG, Megonigal JP, O'Connor RE, Polsky CD, Psuty NP, Richards BA, Sorenson LG, Steele EM, Swanson RS. 2000. The potential impacts of climate change on the mid-Atlantic coastal region. *Clim. Res.* 14: 219-233
- Najjar RG, Pyke CR, Adams MB, Breitburg D, Hershner C, Kemp M, Howarth R, Muholland MR, Paolisso M, Secor D, Sellner K, Wardrop D, Wood R. 2010. Potential climate-change impacts on the Chesapeake Bay. *Estuar. Coast. Shelf S.* 86: 1-20

- Peer AC, Miller TJ. 2014. Climate change, migration phenology, and fisheries management interact with unanticipated consequences. *N. Am. J. Fish. Manage.* 34: 94-110
- Preston BL. 2004. Observed winter warming of the Chesapeake Bay estuary (1949-2002): implications for ecosystem management. *Environ. Manage.* 34: 125-139
- Rice KC, Jastram JD. 2015. Rising air and stream-water temperatures in Chesapeake Bay region, USA. *Climatic Change.* 128: 127-138
- Richards RA, Rago PJ. 1999. A case history of effective fishery management: Chesapeake Bay striped bass. *N. Am. J. Fish. Manage.* 19: 356-375

CHAPTER 1:

Mortality rates and hatch-date distributions for 32 year classes of juvenile striped bass:
Implications for recruitment

ABSTRACT

The Atlantic striped bass fishery collapsed in the late 1970's due to recruitment overfishing and poor habitat quality, was under strict management regulations in the 1980's, and recovered in 1995. Recovery of the fishery resulted from protection of spawning females, favorable environmental conditions, and several years of strong recruitment. The 2018 stock assessment indicated that the striped bass stock is overfished. The purpose of this study was to examine recruitment characteristics of juvenile striped bass during the pre- and post-recovery periods to (1) identify shifts in mortality rates and hatch-date distributions of juvenile striped bass and (2) investigate the relationship between hatch-date distribution and relative abundance of juvenile striped bass. Lengths and otolith-derived daily ages from juvenile striped bass representing three year classes (2011, 2016, and 2017) from the James and Rappahannock subestuaries of the Chesapeake Bay were used to develop subestuary-specific age-length keys. Daily ages of juvenile striped bass from 32 year classes (1986 to 2017) spanning the pre- and post-recovery periods were projected from the age-length keys. Together with seine-survey catch data, the projected daily ages were used to estimate instantaneous daily mortality rates ($Z \text{ day}^{-1}$) for each year class. The effect of hatch-date distribution on relative abundance of juvenile striped bass was explored by examining attributes of the hatch-date distributions, such as median hatch date and hatch duration. Although instantaneous daily mortality rates were relatively constant among the 32 year classes, mean hatch-dates shifted earlier today than prior to 1995. Managers may wish to encourage longer hatching (and spawning) periods by extending season closures to mirror the observed shifts in hatch dates.

INTRODUCTION

Successful recruitment was a key process that promoted the recovery of anadromous striped bass along the Atlantic coast in the 1980's and 1990's. Contemporary landings of the Chesapeake Bay striped bass fishery peaked in the early 1970's, but the fishery experienced significant declines later that decade due to recruitment overfishing (i.e., the harvesting of fish before they mature and spawn) and habitat degradation (Richards & Rago 1999). In the 1980's fisheries managers enacted measures such as size limits, bag limits, and moratoria to protect spawners and enhance the number of two-year-old fish entering the fishery; these measures allowed for reproduction and promoted the age diversity of spawners. Strict regulations, favorable environmental conditions, and several years of relatively high juvenile abundance led to an increase in spawning stock abundance (McGovern & Olney 1996), and ultimately, the recovery of the population in 1995 (Richards & Rago 1999). Although the abundance of striped bass is higher in the post-recovery period (after 1995) than it was in the pre-recovery period (prior to 1994), the population is currently overfished (ASMFC 2019). In addition, environmental conditions such as freshwater flow and temperature have changed (Najjar *et al.* 2010), particularly in striped bass spawning and nursery areas, which may affect key processes such as survival of early life stages (Secor & Houde 1995; North & Houde 2001; Martino & Houde 2010) and recruitment (Szuwalski *et al.* 2015). Management efforts to rebuild the population in the pre-recovery period and sustain the population in the post-recovery period (1995-2017) may no longer be sufficient to insure stability in the population as environmental conditions that affect growth and survival of juvenile striped bass change through time.

In tidal freshwater regions of rivers and subestuaries where anadromous fishes spawn, freshwater discharge introduces terrestrial and upriver nutrients that can increase production and availability of prey for young stages, thereby increasing growth and survival rates of young fishes (Rutherford *et al.* 1997; North & Houde 2003; Purtlebaugh & Allen 2010). Similarly, warm temperatures increase prey abundance (Logan 1985; Franz & Tanacredi 1992; Rutherford *et al.* 1997), induce increased feeding (Houde 1989; Fonds *et al.* 1992; Lloret *et al.* 2014) and promote growth (Booth & Alquezar 2002). Thus, freshwater discharge and temperature may play a key role in survival and recruitment of anadromous fishes, such as striped bass.

Water temperatures in the Chesapeake Bay and its subestuaries have increased, and this trend is projected to continue into the future (Najjar *et al.* 2010; Ding & Elmore 2015; Rice & Jastram 2015; Wagena *et al.* 2018). Projections indicate that warmer temperatures in the Chesapeake Bay may cause stress in temperate species like striped bass (Najjar *et al.* 2010). Furthermore, the magnitude of warming varies spatially and temporally within Chesapeake Bay. In particular, most warming has occurred in the winter and spring (Preston 2004; Najjar *et al.* 2010), and spring coincides with the presence of early life stages of striped bass in nursery areas within subestuaries of the Chesapeake Bay. Although warm water temperatures are associated with growth and survival of young fishes, temperatures that surpass an optimal window can induce stress, and ultimately, lead to mortality in young fishes (Akimova *et al.* 2016; Sswat *et al.* 2018). In the last five years, temperatures greater than 30° C, which is greater than the optimal temperature range of 24-26° C for juvenile striped bass (Cox & Coutant 1981), have been observed more frequently than in the past in nursery areas within the James

and Rappahannock subestuaries of the Chesapeake Bay (Gallagher *et al.* 2017; 2018).

Juvenile striped bass can survive temporarily outside of their optimal window, but growth ceases when water temperatures reach 33.5⁰C (Cox & Coutant 1981). Prolonged exposure to temperatures greater than 30⁰C could result in persistent slow growth during early life, which may result in increased mortality and an overall decrease in juvenile abundance.

Annual indices of juvenile abundance are used to estimate recruitment of striped bass, and such indices indicate that recruitment in this species, like many other fishes, is highly variable from year to year (Jennings *et al.* 2001; Gallagher *et al.* 2018). One view of recruitment variability is that it represents a population-level, adaptive response to highly variable environmental conditions (Fogarty 2001). Indeed, in striped bass, recruitment success is associated with cool water temperatures and high flows in March, April, and May (Martino *et al.* 2006), as well as a high abundance of adult striped bass and a broad female age diversity (Secor 2000). Recruitment success may also be indirectly associated with environmental conditions that vary across time and space, such as temperature, because they often cue spawning behaviors of fishes (Uphoff 1989; Peer & Miller 2014; Fraser *et al.* 2019; Vine *et al.* 2019). For example, adult striped bass enter the subestuaries in the early spring to spawn when water temperatures are 12⁰C or greater (Uphoff 1989). The time period when water temperatures are ideal for spawning may shift annually and also vary among subestuaries and result in slightly different spawning times, and thus different hatch dates of offspring. Hatch dates strongly influence the time at which young fishes encounter favorable (or unfavorable) conditions for survival (Secor & Houde 1995; Lapolla & Buckley 2005; Chimura *et al.* 2009; Lozano *et al.* 2012;

Aldanondo *et al.* 2016; Simonin *et al.* 2016). Variations in hatch dates among year classes and among subestuaries may contribute to annual variations in survival of young fishes, and thus variations in overall year-class strength (Lapolla & Buckley 2005; Aldanondo *et al.* 2016).

One of the seminal hypotheses about recruitment in fishes is Cushing's match-mismatch hypothesis (Cushing 1990); match-mismatch describes the higher survival rates of larvae that occur when first-feeding larvae coincide with an abundance of appropriate prey. In a given year, a shift in hatch date may alter the time at which first-feeding larvae are present, such that offspring with earlier hatch dates may be exposed to more (or less) favorable environmental conditions, and may exhibit higher (or lower) survival rates than their later-hatched conspecifics (Shepherd & Cushing 1980). Thus, annual variability in hatch dates reflects, in part, the influence of environment on spawning. Analysis of hatch dates in fishes can be used to study the dynamics of early-life stages (Secor & Houde 1995; Aldanondo *et al.* 2016; Bogner *et al.* 2016; Simonin *et al.* 2016). For example, Bogner and colleagues (2016) used attributes of the hatch-date distribution (e.g., hatch duration or peak hatch) to understand the effect of hatch-date distribution on the abundance of yellow perch (*Perca flavescens*) and bluegill (*Lepomis macrochirus*) in a North American lake. When hatch duration is long, abundances of larval yellow perch are greater, but larval bluegill abundances are greater when hatch duration is shorter (Bogner *et al.* 2016).

Hatch dates for juvenile fishes can be reconstructed from estimates of daily ages derived from otoliths, which are structures associated with hearing and balance that are located within the inner ear of fishes (Campana & Thorrold 2001). Otoliths grow over

time, and increments are formed as material accumulates along the outside of the otolith. In early-life stages of fishes, formation of these increments often occurs daily and as such, increment counts can be used to determine daily ages of fishes. Daily ages are critical for estimation of early-life-history traits, such as growth and mortality rates, and to understand environmental or species-specific conditions that drive those traits. For example, otoliths were used to show that Atlantic mackerel (*Trachurus trachurus*) exhibit faster growth rates in nearshore habitats than in other habitats (Van Beveren *et al.* 2016). In striped bass, the daily aging technique has been validated (Jones & Brother 1987; Secor & Dean 1989; Kline 1990; Douglas 1995), and daily ages of striped bass have been used to estimate many early life-history traits including, but not limited to, hatch dates, growth rates, and mortality rates of individual year classes (Kline 1990; McGovern & Olney 1991; Secor & Houde 1995; Bradley *et al.* 2017; Vanalderweireldt *et al.* 2019).

If abundance of adult striped bass continues to decline, managers may wish to take steps to encourage strong year classes of juveniles by protecting older females to allow them to spawn, and ensuring that season closures co-occur with the spawning period. Recruitment is determined by the number of offspring that survive to the juvenile and adult stages, and thus, reducing fishing pressure during the spawning season may allow more females to spawn over a longer period of time, thereby producing offspring during a longer period of time in spring. Although striped bass do not exhibit a strong stock-recruitment relationship, a broad distribution in hatch dates would yield offspring with a wide range of probabilities of survival, and possibly, a greater likelihood that offspring would survive into juvenile and adult stages. Therefore, the objectives of this study were to (1) investigate mortality of juvenile striped bass, (2) understand the

relationship between juvenile abundance and hatch-date distribution, and (3) examine changes in hatch dates through time. To address these objectives, I used information on abundance and size of juveniles collected by a long-term annual survey in nursery areas within the James and Rappahannock subestuaries of the Chesapeake Bay. I extracted otoliths from a subset of fish collected from three year classes (2011, 2016, and 2017) to estimate daily ages and develop age-length keys. These age-length keys were then used to estimate age of fish from a time series of lengths from 32 year classes of striped bass (1986-2017). Estimated daily ages provided hatch dates and allowed me to estimate mortality rates of juvenile striped bass within each subestuary. I also partitioned the 32-year time series into the pre-recovery period (1986-1994) and the post-recovery period (1995-2017) to permit comparison of mortality rates and hatch-date distributions of the recovering population of striped bass to those of the current, recovered population (i.e., the population prior to the overfished determination).

METHODS

Fish sampling & otolith preparation

Juvenile striped bass from three year classes (2011, 2016, and 2017) were obtained by the Virginia Institute of Marine Science (VIMS) juvenile striped bass seine survey (hereafter, the VIMS seine survey). The VIMS seine survey samples the Virginia subestuaries of the Chesapeake Bay, and uses a 30.5-m long seine with a 6.4-mm mesh net. It is a fixed-station survey that samples striped bass nursery areas in the Rappahannock (n=12 sites) and James (n=13 sites) subestuaries in July (Figure 1). Other subestuaries are sampled, but I focused my research on the James and Rappahannock subestuaries. The three year classes were selected because they were associated with variable recruitment, such that 2011, 2016, and 2017 year classes represented high, low, and average recruitment, respectively (Gallagher *et al.* 2018).

I used standard methods to prepare otoliths for age determination of juvenile striped bass (Secor *et al.* 1991). For each year class, the left sagittal otolith was removed from 75 randomly selected individuals from each subestuary (3 year classes x 75 fish x 2 subestuaries) for a total of 450 otoliths. Each otolith was mounted in flat embedding molds using epoxy resin. Once hardened, the molds were sectioned transversely with a low-speed Beuhler isomet saw and fixed to a microscope slide using Crystalbond. Each mounted otolith was ground using 320, 600, 800, and 1200 grit sandpaper until the core, which represents the otolith origin, was visible; otoliths were then polished with a microcloth containing a slurry of 0.3 μm alumina micropolish. Each polished otolith was photographed using a Nikon compound microscope at 600-1200X magnification, and NIS Elements BR 3.2 imaging software was used to annotate the images and facilitate

increment counts. I used the ObjectJ plug-in of ImageJ software to count otolith increments and determine age.

Consistency of age determinations

To ensure my age determinations were consistent, I randomly selected a subsample of 40 juvenile striped bass otoliths, representing the two subestuaries and three year classes, and determined increment readings for each of the 40 otoliths multiple times. I conducted these increment readings four times during a period of four weeks; from these four increment readings I calculated the deviance between each pair of readings for each otolith (e.g. first and second, first and third, and so on). With these deviances, I estimated error, bias, and average percent error between pairs of readings of the same otolith (Campana 2001). As used here, error describes the mean magnitude of the deviance between pairs of readings, and bias describes the mean deviance between pairs of readings (Campana *et al.* 1995; Campana 2001). That is, bias incorporates the positive or negative direction of the deviance for each reading of the same otolith. These metrics were estimated with the following formulae:

$$(1) \text{ Error} = \frac{\sum_{j=1}^n |a_{ij} - a_{kj}|}{n}$$

$$(2) \text{ Bias} = \frac{\sum_{j=1}^n a_{ij} - a_{kj}}{n}$$

where n is the total number of otoliths in each reading ($n=40$), a_{ij} and a_{kj} are the estimated ages obtained from otolith j in readings i and k , where $i \neq k$ and $k = 2, 3, \text{ or } 4$ (Gallagher *et al.* 2018). To assess bias, I used paired t -tests to compare mean increment counts from each combination of readings (e.g., readings one and two, one and three, one

and four, and so on), and used an alpha level of 0.05 to assess significance. The average percent error (APE) was estimated for each otolith, j , by estimating the average deviation from the mean age across the 4 readings with the following formula:

$$(3) APE_j = \frac{\sum_{i=1}^4 \frac{|\alpha_{ij} - \bar{\alpha}_j|}{\bar{\alpha}_j}}{4} * 100$$

where α_{ij} is the estimated age for reading i from otolith j and $\bar{\alpha}_j$ is the mean age of otolith j based on four readings (Campana 2001). APE_j was averaged across the 40 otoliths to calculate an index of average percent error (Campana *et al.* 1995).

Daily age estimation

Because temperature during the yolk-sac larval stage affects first-increment deposition, increment counts must be adjusted to yield accurate ages. The following relationship describes the adjusted first day of increment deposition, D , based on mean temperature, T (C°), during the yolk-sac larval stage:

$$(4) D = 11.56 - 0.45T$$

(Houde & Moring 1990). Because fish were collected at the juvenile stage in 2011, 2016, and 2017 and water temperature was not monitored daily in nursery areas, I did not have temperature data for the time during which fish were in the yolk-sac larval stage. To address this deficiency, I estimated the apparent day of first deposition by subtracting the raw increment count from the collection date (expressed as calendar day). Next, I used daily estimates of water temperature during the time the fish were in the yolk-sac larval

stage to calculate the mean temperature during the yolk-sac larval stage. I calculated the average temperature during yolk-sac larval stage using the mean daily temperatures on each of the 10 days prior to the apparent day of first deposition because larvae remain in the yolk-sac stage for 5-10 days after hatching (Secor & Houde 1995). Biweekly temperatures were obtained from the Chesapeake Bay Program's (CBP) water quality monitoring program (Water Quality Database for 1984 to present available at https://www.chesapeakebay.net/what/downloads/cbp_water_quality_database_1984_present). Biweekly temperatures from the CBP database were averaged across monitoring stations within the tidal fresh zone of each subestuary (Figure 2). The biweekly mean temperatures for each subestuary were then linearly interpolated from June to August of each year (1986-2017) to provide estimated mean daily temperatures for the tidal fresh zone of the James and Rappahannock subestuaries. With these daily temperatures, I estimated the mean day of first-increment deposition, D , as 3.78 days (SE = 0.04) using equation (4); D ranged from 1.59 to 6.31 days, depending on year.

Adjusted ages were calculated using the following equation:

$$(5) A = I + D$$

where A represents adjusted age, I represents increment count, and D is day of first-increment deposition, determined from equation (4).

Age-length keys

The relationship between fish length and daily age was used to develop age-length keys (Bettoli & Miranda 2001; Isermann & Knight 2005; Ailloud & Hoenig 2019) for juvenile striped bass from Virginia subestuaries. For this study, age-length keys were

used to estimate daily ages of juvenile striped bass from length information from 32 year classes collected by the VIMS seine survey (1986 – 2017). Age-length keys can be developed for an entire population (e.g., Chesapeake Bay juvenile striped bass), under the assumption that all individuals from the population have a similar age-length relationship (Ailloud & Hoenig 2019). However, individual striped bass may grow at different rates, particularly if they occupy subestuaries with varying prey resources and abundances of conspecifics. Thus, age-length keys were developed for each subestuary (James and Rappahannock) and each year class (2011, 2016, and 2017) using a multinomial logistic model, where age was a function of length category, subestuary, and year class (Rindorf & Lewy 2001; Gerritsen *et al.* 2006). The age-length relationship of juvenile striped bass is linear (Kline 1990), and preliminary observations of my age and length data supported a linear relationship. For these age-length keys, I grouped length into 3-mm bins, from 22 to 89-mm fork length (FL) because not all lengths were represented when I used smaller bins (i.e., 1-mm or 2-mm), and because larger bins would have provided a coarser age-length relationship. I used the method described in Gerritsen *et al.* (2006) in which a simple model is compared with more complex models using likelihood ratio tests to assess support for year-specific or subestuary-specific age-length keys. I did not consider year-specific keys within each subestuary due to low sample size. The simple model was:

$$(6) (Age)_k = \beta_0 + \beta_1 (Length)_l + \varepsilon_l$$

- where $(Age)_k$ = daily age of the k^{th} individual, assumed to be normally distributed;
 β_0 = intercept, overall mean value of age for juvenile striped bass from 32 year classes (from 1986 to 2017) in the James and Rappahannock subestuaries;
 β_1 = regression coefficient accounting for effect of the l^{th} length bin on age;
 $(Length)_l$ = the l^{th} length bin measured in mm;

ε_l = random unexplained error, assumed to be normally distributed with mean of 0 and variance of σ_ε^2 .

The year-class-specific model was:

$$(7) (Age)_{jk} = \beta_0 + (Year)_j + \beta_2(Length)_l + \beta_3(Year * Length)_{jl} + \varepsilon_{jk}$$

- where $(Age)_{jk}$ = daily age of the k^{th} individual in the j^{th} year class (j=1986 to 2017), assumed to be normally distributed;
- β_0 = intercept, overall mean value of age for juvenile striped bass from 32 year classes (from 1986 to 2017) in the James and Rappahannock subestuaries;
- $(Year)_j$ = effect of the j^{th} year class (j=1986 to 2017);
- β_2 = partial regression coefficient accounting for effect of length bin on age;
- $(Length)_l$ = the l^{th} length bin measured in mm;
- β_3 = partial regression coefficient accounting for effect of the interaction of length and year class on age;
- $(Year * Length)_{jl}$ = interaction of length bin and year class;
- ε_{jk} = random unexplained error associated with the k^{th} individual from the j^{th} year class, assumed to be normally distributed with mean of 0 and variance of σ_ε^2 .

Similarly, the subestuary-specific model was:

$$(8) (Age)_{ik} = \beta_0 + (Subestuary)_i + \beta_4(Length)_l + \beta_5(Subestuary * Length)_{il} + \varepsilon_{ik}$$

- where $(Age)_{ik}$ = daily age of the k^{th} individual in the i^{th} subestuary (j=James or Rappahannock), assumed to be normally distributed;
- β_0 = intercept, overall mean value of age for juvenile striped bass from 32 year classes (from 1986 to 2017) in the James and Rappahannock subestuaries;
- $(Subestuary)_i$ = the i^{th} subestuary (i=James or Rappahannock);
- β_4 = partial regression coefficient accounting for effect of length bin on age;
- $(Length)_l$ = the l^{th} length bin measured in mm;
- β_5 = partial regression coefficient accounting for effect of interaction of length bin and subestuary on age;

$(Subestuary * Length)_{il}$ = interaction of length bin and subestuary;
 ε_{ik} = random unexplained error associated with the k^{th}
individual from the i^{th} subestuary, assumed to be
normally distributed with mean of 0 and variance of σ_{ε}^2 .

Because model 6 is nested within model 7 and model 8, likelihood ratio tests were used to compare models 7 and 8 with model 6 (Gerritsen *et al.* 2006).

The age-length key supported by the likelihood ratio test was applied to length measurements collected by the VIMS seine survey to estimate daily ages for juvenile striped bass from 32 year classes within the James and Rappahannock subestuaries.

Instantaneous daily mortality rates (Z)

I developed catch curves from estimated daily ages (1-day bins) and catches from the VIMS seine survey and compared estimated instantaneous daily mortality rates, Z , for the James and Rappahannock subestuaries during the pre-recovery period (1986 to 1994) and the post-recovery period (1995-2017); daily Z estimates were also examined for annual changes among the 32 year classes for fish captured between 1 and 31 July each year. Instantaneous daily mortality rates may be estimated using catch-curve analysis if the following assumptions are met: (1) the population is closed and there is no immigration or emigration, (2) daily Z is independent of age or length, (3) all fish are equally vulnerable to the gear, and (4) the sample is unbiased (Ogle 2016). Catch curves comprise an ascending limb, a dome, and a descending limb. The ascending limb and dome are composed of age- or length-classes of fish that have not fully recruited to the sampling gear. Fish are considered fully recruited to the gear at the age or size that the dome intersects with the descending limb. The descending limb is comprised of fish that

are fully recruited to the gear. The descending limb of the catch curve is linear when the assumptions of the catch curve are met, and the absolute value of the slope of this limb, β_1 , represents the instantaneous daily mortality rate for the month of July (Miranda & Bettoli 2007; Ogle 2016). The slope of the line can be estimated using the following:

$$(9) (\log_e(\text{Catch}))_l = \beta_0 + \beta_1(\text{Age})_l + \varepsilon_l$$

- where $(\log_e(\text{Catch}))_l$ = \log_e -transformed catch corresponding to the 1th age bin, assumed to be normally distributed;
 β_0 = intercept, overall mean \log_e -transformed catch for juvenile striped bass from 32 year classes (from 1986 to 2017) in the James and Rappahannock subestuaries;
 β_1 = regression coefficient accounting for effect of age on \log_e -transformed catch;
 $(\text{Age})_l$ = 1th age bin (daily);
 ε_l = random unexplained error associated with the 1th age bin, assumed to be normally distributed with mean of 0 and variance of σ_ε^2 .

Instead of developing 64 catch curves representing each year class within each subestuary, I used three analyses of covariance to compare the slope of the descending limb, or Z, between two periods, between subestuaries, and among year classes (Pope & Kruse 2007; Ogle 2016). If the difference in slopes was significantly different from zero, I developed separate catch curves and estimates of daily Z for each group (e.g., pre- and post-recovery; Ogle 2016). The recovery-period model was:

$$(10) (\log_e(\text{Catch}))_{kl} = \beta_0 + (\text{Period})_k + \beta_2(\text{Age})_l + \beta_3(\text{Period} * \text{Age})_{kl} + \varepsilon_{kl}$$

- where $(\log_e(\text{Catch}))_{kl}$ = \log_e -transformed catch corresponding to the 1th age bin in the kth recovery period, assumed to be normally distributed;
 β_0 = intercept, overall mean value of \log_e -transformed catch for juvenile striped bass from 32 year classes (from 1986 to 2017) in the James and Rappahannock subestuaries;
 $(\text{Period})_k$ = effect of the kth recovery period (k=pre-recovery or post-recovery);
 β_2 = partial regression coefficient accounting for effect of recovery period;

$$\begin{aligned}
(Age)_l &= 1^{\text{th}} \text{ age bin (daily);} \\
\beta_3 &= \text{partial regression coefficient accounting for effect of} \\
&\quad \text{interaction of recovery period and age;} \\
(Period * Age)_{kl} &= \text{interaction of recovery period and age;} \\
\varepsilon_{kl} &= \text{random unexplained error associated with the } 1^{\text{th}} \text{ age bin} \\
&\quad \text{from the } k^{\text{th}} \text{ recovery period, assumed to be normally} \\
&\quad \text{distributed with mean of 0 and variance of } \sigma_\varepsilon^2.
\end{aligned}$$

The subestuary model was:

$$\begin{aligned}
(11) \quad &(\log_e(Catch))_{il} \\
&= \beta_0 + (Subestuary)_i + \beta_4(Age)_l + \beta_5(Subestuary * Age)_{il} + \varepsilon_{il}
\end{aligned}$$

$$\begin{aligned}
\text{where } (\log_e(Catch))_{il} &= \log_e\text{-transformed catch corresponding to the } 1^{\text{th}} \text{ age bin in} \\
&\quad \text{the } i^{\text{th}} \text{ subestuary, assumed to be normally distributed;} \\
\beta_0 &= \text{intercept, overall mean value of } \log_e\text{-transformed catch for} \\
&\quad \text{juvenile striped bass from 32 year classes (from 1986 to} \\
&\quad \text{2017) in the James and Rappahannock subestuaries;} \\
(Subestuary)_i &= \text{effect of the } i^{\text{th}} \text{ subestuary (i= James or Rappahannock);} \\
\beta_4 &= \text{partial regression coefficient accounting for effect of} \\
&\quad \text{subestuary;} \\
(Age)_l &= 1^{\text{th}} \text{ age bin (daily);} \\
\beta_5 &= \text{partial regression coefficient accounting for effect of} \\
&\quad \text{interaction of subestuary and age;} \\
(Subestuary * Age)_{il} &= \text{interaction of subestuary and age;} \\
\varepsilon_{il} &= \text{random unexplained error associated with the } 1^{\text{th}} \text{ age bin} \\
&\quad \text{from the } i^{\text{th}} \text{ subestuary, assumed to be normally distributed} \\
&\quad \text{with mean of 0 and variance of } \sigma_\varepsilon^2.
\end{aligned}$$

The year-class model was:

$$(12) \quad (\log_e(Catch))_{jl} = \beta_0 + (Year)_j + \beta_6(Age)_l + \beta_7(Year * Age)_{jl} + \varepsilon_{jl}$$

$$\begin{aligned}
\text{where } (\log_e(Catch))_{jl} &= \log_e\text{-transformed catch corresponding with the } 1^{\text{th}} \text{ age bin in} \\
&\quad \text{the } j^{\text{th}} \text{ year class, assumed to be normally distributed;} \\
\beta_0 &= \text{intercept, overall mean value of } \log_e\text{-transformed catch for} \\
&\quad \text{juvenile striped bass from 32 year classes (from 1986 to} \\
&\quad \text{2017) in the James and Rappahannock subestuaries;} \\
(Year)_j &= \text{effect of the } j^{\text{th}} \text{ year class (j=1986 to 2017);} \\
\beta_6 &= \text{partial regression coefficient accounting for effect of year} \\
&\quad \text{class;} \\
(Age)_l &= 1^{\text{th}} \text{ age bin (daily);}
\end{aligned}$$

$$\begin{aligned} \beta_7 &= \text{partial regression coefficient accounting for effect of} \\ &\quad \text{interaction of year class and age;} \\ (Year * Age)_{jl} &= \text{interaction term of year class and age bin;} \\ \varepsilon_{jl} &= \text{random unexplained error associated with the } l^{\text{th}} \text{ age bin in} \\ &\quad \text{jth year class, assumed to be normally distributed with mean} \\ &\quad \text{of 0 and variance of } \sigma_{\varepsilon}^2. \end{aligned}$$

A significant interaction between age and period, year class, or subestuary indicated that the difference between slopes of the descending limb of the catch curves differed from zero. This necessitated a separate catch curve for each group and a separate estimate of daily Z. For instance, if the interaction between period and age in model 10 was significant, the slope of the descending limb (Z) for fish collected during the pre-recovery period was significantly different from the slope of the descending limb (Z) for fish collected during the post-recovery period, requiring a separate catch-curve analysis (and daily Z estimates) for each period. I estimated 95% confidence intervals of the regression coefficients for age to compare the resulting daily Z estimates through time, between the pre-recovery and post-recovery period (1986 to 2017) and among subestuaries (James and Rappahannock).

Hatch-date distributions

To reduce bias in the analysis of hatch-date distributions, I considered estimated hatch dates only for juvenile fish that were fully recruited to the seine. Because growth rates vary through time and space, and because these variations may alter the age at which fish fully recruit to the gear, I conducted a graphical investigation of catch-at-length to identify the length at which juvenile striped bass were recruited to the seine. For this analysis catches were grouped into individual length classes (1 mm bins). Based on

this graphical analysis, the length at which juvenile striped bass were fully recruited to the seine was 55 mm, and thus only fish greater than 55 mm were included in the analysis of hatch-date distributions. More specifically, I used the estimated daily ages derived from age-length keys but only for individuals greater than 55 mm. I subtracted the estimated daily age of each fish from the date of collection to estimate hatch date for all juveniles captured by the VIMS seine survey between 1 July and 31 July in the James and Rappahannock subestuaries from 1986 to 2017. For example, a 50-day old juvenile captured on calendar day 170 had an estimated hatch date of calendar day 120. I developed hatch-date distributions for each year class from 1986 to 2017, rather than subestuary specific hatch-date distributions for each year class because the James and Rappahannock subestuaries appeared to have similar hatch-date distributions during the 32-year time span (see results).

In addition to restricting my analysis to only those fish that had fully recruited to the seine, I also considered the effects of cumulative mortality on hatch-date distributions. Cumulative mortality may occur because young fish experience fewer days of mortality by the time of collection than older fish, causing a mortality differential between age cohorts. The cumulative mortality differential can affect the observed hatch-date distribution, such that the abundance of young fish (represented by later hatch dates) appears much higher than the abundance of older fish (represented by earlier hatch dates). Cumulative mortality differential between older and younger individuals is reduced when fish are collected at a relatively older age or during a time in which mortality rates are low. In my study, I restricted analyses to fish collected between 1 and 31 July; all these fish were juveniles. To explore the potential effect of cumulative mortality on hatch-date

distribution, I calculated abundances of cohorts under a constant daily mortality assumption. For this exercise, I assumed juveniles experienced a mortality rate of 1% per day (Secor *et al.* 1995). I organized individuals into 15-day cohorts, and compared the resulting hatch-date distribution with the observed hatch-date distribution. If cumulative mortality was a concern, then the observed hatch-date distribution will appear skewed in relation to the mortality-adjusted hatch-date distribution. More specifically, the observed hatch-date distribution would show a relatively greater abundance of juveniles hatched later in the season relative to the distribution of the mortality-adjusted hatch-dates.

Relationship between hatch-date distribution & abundance of juvenile striped bass

I calculated multiple attributes of the annual hatch-date distributions including earliest, latest, peak, and median hatch dates (Table 1). I also calculated hatch duration (i.e., range) and truncated hatch duration, to remove the earliest and latest 1% of hatch dates. The truncated hatch duration reduces the potential error resulting from the application of age-length keys that I used to estimate daily ages and resulting hatch dates. More specifically, the estimated hatch dates that occur especially early (mid-March) and especially late (mid-June) may not be representative of actual hatch dates exhibited by the 32 year classes assessed in this study, and may instead result from unexplained, random error associated with my age-length key.

A generalized additive model (GAM) was used to describe the effects of attributes of annual hatch-date distributions on annual relative abundance of juvenile striped bass for 1986 to 2017. Annual indices of abundance of juvenile striped bass were provided by the VIMS seine survey and represented relative abundance. Graphical inspection of the

raw data suggested that the relationship between juvenile striped bass abundance and hatch-date distribution attributes may not be linear, so I applied a GAM. Pearson's correlation (r) analysis was used to identify hatch-date attributes that were correlated with one another. Because truncated hatch duration is a direct result of first and last hatch, preliminary results suggested that first and last hatch were highly, significantly correlated with truncated hatch duration ($r_{\text{first hatch}} = -0.69$, $p_{\text{first hatch}} < 0.05$; $r_{\text{last hatch}} = 0.51$, $p_{\text{last hatch}} < 0.05$). I removed from consideration those attributes whose correlation was significantly different from zero and retained three attributes: truncated duration, peak hatch, and median hatch date. Further, the possibility of collinearity was explored with the `ols_vif_tol()` command in the `olsrr` package in R, which calculates tolerance values for each factor (tolerance values less than 0.1 indicate the presence of collinearity). I fitted the following GAM using non-parametric smoothing factors in the `mgcv` package in R:

$$(14) (Abundance)_l = \alpha + g_1(Truncated\ duration) + g_2(Peak\ hatch) + g_3(Median\ hatch) + \varepsilon_l$$

where $(Abundance)_l$ = juvenile striped bass abundance of the l^{th} year class (l =from 1986 to 2017), assumed to be normally distributed;
 α = intercept, overall mean abundance of juvenile striped bass;
 g_{1-3} = nonparametric smoothing functions for truncated hatch duration, peak hatch date, and median hatch date;
 ε_l = random unexplained error, assumed to be normally distributed with mean of 0 and variance of σ_{ε}^2 .

I evaluated model diagnostics using the `gam.check()` command in the `mgcv` package in R, using plots to assess the reasonableness of the assumptions of normality (quantile-quantile plot) and homogeneity of variance (residual plot), as well as adequacy of model fit (plots of residuals versus fitted). Preliminary inspection of the diagnostic

plots, especially the residuals versus fitted plot, showed that the assumption of homogeneity of variance was violated. I attempted to resolve this issue by modifying model (14) in one of two ways: (1) use of the gamma distribution to describe the relative abundance of juvenile striped bass and the negative reciprocal as the link function, and (2) use of the natural-log transformed relative abundance. Both solutions violated the assumption of homogeneity of variance, and neither solution resulted in residuals that reasonably met the assumption of normality. Given the violated assumptions, I assessed the relationship between attributes of the hatch-date distributions and relative abundance of juvenile striped bass with Spearman's rank correlation, which is a non-parametric alternative to linear regression that measures the direction and strength of the relationship between two ranked variables (Gauthier 2001). Spearman's rank correlation tests were conducted with the *cor.test()* command in R, which yielded an S-statistic, p-value, and an estimate of rho for each attribute of the hatch-date distribution and relative abundance.

Comparison of hatch-date distributions for 32 year classes

To understand how hatch-date distributions of juvenile striped bass changed through time, I developed a nested analysis of covariance (ANCOVA); here, hatch date (calendar day) was modeled as a function of subestuary, period, and year class (1986-2017) nested within period. Year was nested within period because each year class occurred within a single period (e.g., 1988 occurred within the pre-recovery period). I included temperature at hatch as a covariate to account for changing water temperatures in striped bass nursery areas through time, and to allow me to compare the mean hatch date in each subestuary, period, and year-class at a common temperature. Temperature at

hatch was estimated as described previously. The initial statistical model fitted to the data using the `lm()` function in R (R Core Team 2019) was:

$$(15) \text{ (Hatch date)}_{ijkl} = \beta_0 + (\text{Subestuary})_i + (\text{Period})_k + (\text{Year(Period)})_{jk} + \beta_1(\text{Temp}) + \varepsilon_{ijkl}$$

where $(\text{Hatch date})_{ijkl}$ = The hatch date of the l^{th} individual in the i^{th} subestuary and the j^{th} year class within the k^{th} period, assumed to be normally distributed;

β_0 = intercept, overall mean hatch date;

Subestuary_i = effect of the i^{th} subestuary (i = James or Rappahannock);

Period_k = effect of the k^{th} period (j = pre-recovery or post-recovery);

$(\text{Year(Period)})_{jk}$ = Effect of the j^{th} year class nested within the k^{th} recovery period (i.e., 1986 to 1994 year classes in the pre-recovery period and 1995 to 2017 year classes in the post-recovery period);

β_1 = regression coefficient accounting for effect of temperature during hatch;

(Temp) = Temperature during hatching measured in degrees Celsius;

ε_{ijkl} = random unexplained error associated with the l^{th} individual in the i^{th} subestuary and the j^{th} year class within the k^{th} period, assumed to be normally distributed with mean of 0 and variance of σ_ε^2 .

All factors in the model were considered fixed effects. I examined residuals to assess model fit and the assumption of homogeneity of variance. I also examined two-way interaction plots to determine if interactions between predictors were present, but did not detect interactions.

RESULTS

Consistency of age determinations

Aging error, or the mean magnitude of the deviance in estimated increment counts between two readings, ranged from 4.5 to 8 days (N = 40 otoliths). The mean average percent error (APE) across individual otoliths was 5.8% and ranged from 2.0 to 17%. Four otoliths or 10% of the subsampled otoliths had an APE greater than 10%. Furthermore, the 4 otoliths with an APE greater than 10% were equally representative of all sampled otoliths in that they encompassed all three year classes and both subestuaries. Bias ranged from -2.4 to 2.0 days across readings. I found a significantly negative age bias ($t = -2.61$, $p < 0.05$) between the second and third readings (2.3 days), but the bias was non-significant for all other reading combinations (Table 2). My error, bias, and APE estimates indicated that my age determinations did not exhibit a systemic bias, and thus, were used in further analyses.

Age-length keys

Although the age-length relationship varied between subestuaries (LR Statistic = 151; $p < 0.05$), I was not able to detect differences in the age-length relationship among year classes (LR Statistic = 260; $p = 0.07$). Based on these results, I developed age-length keys for each subestuary using the range of lengths observed in the VIMS seine survey (James: 28 to 89-mm FL; Rappahannock: 22 to 69-mm FL); these keys were then used to estimate daily ages of striped bass from the 32 year classes (1986-2017) using observed lengths. The average length of juvenile striped bass across 32 year classes was 62 mm (95% confidence interval [CI] = 59.9 – 63.9 mm). The average 62-mm juvenile striped

bass was about 74 days old (95% CI: 73.6 – 75.3 days) in the James subestuary, and 81 days old (95% CI: 79.4 – 82.0 days) in the Rappahannock subestuary.

Instantaneous daily mortality rates (Z)

For all catch curves the descending limb began at 80 days after hatch, and this was treated as the age of recruitment to the seine. I used the three ANCOVAs (models 10, 11, and 12) to compare daily Z estimates for the month of July among groups holding all other effects constant. I used model 10 to compare daily Z across periods, and found that the interaction between age and period was not significant ($F_{\text{Age*Period}} = 0.04$, $p = 0.84$), whereas the mean effects of age and period were significant factors explaining the variation in observed catches ($F_{\text{Age}} = 98.2$, $p < 0.01$; $F_{\text{Period}} = 54.8$, $p < 0.01$). Daily Z was estimated for each period from model 10 such that the absolute value of the slope of the line was the estimate of daily Z for the post-recovery period, and the absolute value of the slope of the line plus the effect due to period was the daily Z estimate for the pre-recovery period. However, based on overlapping 95% confidence intervals, the daily Z estimates were not significantly different among periods: $Z = 0.132 \text{ day}^{-1}$ (95% CI: 0.097-0.138 day^{-1}) in the pre-recovery period and $Z = 0.126 \text{ day}^{-1}$ (95% CI: 0.088-0.158 day^{-1}) in the post-recovery period. Model 11 computed estimates of daily Z for the subestuaries, and indicated that the interaction between age and subestuary was not significant ($F_{\text{Interaction}} = 0.69$, $p = 0.41$); age was a significant factor in the model ($F_{\text{Age}} = 24.1$, $p < 0.01$), but subestuary was not ($F_{\text{Subestuary}} = 0.01$, $p = 0.93$). Therefore, this model indicates no difference in daily Z for the month of July between subestuaries, and suggests a single daily Z estimate of 0.106 day^{-1} (95% CI: 0.031-0.181 day^{-1}),

representing the instantaneous daily mortality rate of juvenile striped bass from either subestuary. I used model 12 to compare daily Z estimates for the month of July across the 32 year classes (1986 to 2017). In model 12, the interaction between age and year class was not significant ($F = 1.09$, $p = 0.38$), and the main effects of age and year class were significant factors in the model ($F_{\text{Age}} = 1753.5$, $p < 0.01$; $F_{\text{Year-class}} = 23.8$, $p < 0.01$). Estimated daily Z ranged from 0.061 day^{-1} (2012) to 0.218 day^{-1} (1995), and averaged 0.147 day^{-1} (SE: 0.006) for the 32 year classes analyzed here (Table 3). However, the 95% confidence intervals for these estimates overlapped, suggesting that instantaneous daily mortality rates of juveniles in July did not vary among year classes (Figure 3). Based on the observed daily Z estimates, the instantaneous monthly mortality estimates for the month of July (within each year class) ranged from 1.89 month^{-1} (2012) to 6.76 month^{-1} (1995). Discrete mortality rates (A) ranged from 0.06 day^{-1} for the 2012 year class to 0.20 day^{-1} for the 1995 year class (Table 3).

Relationship between hatch-date distributions & abundance of juvenile striped bass

The hatch-date distributions of 32 year classes of juvenile striped bass in the James and Rappahannock subestuaries did not change as a result of cumulative mortality. That is, cumulative mortality differential between younger cohorts and older cohorts was minimal, such that the observed and mortality-adjusted hatch-date distributions did not differ appreciably (Figure 4A and B).

No significant correlations were observed between attributes of the hatch-date distributions (truncated hatch duration, median hatch, peak hatch, first hatch, and last hatch) and relative abundance of juvenile striped bass (Table 4). However, the

Spearman's rank correlation associated with truncated hatch duration was marginally significant ($\rho = 0.30$, $p = 0.095$).

Comparison of hatch-date distributions for 32 year classes

Hatch-date distributions of juvenile striped bass larger than 55 mm (i.e., length at which fish were fully recruited to the seine) depended on period, year class nested within period, and temperature at time of hatching. Hatch-dates pooled across 32 year classes from the James and Rappahannock subestuaries were normally distributed (Figure 5). Although my model results suggested that significantly later hatching (about 2 days) occurred in the Rappahannock subestuary compared with the James subestuary, I could not resolve this difference with my aging error of 4 to 8 days. As a result, and to simplify the model, subestuary was omitted from the model, and I retained period, year class nested within period, and temperature at time of hatching to explain the variation in mean hatch dates. This model accounted for 73.3% of the variation in mean hatch date across all year classes ($R^2 = 0.7326$, $p < 0.05$). Overlapping confidence intervals on interaction plots between subestuary and temperature during hatching indicated that the interaction, if present, was not strong (Figure 6). Other two-way interactions were minor or not present (i.e., interactions between subestuary, year class, recovery period, and temperature during hatch; Figure 6). The histogram of residuals (Figure 7A) and Q-Q plot (Figure 7B) indicated that the assumption of normality was met. I found no evidence of a pattern in the residuals to indicate heterogeneity of variance (Figure 7C). Box and whisker plots grouped by year class (Figure 7E), period (Figure 7F), and low (5.0 – 18.4

°C) and high (18.5 – 29.0 °C) temperature during hatching (Figure 7G) indicated that groups appeared to exhibit similar variances.

Mean hatch dates during the pre-recovery period (1986-1995) were significantly later than mean hatch dates during the post-recovery period (1996-2017; $F = 452.41$; $p < 0.01$). The least-squares mean hatch date during the pre-recovery period was day 125.8 (95% CI: 125.4-126.2), or May 5th, and the least-squares mean hatch date during the post-recovery period was day 121.9 (95% CI: 121.7-122.1), or May 1st. Mean hatch date varied among year classes ($F = 233.00$; $p < 0.01$), and appeared to decline through time, with mean hatch dates occurring earlier in recent year classes (Figure 8). The covariate, mean temperature during hatching, was also a significant factor in the model ($F=18586$; $p < 0.01$). The partial-regression coefficient for mean temperature at time of hatching was 3.89 (95% CI: 3.83-3.94). That is, the model-based relationship indicates that larvae that hatch later in the spring do so in warmer water temperatures.

Overall, hatch-distribution attributes shifted through time, but hatch duration appeared similar (about 48 to 65 days) regardless of year class or recovery period (Figure 10). Three observations, representing the 1986, 1988, and 1990 year classes have truncated hatch durations less than 30 days (Figure 10), but this likely reflected changes in the manner in which the VIMS seine survey completed the sampling in those years. Because the 1986, 1988, and 1990 year classes were each sampled during only three or fewer days in July it is likely that fish that were hatched later in the season were not collected, and reduced sampling in these years may have resulted in the appearance of a shorter truncated hatch duration. Additionally, attributes of the hatch-date distribution of 32 year classes of juvenile striped bass in the James and Rappahannock subestuaries

shifted to earlier dates in the post-recovery period. These hatch-date attributes included: earliest hatch, latest hatch, peak hatch, and median hatch (Table 1). The shortest hatch duration, excluding the 1986, 1988, and 1990 year classes, occurred in 1989 and lasted 41 days; the longest hatch duration occurred in 1998 and lasted 74 days. Although hatch duration varied annually, average hatch duration across year-classes was about 65.3 (standard error [SE] = 1.87) days. Truncated hatch duration, which removes the extremes of hatch duration, averaged 44.8 (SE = 1.33) days, and the shortest truncated hatch duration occurred in 1998 and lasted about 23.3 days; the longest truncated hatch duration occurred in 1996 and lasted about 58.3 days.

DISCUSSION

Between 1986 and 2017, instantaneous daily mortality rates (Z) of juvenile striped bass from the James and Rappahannock subestuaries in July were relatively constant, but mean hatch-dates varied among 32 year classes. Further, mean hatch dates in recent years shifted to earlier in the spring compared with those observed in years prior to 1995. If hatch timing affects the time at which juvenile striped bass encounter favorable environmental conditions for survival, then the results of my study suggest that a shift in hatch dates may mirror shifts in favorable environmental conditions through time, and thus may have contributed to the constant daily mortality rates I observed in July among year classes. The observed changes at the juvenile stage suggest responses at the adult stage, namely, spawning behavior may be changing, perhaps as a result of a changing environment. Such alterations in the reproductive behaviors of adult striped bass may have economic and ecologic impacts in the Chesapeake Bay. For example, if the season closure designed to protect spawning females from harvest is not adjusted to mirror the earlier hatch dates, and presumably earlier spawning times, observed in recent times then spawners may be harvested before they have an opportunity to spawn. Removal of spawners before they produce offspring may contribute to the recently observed decline in abundance of the striped bass population.

Instantaneous daily mortality rates (Z)

Instantaneous daily mortality rates of juvenile striped bass in July were relatively constant between recovery periods and across the James and Rappahannock subestuaries.

Although variable mortality rates are characteristic of the early life stages of most fishes, I observed little annual variability in instantaneous daily mortality rates for juvenile striped bass in July. However, variations in instantaneous daily mortality rates among year classes were difficult to discern because of the high uncertainty around estimates of mortality; this level of uncertainty likely resulted from the small number of fish in each daily age bin of the catch-curve analysis. Catch curves developed with age bins of 3 to 5 days can help to increase the number of observations per age bin, and this could result in greater certainty around instantaneous daily mortality estimates, however, such estimates will be coarser estimates of instantaneous daily mortality. Uncertainty around estimates of instantaneous daily mortality rates in my study may also be due to violation of the assumptions of the catch-curve model. Catch-curve analyses assume a closed population (e.g., no recruitment) with population losses occurring only as a result of mortality. Additionally, all fish are assumed to be equally susceptible to the sampling gear. Two protocols were used to ensure that the samples used in this analysis satisfied those assumptions: (1) only fish less than 89 mm were included in the analysis and (2) the time frame for estimation of instantaneous daily mortality rates was limited to July. Juvenile fish less than 89 mm in July are not large enough to evade the seine net and thus, all other factors being equal, their vulnerability to capture should be fairly constant. However, my estimates of mortality represent apparent mortality rates because juvenile fish may leave nearshore areas that are sampled by the seine. Thus my estimates of apparent mortality represent losses from the population of juveniles that are available to the seine. If habitat use remained relatively similar during the 32-year period of my study, then my estimates of apparent mortality suggest that mortality was relatively constant, albeit variable among

year classes. If habitat use varied during the 32-year period, then my estimates of mortality include losses due to the lack of availability of fish to the seine. The third possibility is that instantaneous daily mortality rates are indeed relatively constant for juvenile striped bass in July. This is supported by the observation that mortality at the juvenile stage of fishes is generally more stable than at the egg or larval stages (Houde 1989; Campana 1991; Lorenzen & Camp 2019). Future studies should estimate instantaneous daily mortality rates at a younger life stage (e.g., larval) to better investigate potential variation in mortality of pre-recruited striped bass among year classes and relate observed mortality rates to overall year-class strength.

Most mortality estimates for young striped bass that have been published to date pertain to larvae and young juveniles (McGovern & Olney 1991; Secor & Houde 1995; Kimmerer *et al.* 2000), and because mortality is highest at these earlier life stages I expected these rates would be greater than what I observed for juvenile striped bass in July in the Chesapeake Bay. Winter mortality in juvenile striped bass has also been studied because losses in winter are hypothesized to be high during this time as a result of low water temperatures and limited prey; these conditions can increase stress and lead to death (Hurst & Conover 2003; Martino & Houde 2012). Therefore, I expected to observe lower mortality rates in my study because the juvenile striped bass I examined were collected in July (summer). However, the instantaneous daily mortality rates in my study are particularly high in comparison to those reported in studies of larval (Secor & Houde 1995), early-juvenile (Secor *et al.* 1995), and late-juvenile (winter; Hurst & Conover 2003) striped bass, providing further evidence that my estimates represent an apparent mortality.

Hatch-date distributions and relative abundance of juvenile striped bass

Attributes of the hatch-date distributions of fishes, such as longer hatch durations influence the likelihood that some portion of the young fish will encounter favorable conditions for growth and survival (Bogner *et al.* 2016). In my study, attributes of the hatch-date distribution were not associated with relative abundance of juvenile striped bass. However, truncated hatch duration was associated with a marginally significant Spearman's correlation value of 0.30 ($p = 0.095$), suggesting that truncated hatch duration may be a useful attribute to characterize a year class of juvenile striped bass. Observed truncated hatch durations were relatively long, ranging over two to three months, which is consistent with a previous study that found that striped bass exhibit protracted spawning behaviors (Secor 2000). Protracted spawning is often associated with recruitment success because such behaviors increase the chances that at least some young fish will encounter favorable environmental conditions for survival. This idea is called the window of opportunity hypothesis, and is an extension of Cushing's match-mismatch hypothesis (Bogner *et al.* 2016). The window of opportunity hypothesis states that, within a given year, and when optimal environmental conditions vary temporally, fish that spawn during a protracted period have a recruitment advantage over those that spawn during a shorter period (Humphries *et al.* 2013). Protracted spawning behaviors likely yield longer hatch durations, which result in greater mean relative abundances of larval yellow perch (*Perca flavescens*) and age-1 bluegill (*Lepomis macrochirus*; Bogner *et al.* 2016), and these relationships were attributed to a long hatch duration buffering against environmental variation in spring for larval yellow perch and environmental

variation in summer for age-1 bluegill. Although I did not observe a significant recruitment advantage from longer truncated hatch durations, perhaps a larger sample size of year classes, particularly those associated with especially strong or weak recruitment strength, would show a stronger relationship between truncated hatch duration and relative recruitment of juvenile striped bass.

Mean hatch dates for striped bass varied annually and occurred earlier in 2017 than they did prior to 1995, when the fishery was declared recovered. Two possibilities exist to explain this observed shift: (1) earlier warming of water temperatures in spring in spawning and nursery areas and (2) a greater abundance of older females in recent times. Water temperatures in the Chesapeake Bay have increased since 1949 (Preston 2004), and this increase is mostly due to higher temperatures during winter and spring (Preston 2004; Najjar *et al.* 2010). Adult striped bass are cued to begin their spawning migration when water temperatures reach about 12⁰C (Uphoff 1989). Temperatures may reach 12⁰C earlier in the spring now than prior to 1995, which could prompt earlier spawning runs, and result in earlier hatch dates. Indeed, the onset of spawning for striped bass in the Hudson River Estuary has shifted earlier since 1950, such that observations of annual egg counts indicate that spawning occurred 6.8 days earlier in 2012 than in 1976 (Nack *et al.* 2019). This change is consistent with the observed shift in hatch dates in my study. On an annual basis, movement of spawners into the Chesapeake Bay is largely influenced by spring water temperatures, and earlier warming results in earlier migrations (Peer & Miller 2014). Further, results of my study showed a correlation between temperature and hatch date, such that fish hatched later in the season experience warmer temperatures during hatching; this is as expected because hatching occurs between late-March and

early-June, as temperatures warm from spring into summer. The model-based relationship between hatch date and temperature is likely a result of the importance of temperature in cueing the spawning migration. As water temperatures increased through time, adult striped bass may have been cued to begin their spawning migration earlier, and thus hatch dates have shifted earlier today (2017) than prior to 1995. A second potential explanation for the observed shift in mean hatch dates is that the abundance of adult striped bass increased after recovery in 1995, and the more stable population included a greater relative abundance of older females (ASMFC 2019). The hatch-date distribution of striped bass may be relatively stable, and the observed shift of hatch dates in this study may partially reflect the contribution resulting from the greater abundance of early-spawning, older females (i.e., 8 years and older) in the post-recovery spawning population.

Daily ages were not available for samples from 32 year classes, so I used daily ages projected from age-length keys developed from otolith-derived ages from three post-recovery year classes from the James and Rappahannock subestuaries of the Chesapeake Bay to reconstruct the age composition of these year classes. As such, the results of my study were influenced by the limited number of samples used to construct age-length keys. For instance, otolith-derived daily ages are associated with aging bias and error. Most aging studies are careful to report aging error, bias, and average percent error (Campana 1991; Campana 1995; Gallagher *et al.* 2018). Common practice is to disregard otoliths with an average percent error greater than 10%, and instead calculate average percent error for the subset of otoliths with low (<10%) average percent error. I did not remove any aged-otoliths from my analysis. Although I did not use these metrics to make

adjustments to otolith-derived ages, I did consider error, bias, and average percent error in model selection and interpretation. More specifically, subestuary was not included in the model that described hatch date as a function of time (period and year class) and temperature (temperature during hatching) because the difference in mean hatch date between the James and Rappahannock subestuaries was two days which fell within the range of my aging bias and error. The difference in mean hatch date between the pre-recovery period and the post-recovery period (about 4 days) is within the range of my ageing error (4 to 8 days) also, but larger than the estimate of ageing bias (about -2 to 2 days), and was therefore used to interpret difference in mean hatch date between the two periods. Further, period was used as a nesting factor in my analysis, so although the difference between the pre-recovery and the post-recovery period falls within the range of aging error, the overall declining trend in mean hatch date from 1986 to 2017 supports the finding that mean hatch dates have shifted earlier today than prior to 1995.

Another source of potential error comes from the limitations of the application of age-length keys to length data. The assumption of an age-length key is that growth rates are similar among the groups of fish for which the key is used (Bettoli & Miranda 2001; Isermann & Knight 2005; Ogle 2016; Ailloud & Hoenig 2019). If growth rates are not similar among groups (e.g., between subestuaries), then the ages projected from the age-length key are not representative of the age structure of the sub-populations. I assessed the need for year- and subestuary-specific keys to curb this potential error, and developed James- and Rappahannock-specific age-length keys. Moreover, when I compared age-length relationships among year classes, there was a marginally significant difference among year classes ($p = 0.09$) suggesting that a year-class-specific age-length key may be

necessary. The marginal significance likely resulted from the low sample size for three of the year classes considered in my study; low sample sizes hamper the ability to detect the actual difference in the age-length relationships among year classes. Note, however, that the otolith-derived ages used to develop these keys were selected from three year classes that represented low, average, and high abundances of juveniles. Using observations from year classes that exhibit varying levels of abundance increased the chance that the sample of juvenile striped bass used to develop the age-length keys was representative of the populations of juvenile striped bass to which the age-length keys were applied. Nevertheless, additional year classes may be necessary to further refine age-length keys for juvenile striped bass.

Cumulative mortality, or the disproportionate mortality experienced by older versus younger juveniles, may have influenced the hatch-date distributions developed in this study. Cumulative mortality differentials between older and younger juveniles can skew hatch-date distributions and result in an apparent increase in the abundance of young fish which is not representative of the population. In this study, the observed hatch-date distribution did not vary from the mortality-adjusted hatch-date distribution, which suggests that the cumulative mortality differential between younger and older juveniles may be small. This likely occurred because I considered fish from the juvenile stage when hatch-date distributions have stabilized. Cumulative mortality differentials between young and old fish may be corrected by multiplying the inverse of the survival rate by the number of fish in each daily cohort (Method 1983; Yoklavich & Bailey 1990). I did not apply such adjustments to hatch-date distributions derived from juvenile striped

bass because these corrections are appropriate only when mortality rates are high, e.g., in larval fish.

The magnitude of climate-change effects varies with latitude along the Atlantic coast, thereby increasing the need to understand environmental effects on the recruitment of striped bass throughout its native range. My study of annual estimates of juvenile mortality rates and hatch-date distributions provides a first look at coarse changes in the population dynamics of juvenile striped bass during three decades. As environmental conditions continue to change, it will be important to understand the relationship between hatch date and growth and survival of individuals within a year class. For example, future studies should investigate mortality rates of cohorts within a single year class to gain a better understanding of the relationship between median hatch dates and relative abundance. A study of sub-cohort mortality and growth rates may provide insight into factors that differentiate juvenile striped bass that survive and those that do not. Moreover, a contemporary study addressing differences among sub-cohort characteristics may be compared with results from studies conducted in the pre-recovery period, namely, Secor & Houde (1995) and McGovern & Olney (1996). I would expect such a comparison to show that the sub-cohorts that contribute most to overall year-class strength today (1996 to 2017) are not the same sub-cohorts that contributed most to overall year-class strength in the earlier studies, or that the sub-cohorts that contribute most to overall year-class strength today exhibit different growth rates than those from the earlier studies.

Although I examined hatch-date distributions and mortality rates of juvenile striped bass across two subestuaries within the Chesapeake Bay, future studies may

consider these recruitment characteristics across larger spatial scales, and throughout the species' native range (Nova Scotia to South Carolina). That is, a study that includes striped bass collected from multiple spawning rivers along its native range (e.g., Hudson and Delaware rivers) may also shed light on factors that affect mortality rates and hatch dates of juvenile striped bass. For example, growth rates of juvenile striped bass are higher in the northern portions of the species' range than in the southern portion (Conover *et al.* 1997), and perhaps hatch-date distributions and mortality rates at the juvenile stage vary along the range, as well. Notably, the effect of temperature during hatching on mean hatch date may vary across a larger spatial scale because temperature varies with latitude, and thus, the relationship between mean hatch date and temperature during hatching may change towards the northern limit of the species range. Differences in recruitment characteristics across the species range may be especially important as environmental conditions change as a result of climate change.

Never before have hatch-date distributions and mortality rates of juvenile striped bass been studied during three decades. The use of a long time series in this study shows that hatch timing can and has shifted earlier, and this information can be used to guide management regulations such as season closures. For example, the recreational striped bass fishery in the Virginia portion of the Chesapeake Bay, which targets adults from 51 to 71 cm (20-28 inches), is closed from 1 April to 15 May to protect spawning females, but my study shows that hatching occurs as early as late-March and as late as late-May to early-June. Noting that spawning and hatching are successive events, the earlier hatch dates of recent year classes imply an earlier presence of adult striped bass in the tidal freshwater regions of these subestuaries. The model-based relationship between

temperature during hatching and mean hatch date further supports the hypothesis that temperature is closely related to spawning and hatching. Recreational season closures have not been adjusted in many years, a practice which may negatively affect production of offspring because harvest of spawners may occur before spawners have an opportunity to reproduce. During cool years in the Chesapeake Bay, spawner movements co-occur with the trophy fishery and spawners may be harvested prior to spawning (Peer & Miller 2014). Alternatively, earlier hatch dates may reflect greater survival of earlier-hatched offspring. Striped bass may continue to hatch earlier as waters continue to warm in the region (Peer & Miller 2014; Nack *et al.* 2019), and as such, management measures that promote age diversity of females will be necessary to maintain longer spawning periods and the resulting longer hatch durations. Although a season closure that encompasses the entire protracted spawning period may be contentious, protection of spawners during the earlier portion of the spawning period (March) may result in the greater contribution of older females to spawning, which could be especially influential because older females produce larger offspring with a higher chance of survival (Zastrow *et al.* 1989).

Conclusions and recommendations

Studies of population attributes of juvenile striped bass will be necessary into the future because water temperatures, which are closely associated with hatch timing, are projected to increase in the Chesapeake Bay (Najjar *et al.* 2010). It will be important to understand how hatch timing continues to shift in response to those temperature changes, and the effect of shifts in hatch timing on mortality of early life stages of striped bass. In my study, instantaneous daily mortality rates were estimated during the juvenile stage

and were relatively constant regardless of the hatch-date distribution of a particular year class; future studies should measure mortality rates during the larval stage because mortality is especially high, has not yet stabilized and may show annual variation. Annual variability in larval daily mortality rates could be used to investigate the effects of hatch timing on survival of young striped bass, and thus elucidate the influence of hatch timing on overall recruitment. It will also be important to understand the relationship between hatch-date distributions and spawner demography because such an understanding could result in more targeted management measures. For example, if hatch duration is driven by age diversity, managers could consider altering size limits or the timing of the trophy fishery to protect older females. However, future studies should aim to age females as they move into the Chesapeake Bay to spawn, and compare those age distributions to hatch-date distributions of juveniles. This process would not only provide a direct relationship between the age distribution of spawners and the resulting hatch-date distribution, but would also provide an indication of the effect of female age on survival of the juvenile stage because only those fish that survive to the juvenile stage will be included in the assessment. A complete understanding of recruitment is unattainable, but investigating the causes and effects of shifting hatch dates for striped bass could allow fisheries managers to make predictions regarding future populations of striped bass, and thus ensure sustainable management of the fishery.

LITERATURE CITED

- Ailloud LE, Hoenig JM. 2019. A general theory of age-length keys: combining the forward and inverse keys to estimate age composition from incomplete data. *ICES J. Mar. Sci.* fxz072
- Akimova A, Hufnagl M, Kreuz M, Peck MA. 2016. Modeling the effects of temperature on the survival and growth of North Sea cod (*Gadus morhua*) through the first year of life. *Fish. Oceanogr.* 25: 193-209
- Aldanondo N, Cotano U, Goikoetxea N, Boyra G, Ibaibarriaga L, Irigoien X. 2016. Interannual differences in growth and hatch-date distributions of early juvenile European anchovy in the Bay of Biscay: implications for recruitment. *Fish Oceanogr.* 25(2): 147-163
- Atlantic State Marine Fisheries Commission (ASMFC). 2016. Atlantic striped bass stock assessment update. ASMFC, Arlington, Virginia
- Atlantic State Marine Fisheries Commission (ASMFC). 2013. Atlantic striped bass benchmark stock assessment. ASMFC, Arlington, VA
- Atlantic States Marine Fisheries Commission (ASMFC). 2019. Summary of the 2019 benchmark stock assessment of Atlantic striped bass. ASMFC, Arlington, Virginia
- Bettoli PW, Miranda LE. 2001. A cautionary note about estimating mean length at age with subsampled data. *N. Am. J. Fish. Manage.* 21: 425-428
- Bogner DM, Kaemingk MA, Wuellner MR. 2016. Consequences of hatch phenology on stages of fish recruitment. *Plos One.* 11: e0164980

- Booth D, Alquezar R. 2002. Food supplementation increases larval growth, condition and survival of *Acanthochromis polyacanthus*. *J. Fish. Biol.* 60: 1126-1133
- Bradley CE, RiceJa, Aday DD, Hightower JE, Rock J, Lincoln KL. 2018. Juvenile and adult striped bass mortality and distribution in an unrecovered coastal population. *N. Am. J. Fish. Manage.* 38: 104-119
- Burnham KP, Anderson DR. 2004. Multimodel inference: understanding AIC and BIC in model selection. *Sociol. Method. Res.* 33: 261-304
- Campana SE, Annand MC, McMillan JI. 1995. Graphical and statistical methods for determining the consistency of age determinations. *T. Am. Fish. Soc.* 124: 131-138
- Campana SE. 2001. Accuracy, precision and quality control in age determinations, including a review of the use and abuse of age validation methods. *J. Fish Biol.* 59: 197-242
- Campana SE, Thorrold SR. 2001. Otoliths, increments, and elements: keys to a comprehensive understanding of fish populations? *Can. J. Fish. Aquat. Sci.* 58: 30-38
- Chimura M, Watanabe Y, Okouchi H, Shirafuji N, Kawamura T. 2009. Hatch-period-dependent early growth and survival of Pacific herring *Clupea pallasii* in Miyako Bay, Japan. *J. Fish Biol.* 74: 604-620
- Conover DO, Brown JJ, Ehtisham A. 1997. Countergradient variation in growth of young striped bass (*Morone saxatilis*) from different latitudes. *Can. J. Fish. Aquat. Sci.* 54: 2401-2409

- Cox DK, Coutant CC. 1981. Growth dynamics of juvenile striped bass as functions of temperature and ration. *T. Am. Fish. Soc.* 110: 226-238
- Cushing DH. 1990. Plankton production and year-class strength in fish populations – an update of the match mismatch hypothesis. *Adv. Mar. Biol.* 26: 249-293
- Ding H, Elmore AJ. 2015. Spatio-temporal patterns in water surface temperature from Landsat time series data in the Chesapeake Bay, USA. *Remote Sens. Environ.* 168: 335-348
- Douglas SG. 1995. Validation of daily increment formation on otoliths with applications to wild striped bass (*Morone saxatilis*) at the northern limit of its range. MS Thesis. Acadia University, Nova Scotia.
- Fogarty MJ, Myers RA, Bowen KG. 2001. Recruitment of cod and haddock in the North Atlantic: a comparative analysis. *ICES J. Mar. Sci.* 58: 952-961
- Fonds M, Cronie R, Vethaak AD, Van der Puyl P. 1992. Metabolism, food consumption, and growth of plaice (*Pleuronectes platessa*) and flounder (*Platichthys flesus*) in relation to fish size and temperature. *Neth. J. Sea Res.* 29: 127-143
- Franz DR, Tanacredi JT. 1992. Secondary production of the amphipod *Amplisca abdita* Mills and its importance in the diet of juvenile winter flounder (*Pleuronectes americanus*) in Jamaica Bay, New York. *Estuaries.* 15: 193-203
- Fraser GS, Bestgen KR, Winkelman DL, Thompson KG. 2019. Temperature – not flow – predict native fish reproduction with implications for climate change. *T. Am. Fish. Soc.* 148: 509-527
- Gallagher BK, Fabrizio MC, Tuckey TD. 2017. Estimation of juvenile striped bass relative abundance in the Virginia portion of the Chesapeake Bay. Annual

Progress Report: 2017-2018. Virginia Institute of Marine Science, William & Mary.

Gallagher BK, Fabrizio MC, Tuckey TD. 2019. Estimation of juvenile striped bass relative abundance in the Virginia portion of the Chesapeake Bay. Annual Progress Report: 2018-2019. Virginia Institute of Marine Science, William & Mary.

Gallagher BK, Piccoli PM, Secor DH. 2018. Ecological carryover effects associated with partial migration in white perch (*Morone Americana*) within the Hudson River Estuary. *Estuar. Coast. Mar. Sci.* 200: 277-288

Gauthier TD. 2001. Detecting trends using Spearman's rank correlation coefficient. *Environ. Forensics.* 2: 359-362

Gerritsen HD, McGrath D, Lordan C. 2006. A simple method for comparing age-length keys reveals significant regional differences within a single stock of haddock (*Melanogrammus aeglefinus*). *ICES. J. Mar. Sci.* 63: 1096-1100

Houde ED. 1989. Comparative growth, mortality, and energetic of marine fish larvae: temperature and implied latitudinal effects. *Fish B-NOAA.* 87: 471-495

Houde ED, Morin LG. 1990. Temperature effects on otolith daily increment deposition in striped bass and white perch larvae. pp 57-91. Egg production and larval dynamics of striped bass and white perch in the Potomac River and Upper Chesapeake Bay. Volume II. Report to the Maryland Department of Natural Resources. Contract No. F145-88-008. University of Maryland, Center for Environmental and Estuarine Studies, Solomons, Maryland

- Humphries P, Richardson A, Wilson G, Ellison T. 2013. River regulation and recruitment in a procatod-spawning riverine fish. *Ecol. Appl.* 23: 208-225
- Hurst TP, Conover DO. 2003. Seasonal and interannual variation in the allometry of energy allocation in juvenile striped bass. *Ecology.* 84: 3360-3369
- Hurvich CM, Tsai C-L. 1989. Regression and time series model selection in small samples. *Biometrika.* 76: 297-307
- Isermann DA, Knight CT. 2005. A computer program for age-length keys incorporating age assignment to individual fish. *N. Am. J. Fish. Manage.* 25: 1153-1160
- Jennings S, Kaiser MJ, Reynolds JD. 2001. Marine Fisheries Ecology. Blackwell Publishing company, Oxford, UK
- Jones C, Brother EB. 1987. Validation of the otolith increment aging technique for striped bass, *Morone saxatilis*, larvae reared under suboptimal feeding conditions. *Fish B-NOAA.* 85: 171-178
- Kimmerer WJ, Cowan JH, Miller LW, Rose KA. 2000. Analysis of an estuarine striped bass (*Morone saxatilis*) population: influence of density-dependent mortality between metamorphosis and recruitment. *Can. J. Fish. Aquat. Sci.* 57: 478-486
- Kline L. 1990. Population dynamics of young-of-the-year striped bass, *Morone saxatilis*, populations, based on daily increments. PhD Dissertation. William & Mary, Virginia
- Lapolla A, Buckley LJ. 2005. Hatch date distributions of young-of-year haddock *Melanogrammus aeglefinus* in the Gulf of Maine/Georges Bank region: implications for recruitment. *Mar. Ecol. Prog. Ser.* 290: 239-249

- Lloret J, Shulman G, Love RM. 2014. Condition and health indicators of exploited marine fishes. John Wiley, Chichester, UK
- Logan DT. 1985. Environmental variation and striped bass population dynamics: A size dependent mortality model. *Estuaries*. 8: 28-38
- Lorenzen K, Camp, EV. 2019. Density-dependence in the life history of fishes: When is a fish recruited? *Fish. Res.* 217: 5-10
- Lozano C, Houde ED, Wingate RL, Secor DH. 2012. Age, growth, and hatch dates of ingressing larvae and surviving juveniles of Atlantic menhaden *Brevoortia tyrannus*. *J Fish Biol.* 8: 1665-1685
- Martino EM, Houde ED. 2010. Recruitment of striped bass in Chesapeake Bay: spatial and temporal environmental variability and availability of zooplankton prey. *Mar. Ecol. Prog. Ser.* 409: 213-228
- McGovern JC, Olney JE. 1996. Factors affecting survival of early life stages and subsequent recruitment of striped bass on the Pamunkey River, Virginia. *Can J Fish Aquat Sci.* 53: 1713-1726
- Methot RD. 1983. Seasonal variation in survival of larval northern anchovy, *Engraulis mordax*, estimated from the age distribution of juveniles. *Fish. Bull.* 81: 741-750
- Miranda LE, Bettoli PW. 2007. Mortality. *Analysis and interpretation of freshwater fisheries data*. American Fisheries Society, Bethesda, Maryland, 229-277
- Nack CC, Swaney DP, Limburg KE. 2019. Historical and projected changes in spawning phenologies of American shad and striped bass in the Hudson River Estuary. *Mar. Coast. Fish.* 11 271-284

- Najjar RG, Pyke CR, Adams MB, Breitburg D, Hershner C, Kemp M, Howarth R, Muholland MR, Paolisso M, Secor D, Sellner K, Wardrop D, Wood R. 2010. Potential climate-change impacts on the Chesapeake Bay. *Estuar Coast. Shelf S.* 86: 1-20
- North EW, Houde ED. 2001. Retention of white perch and striped bass larvae: Biological-physical interactions in Chesapeake Bay estuarine turbidity maximum. *Estuaries.* 24: 756-769
- North EW, Houde ED. 2003. Linking ETM physics, zooplankton prey, and fish early-life histories to striped bass *Morone saxatilis* and white perch *M. americana* recruitment. *Mar. Ecol. Prog. Ser.* 260: 219-236
- Ogle DH. 2016. Introductory fisheries analysis with R. Boca Raton, FL-CRC Press.
- Pope KL, Kruse CG. 2007. Condition. *In* Analysis and interpretation of freshwater fisheries data. *Edited by* CS Guy and ML Brown. *American Fisheries Society, Bethesda, Maryland,* 423-471
- Peer AC, Miller TJ. 2014. Climate change, migration phenology, and fisheries management interact with unanticipated consequences. *N. Am. J. Fish. Manage.* 34: 94-110
- Preston BL. 2004. Observed winter warming of the Chesapeake Bay estuary (1949-2002): implications for ecosystem management. *Environ. Manage.* 34: 125-139
- Purtlebaugh CH, Allen MS. 2010. Relative abundance, growth, and mortality of five age-0 estuarine fishes in relation to discharge of the Suwannee River, Florida. *T. Am. Fish. Soc.* 139: 1233-1246

- Quinn GP, Keough MJ. 2002. Experimental design and data analysis for biologists.
Cambridge University Press, Cambridge, UK
- R Core Team. 2019. R: A language and environment for statistical computing. R
foundation for statistical computing, Vienna, Austria
- Rice KC, Jastram JD. 2015. Rising air and stream-water temperatures in Chesapeake Bay
region, USA. *Climatic Change*. 128: 127-138
- Richards RA, Rago PJ. 1999. A case history of effective fishery management:
Chesapeake Bay striped bass. *N. Am. J. Fish. Manage.* 19: 356-375
- Rindorf A, Lewy P. 2001. Analysis of length and age distributions using continuation-
ratio logits. *Can. J. Fish. Aquat. Sci.* 58: 1141-1152
- Rutherford ES, Houde ED, Nyman RM. 1997. Relationship of larval-stage growth and
mortality to recruitment of striped bass, *Morone saxatilis*, in Chesapeake Bay.
Estuaries. 20: 174-198
- Secor DH, Dean JM. 1989. Somatic growth effects on the otolith-fish size relationship in
young pond-reared striped bass, *Morone saxatilis* (Walbaum). *Can. J. Fish.*
Aquat. Sci. 46: 113-121
- Secor DH, Dean JM, Laban EH. 1991. Manual for otolith removal and preparation for
microstructure examination. Belle W. Baruch Institute for Marine Biology and
Coastal Research, University of South Carolina, Columbia, South Carolina.
- Secor DH, Houde ED. 1995. Temperature effects on the timing of striped bass egg
production, larval viability, and recruitment potential in the Patuxent River
(Chesapeake Bay). *Estuaries*. 18: 527-544

- Secor DH, Houde ED, Monteleone DM. 1995. A mark-release experiment on larval striped bass *Morone saxatilis* in a Chesapeake Bay tributary. *ICES J. Mar. Sci.* 52: 87-101.
- Secor DH. 2000. Spawning in the nick of time? Effect of adult demographics on spawning behaviour and recruitment in Chesapeake Bay striped bass. *ICES J. Mar. Sci.* 57: 403-411
- Shelton AO, Mangel M. 2011. Fluctuations in fish populations and the magnifying effects of fishing. *PNAS.* 108: 7075-7080
- Shepherd JG, Cushing DH. 1980. A mechanism for density dependent survival of larval fish as the basis for a stock-recruitment relationship. *J Conseil.* 29: 160-167
- Sswat M, Stiasny MH, Jutfelt F, Riebessell U, Clemmesen C. 2018. Growth performance and survival of larval Atlantic herring, under the combined effects of elevated temperatures and CO₂. *Plos One.* 13: e019147
- Szuwalski CS, Vert-Pre KA, Punt AE, Branch TA, Hilborn R. 2015. Examining common assumptions about recruitment: a meta-analysis of recruitment dynamics for worldwide marine fisheries. *Fish Fish.* 16: 633-648
- Uphoff Jr. JH. 1989. Environmental effects on survival of eggs, larvae, and juveniles of striped bass in the Choptank River, Maryland. *T Am Fish Soc.* 118: 251-263
- Van Beveren E, Klein M, Serrao EA, Goncalves EJ, Borges R. 2016. Early life history of larvae and early juvenile Atlantic horse mackerel *Trachurus trachurus* off the Portuguese west coast. *Fish. Res.* 183: 111-118

- Vine JR, Holbrook SC, Post WC, Peoples BK. 2019. Identifying environmental cues for Atlantic sturgeon and shortnose sturgeon spawning migrations in the Savannah River. *T. Am. Fish. Soc.* 148: 671-681
- Wagena MB, Collick AS, Ross AC, Najjar RG, Rau B, Sommerlot AR, Fuka DR, Kleinman PJA, Easton ZM. 2018. Impact of climate change and climate anomalies on hydrologic and biogeochemical processes in an agricultural catchment of the Chesapeake Bay watershed, USA. *Sci. Total. Environ.* 637-368: 1443-1454
- Yoklavich MM, Bailey KM. 1990. Hatching period, growth and survival of young walleye Pollock *Theragra chalcogramma* as determined from otolith analysis. *Mar. Ecol. Prog. Ser.* 64: 13-23
- Zastrow CE, Houde ED, Saunders EH. 1989. Quality of striped bass *Morone saxatilis* eggs in relation to river resources and female weight. *J Conseil.* 191: 34-42

Table 1. Attributes of the hatch-date distribution of 32 year classes of juvenile striped bass in the James and Rappahannock subestuaries of the Chesapeake Bay. Hatch-date distributions were developed from daily ages that were estimated using subestuary-specific age-length keys. Truncated hatch duration was calculated by removing the earliest and latest 1% of hatch dates, and rounded to the nearest day. Unless otherwise noted, all attributes were calculated using calendar days.

Year class	Earliest hatch date	Latest hatch date	Median hatch date	Peak hatch date	Mean hatch date	Hatch duration (days)	Truncated hatch duration (days)
1986	95	134	119	117	119.9	39	29
1987	99	149	124	125	123.5	50	47
1988	115	139	124.5	137	125.7	24	24
1989	106	147	129.5	129	129.9	41	35
1990	105	153	131	132	130.6	48	29
1991	101	148	126	134	126.0	47	45
1992	92	153	128	125	128.2	61	48
1993	89	155	124	136	122.9	66	52
1994	87	149	122	127	121.7	62	51
1995	103	153	123.5	111	123.3	50	38
1996	86	154	117	109	117.0	68	59
1997	94	151	119.5	124	119.0	57	46
1998	78	152	124	129	123.5	74	47
1999	97	148	126	128	124.4	51	45
2000	99	157	128	127	129.4	58	42
2001	89	151	120	123	120.6	62	50
2002	87	145	123	128	122.2	58	48
2003	84	154	128	134	127.6	70	52
2004	90	153	119	110	118.7	63	51
2005	91	145	119	109	118.1	54	48
2006	98	148	127	125	127.1	50	43
2007	83	151	122	123	121.5	68	53
2008	88	154	123	126	122.8	66	54
2009	94	151	124	124	122.9	57	43
2010	93	156	125	129	124.8	63	43
2011	103	157	129.5	127	129.3	54	47
2012	89	144	112.5	113	112.7	55	49

2013	92	158	119.5	116	120.4	66	45
2014	91	160	123	118	122.7	69	41
2015	98	145	126	131	124.5	47	47
2016	96	144	121	120	123.0	48	42
2017	94	148	119	124	120.1	54	48

Table 2. Paired *t*-test statistics comparing mean otolith increment counts of each of the six pairs of reading combinations for striped bass otoliths. Each reading included increment counts from 40 striped bass otoliths subsampled across three year classes (2011, 2016, and 2017) within the James and Rappahannock subestuaries. Pairs exhibiting significant differences ($p < 0.05$) are highlighted with bold text.

Reading combination	t	p-value
1 & 2	1.66	0.11
1 & 3	-0.14	0.89
1 & 4	-0.18	0.86
2 & 3	-2.61	0.01
2 & 4	-2.00	0.05
3 & 4	-0.10	0.92

Table 3. Estimated instantaneous daily mortality rates for the month of July and their 95% confidence intervals (CI) for 32 year classes (1986-2017) of juvenile striped bass from the James and Rappahannock subestuaries of the Chesapeake Bay. For ease of interpretation, discrete mortality rate, or the proportion of the population that is lost through mortality, was calculated with $1 - e^{-Z}$ and the monthly Z (for July) was calculated using daily Z estimates.

Year class	Daily			Monthly	
	instantaneous mortality rate (day ⁻¹)	Lower 95% CI (day ⁻¹)	Upper 95% CI (day ⁻¹)	instantaneous mortality rate (month ⁻¹ , for July)	Discrete daily mortality rate (% day ⁻¹)
1986	0.157	0.073	0.242	4.87	0.146
1987	0.100	0.037	0.164	3.10	0.095
1988	0.084	0.028	0.140	2.60	0.081
1989	0.130	0.019	0.240	4.03	0.122
1990	0.143	0.006	0.281	4.43	0.134
1991	0.166	0.046	0.286	5.15	0.153
1992	0.115	0.061	0.168	3.57	0.109
1993	0.137	0.089	0.186	4.25	0.128
1994	0.168	0.094	0.241	5.21	0.155
1995	0.218	0.150	0.287	6.76	0.196
1996	0.118	0.079	0.158	3.66	0.111
1997	0.168	0.086	0.250	5.21	0.155
1998	0.156	0.101	0.212	4.84	0.145
1999	0.123	0.042	0.204	3.81	0.116
2000	0.127	0.080	0.173	3.94	0.119
2001	0.171	0.125	0.218	5.30	0.157
2002	0.141	0.084	0.199	4.37	0.132
2003	0.155	0.106	0.205	4.81	0.144
2004	0.165	0.118	0.213	5.12	0.152
2005	0.155	0.081	0.230	4.81	0.144
2006	0.139	0.068	0.209	4.31	0.129
2007	0.158	0.108	0.208	4.89	0.146
2008	0.164	0.103	0.225	5.08	0.151
2009	0.195	0.126	0.264	6.05	0.177
2010	0.210	0.150	0.270	6.51	0.189
2011	0.177	0.127	0.227	5.49	0.162
2012	0.061	0.000	0.151	1.89	0.060

2013	0.130	0.046	0.213	4.03	0.122
2014	0.124	0.087	0.160	3.84	0.116
2015	0.125	0.084	0.167	3.88	0.118
2016	0.185	0.129	0.241	5.74	0.169
2017	0.131	0.073	0.190	4.06	0.123

Table 4. Spearman’s rank correlation (ρ) which measured the relationship between rankings of the attributes of the hatch-date distributions and rankings of the relative abundance of juvenile striped bass from 32 year classes in the James and Rappahannock subestuaries of the Chesapeake Bay. There were no significant correlations between attributes and relative abundance.

Attribute of the hatch-date distribution	ρ	S-statistic	p-value
Truncated hatch duration	0.30	3818	0.095
Median hatch date	-0.03	5601	0.886
Peak hatch date	0.15	4637	0.412
First hatch date	-0.03	5628	0.864
Last hatch date	0.22	4242	0.221

Figure 1. VIMS seine survey sites from which 32 year classes of juvenile striped bass (1986-2017) were sampled from the James and Rappahannock subestuaries of the Chesapeake Bay.

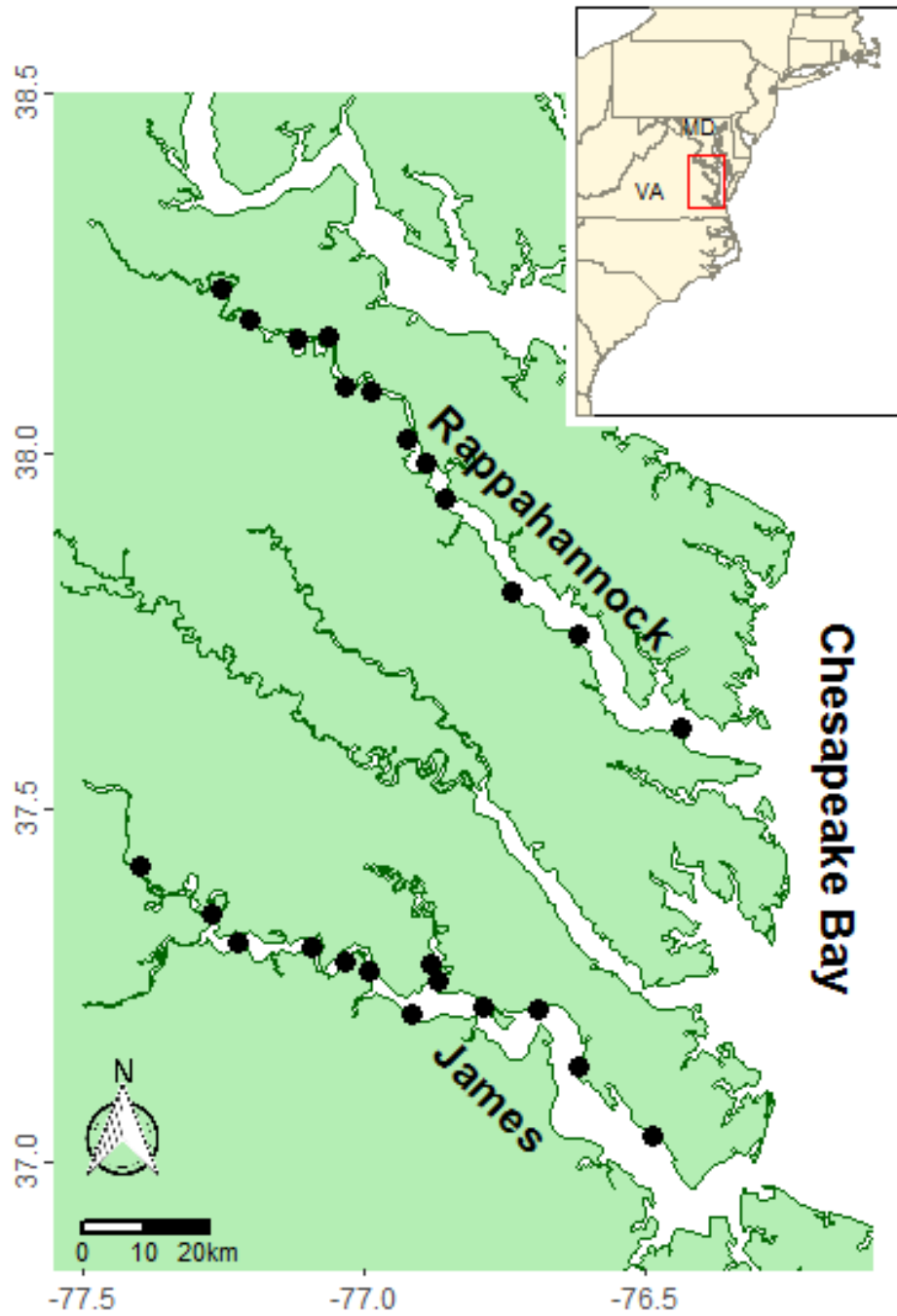


Figure 2. Temperature stations monitored by the Chesapeake Bay Program in tidal fresh (TF) regions of the James and Rappahannock subestuaries. Daily temperature values were linearly-interpolated from approximately biweekly monitoring data collected at each site, and were used to estimate mean temperature during hatch and during the yolk-sac larval stage.

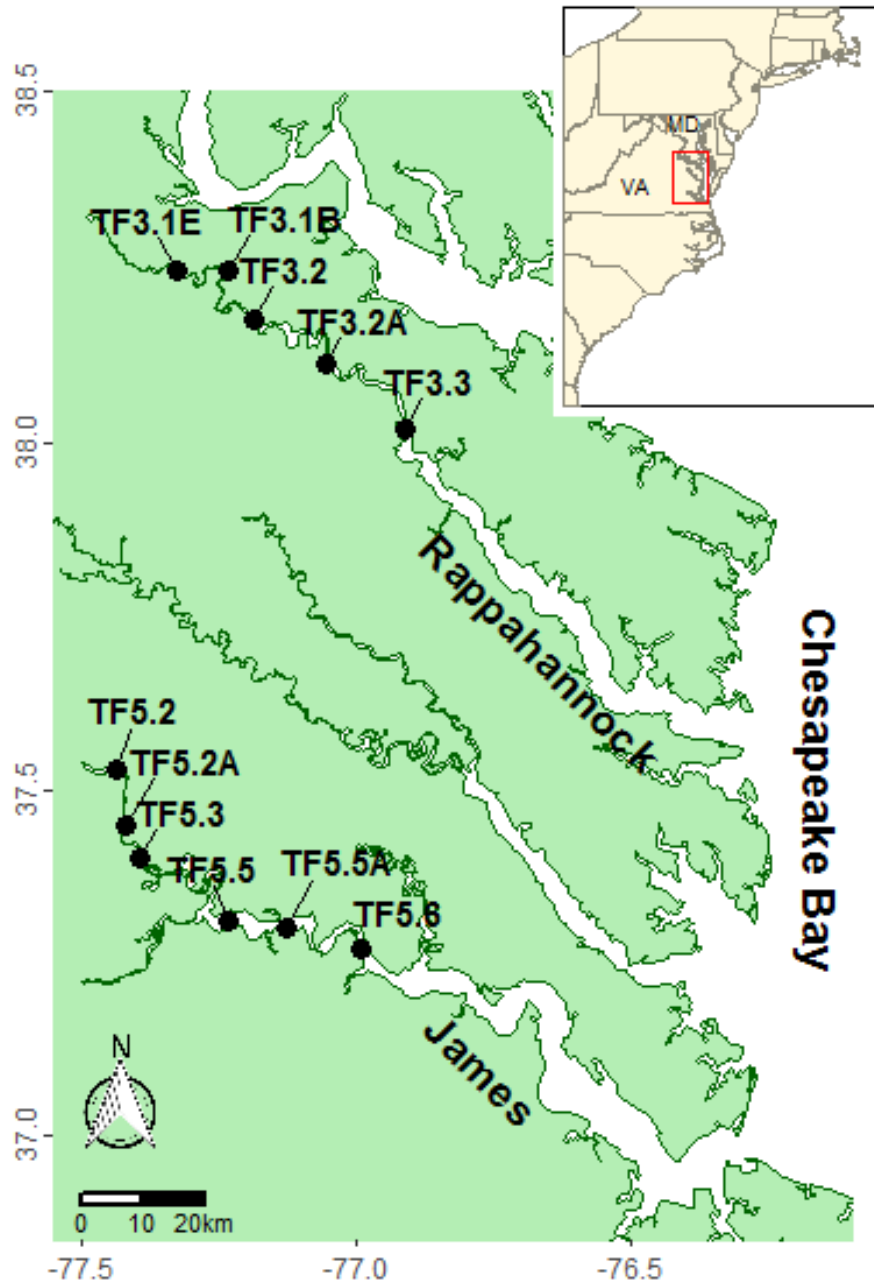


Figure 3. Estimated daily instantaneous total mortality rate (Z , day^{-1}) of juvenile striped bass in July from 1986 to 2017 in the James and Rappahannock subestuaries of the Chesapeake Bay. Gray bars represent 95% confidence intervals. The lower confidence interval for the 2012 year class was negative, and thus truncated at zero.

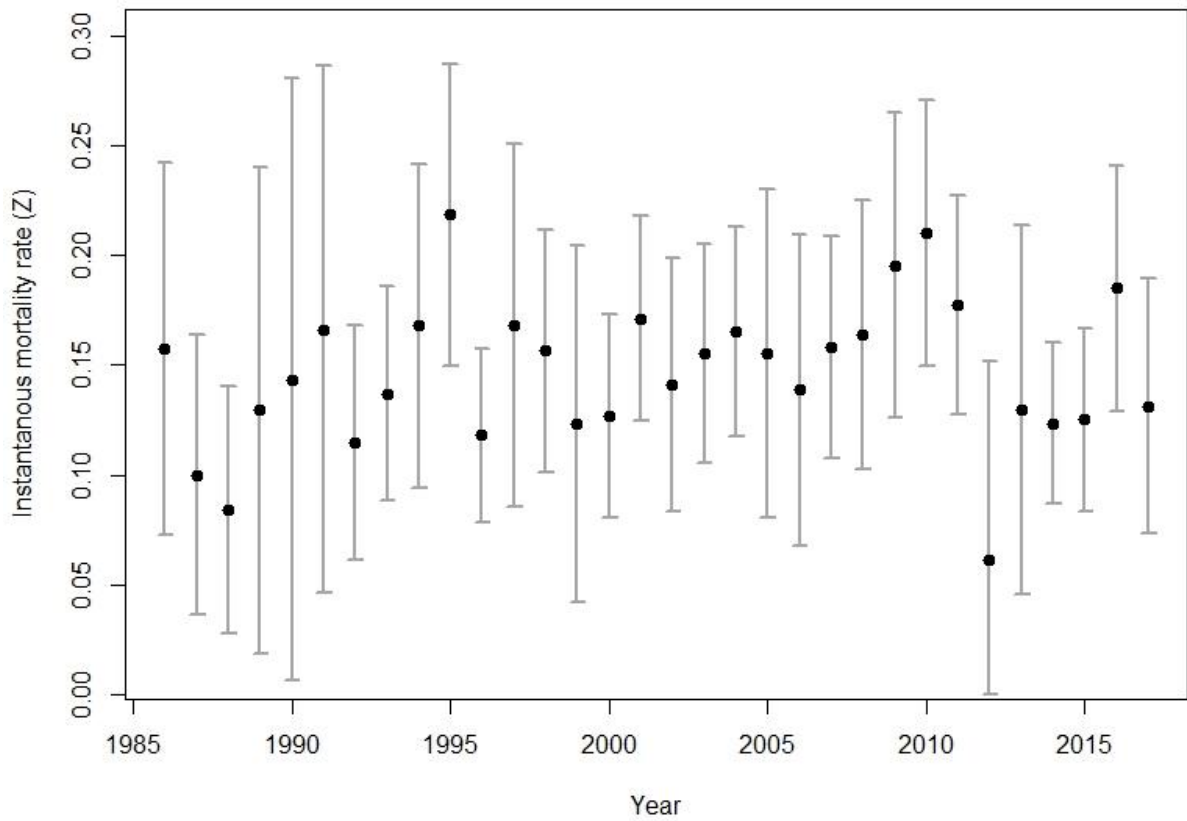


Figure 4. The abundance (A) and percent of the total population (B) of juvenile striped bass within a 15-day cohort assuming no differential mortality between older and younger cohorts (black line) and assuming a loss of 1% per day (gray line; Secor *et al.* 1995). A greater proportional abundance of older cohorts of juvenile striped bass is expected in the mortality-adjusted distribution (gray line) than in the non-adjustment distribution (black line) if the differential mortality between older and younger cohorts is high.

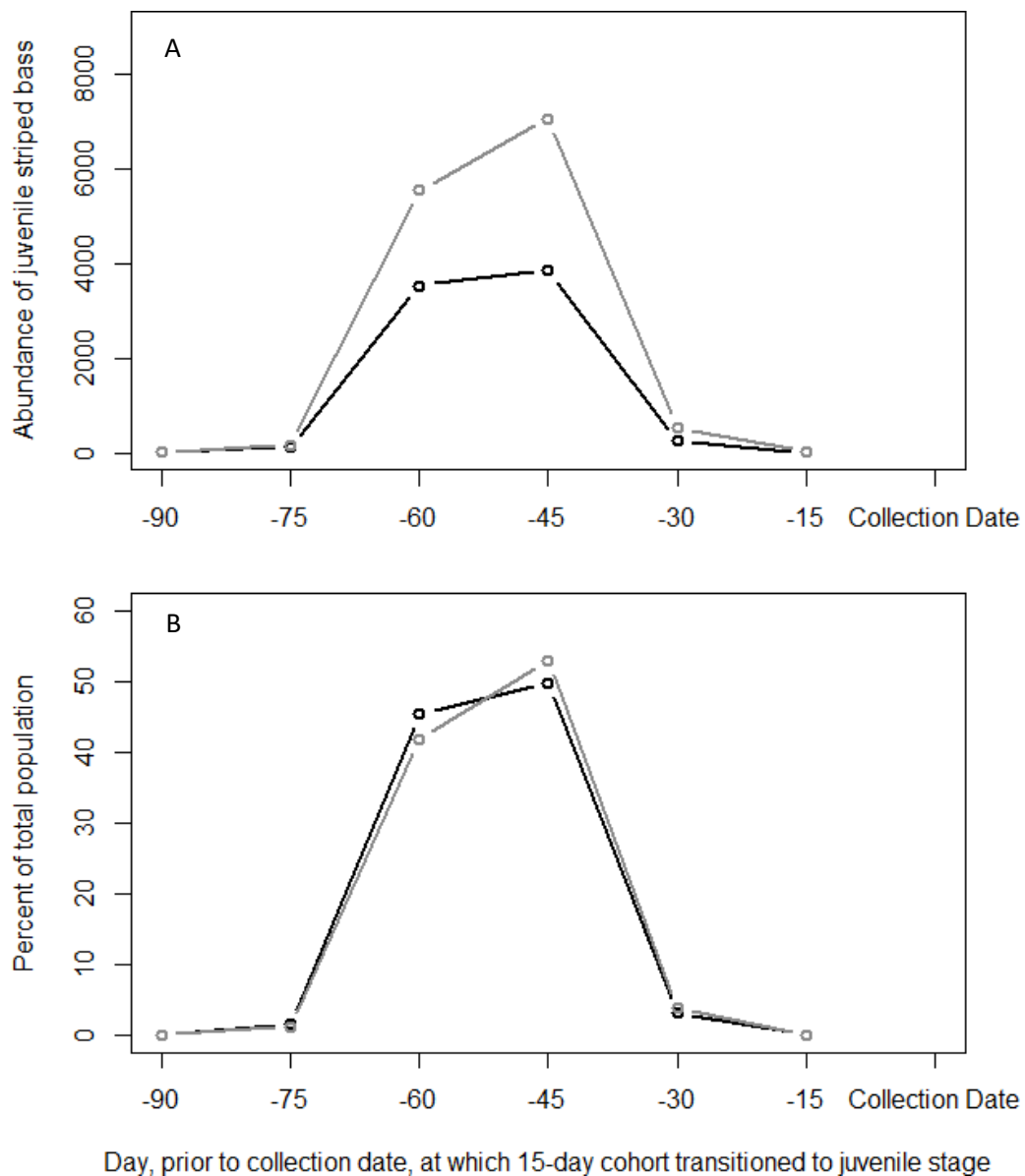


Figure 5. Hatch-date distribution of juvenile striped bass from the James and Rappahannock subestuaries of the Chesapeake Bay. Hatch dates range between calendar days 78 and 169 and represent fish sampled from 1986 to 2017. The mean hatch date was 123.00 (SE = 0.14), which is May 3rd.

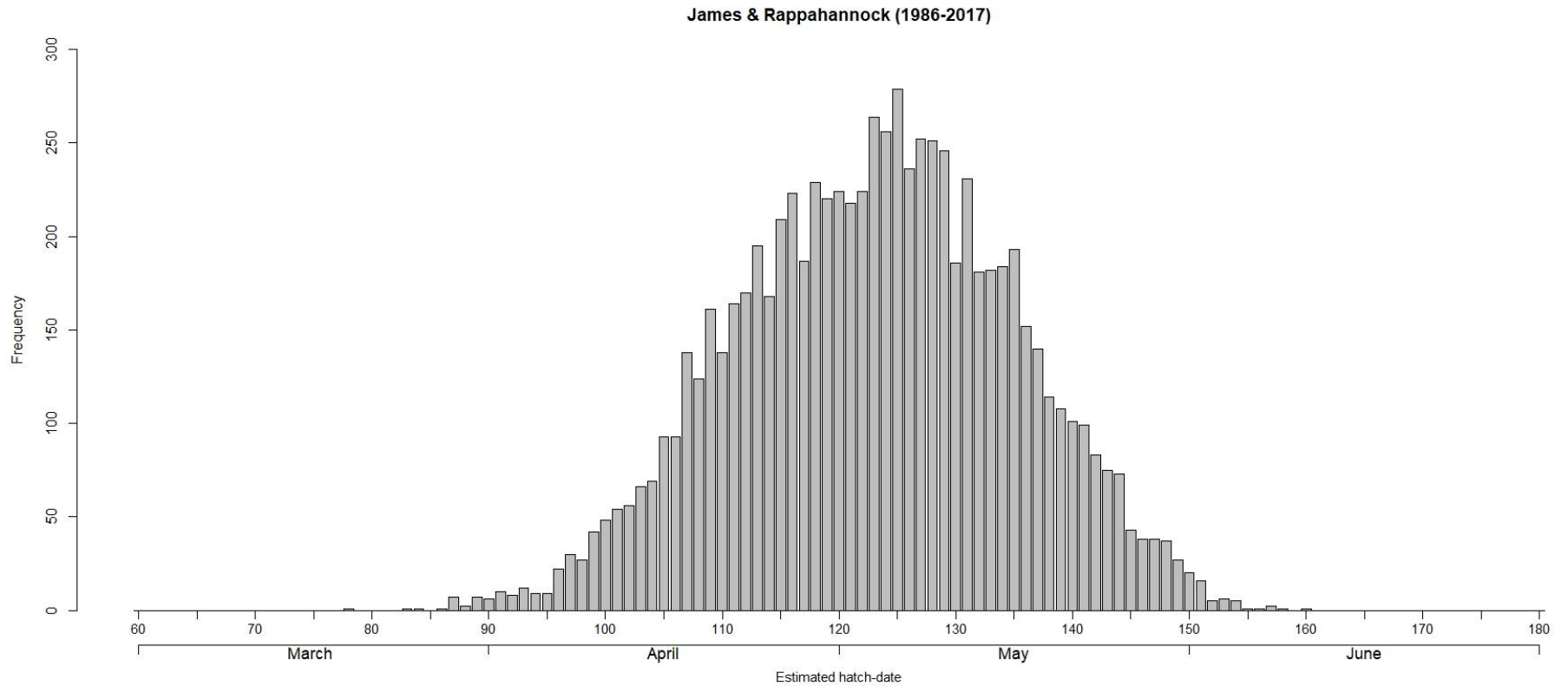
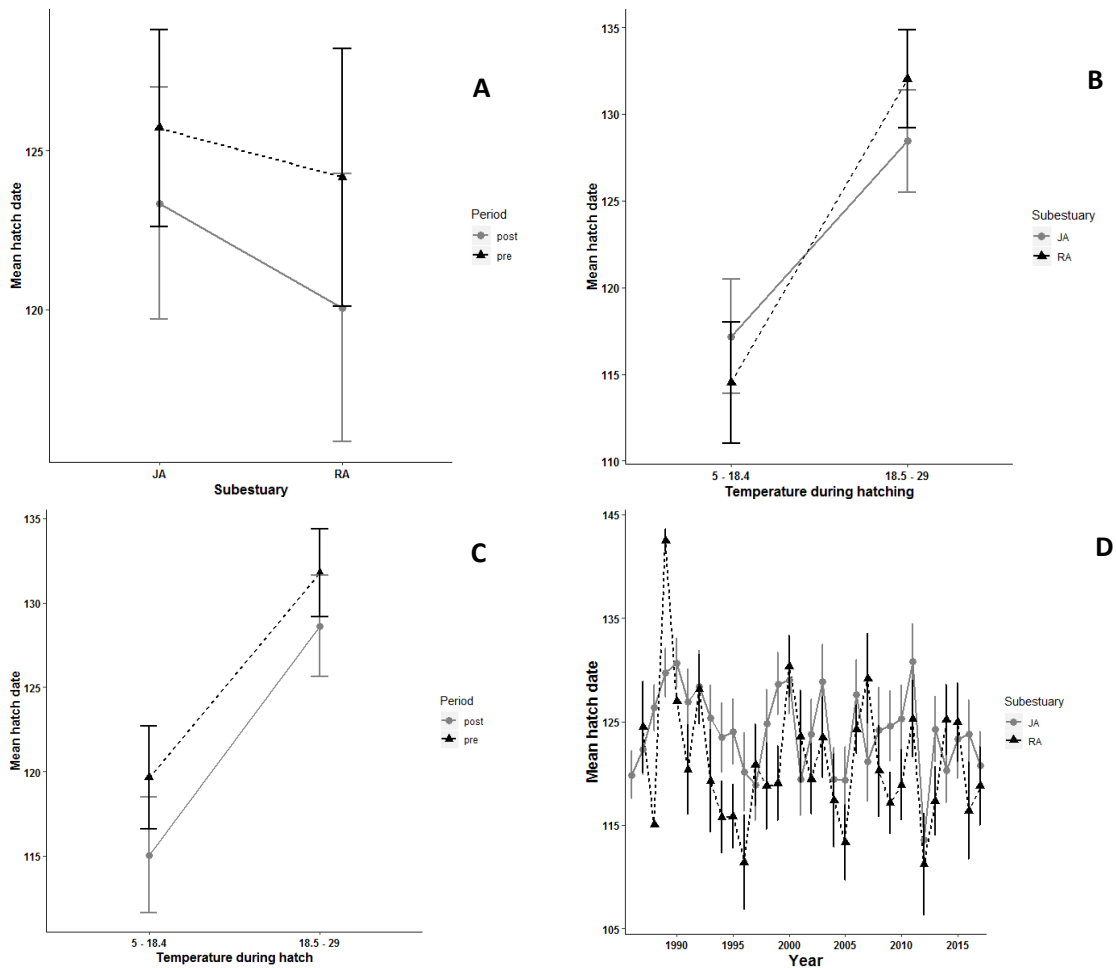
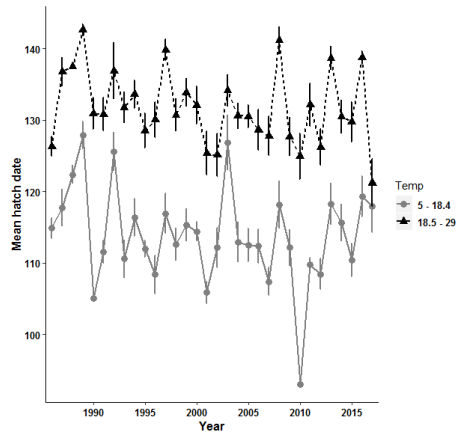


Figure 6. Interaction plots for subestuary, period, year, and temperature during hatch for 32 year classes (1986-2017) of juvenile striped bass in the James (JA) and Rappahannock (RA) subestuary of the Chesapeake Bay. There were no notable interactions between subestuary and period (A), temperature during hatch and period (C), year class and subestuary (D), or year and temperature during hatch (E). Panel B suggests a possible interaction between subestuary and temperature during hatching because the lines for the James (JA; black) and Rappahannock (RA; gray) subestuaries intersect; however, the 95% confidence intervals for low (5.0 - 18.4 °C, N = 3707) and high (18.5 - 29.0 °C, N = 4086) temperature bins overlap, which suggests that the interaction observed may not be strong. The threshold for the temperature bins was based on the observed mean (18.5°C).





E

Figure 7. Diagnostic plots from the analysis of covariance where hatch date of 32 year classes of juvenile striped bass within the James and Rappahannock subestuaries of the Chesapeake Bay was a function of period (pre- or post-), year nested within period (pre: 1986-1994; post: 1995-2017), and temperature during hatching was a covariate. The histogram of residuals (A) and Q-Q plot (B) show that the model meets the assumption of normality. For the most part, the values in the fitted versus residuals plot are evenly distributed around zero, and the assumption of homogeneity of variance appears reasonable. To further explore this assumption, box and whisker plots that group hatch dates by year class (E), period (F), and temperature during hatching (G) were used to compare variance among groups. Most year classes exhibited similar variances ranging from 110 to 163, and only four year classes exhibited variance values less than 110 ($\sigma_{1986}^2 = 51.7$, $\sigma_{1988}^2 = 53.7$, $\sigma_{1989}^2 = 56.9$, $\sigma_{1990}^2 = 55.0$). However, year class is nested within period in this model, and variance was similar among the pre- and post- recovery periods ($\sigma_{pre-recovery}^2 = 118$, $\sigma_{post-recovery}^2 = 148$). Temperature during hatching was grouped into low (5.0-18.4 °C, N = 3707) and high (18.5-29.0 °C, N = 4086) temperature groups, and variance appeared similar across the two temperature groups ($\sigma_{low}^2 = 115$, $\sigma_{high}^2 = 88.0$). Considering the similar variances among groups and the normal distribution of the residuals, I concluded that the assumption of homogeneity of variance was reasonably met. The predicted versus observed plot (D) shows an even distribution around the one-to-one line, indicating that this model can be used to make predictions about mean hatch dates.

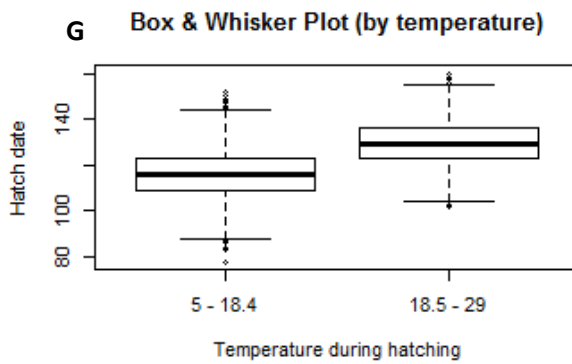
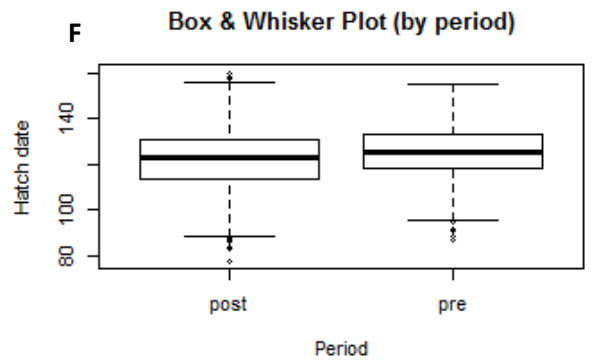
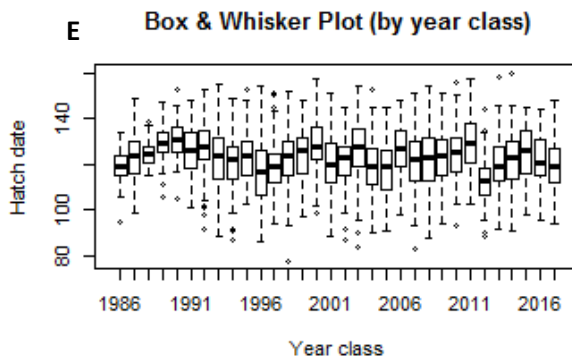
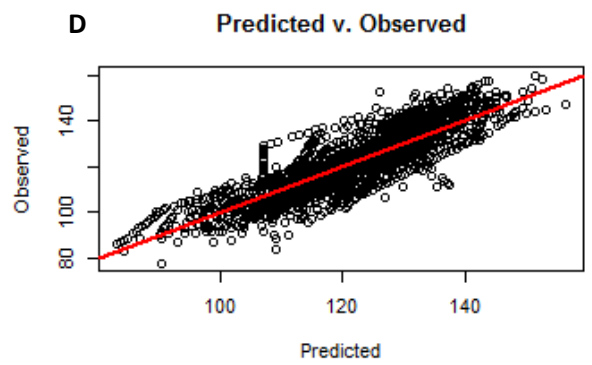
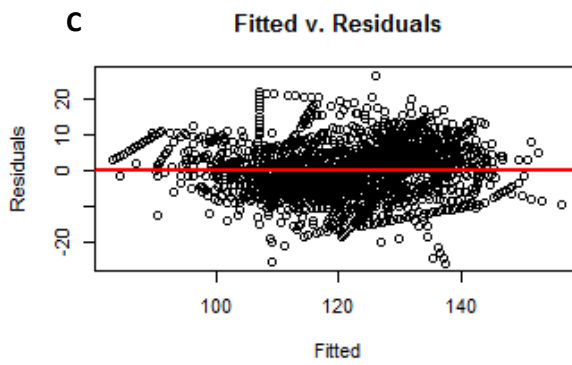
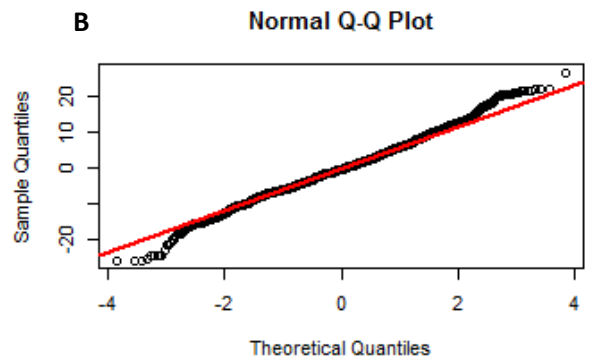
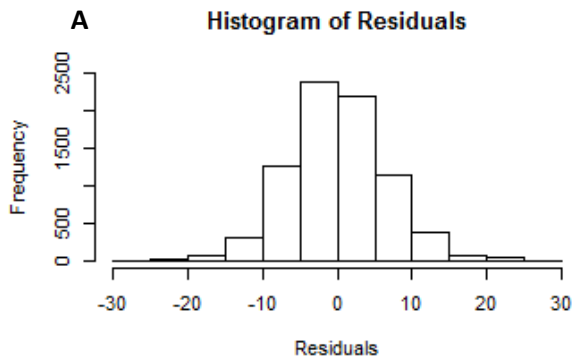


Figure 8. Estimated least-squares mean hatch date (calendar day), adjusted for temperature during hatching, and 95% confidence intervals for 32 year classes of juvenile striped bass in the James and Rappahannock subestuaries of the Chesapeake Bay. These means are from the analysis of covariance in which hatch date was a function of period and year nested within period, and temperature during hatching was the covariate. The solid line is a regression fit to mean hatch date through time, and shows the decline in hatch date through time. The solid line is for display purposes only and is not intended to be a predictive function.

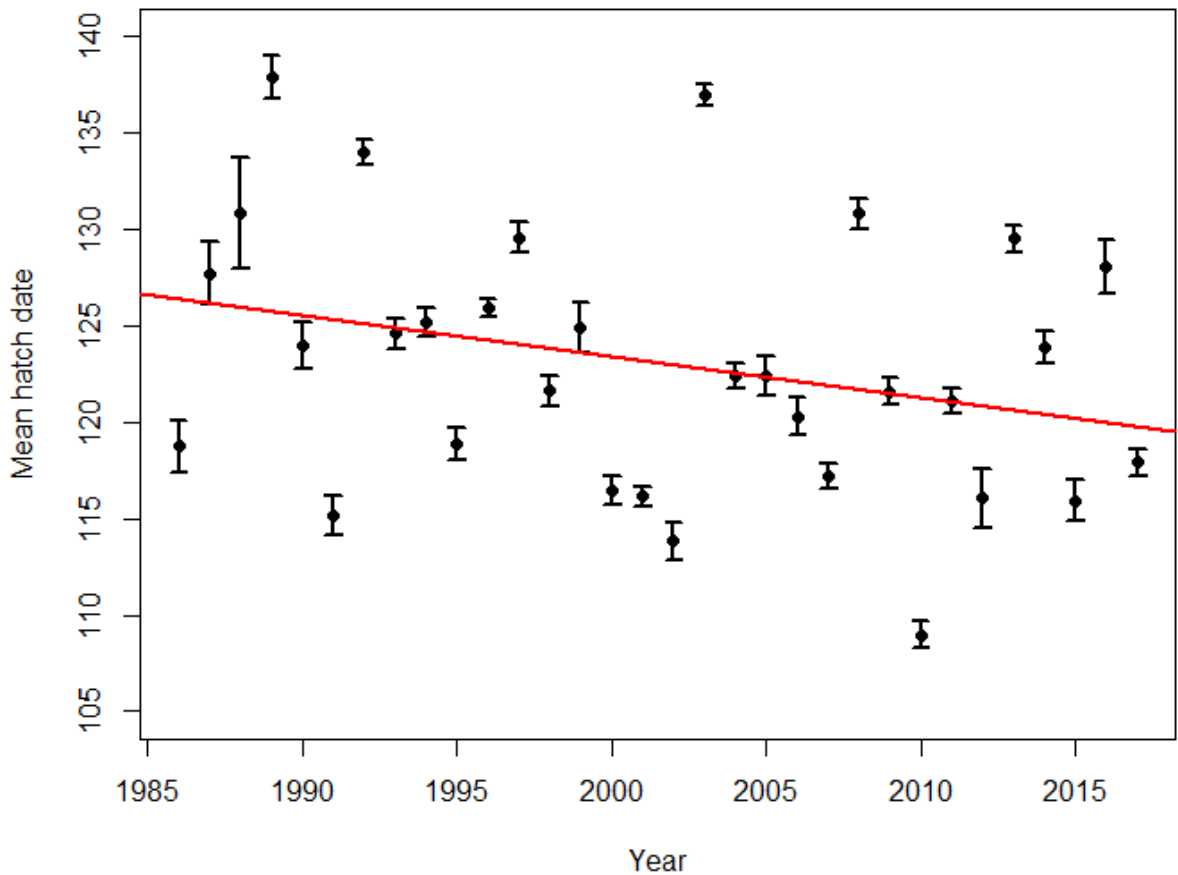


Figure 9. A partial regression plot showing the model-based relationship between temperature during hatching and hatch date from the analysis of covariance in which hatch date of juvenile striped bass in the James and Rappahannock was a function of period and year nested within period, and temperature during hatching was the covariate. The solid line represents the correlation between temperature during hatching and hatch date (calendar day), and the gray dots represent the observed temperature on a given hatch date.

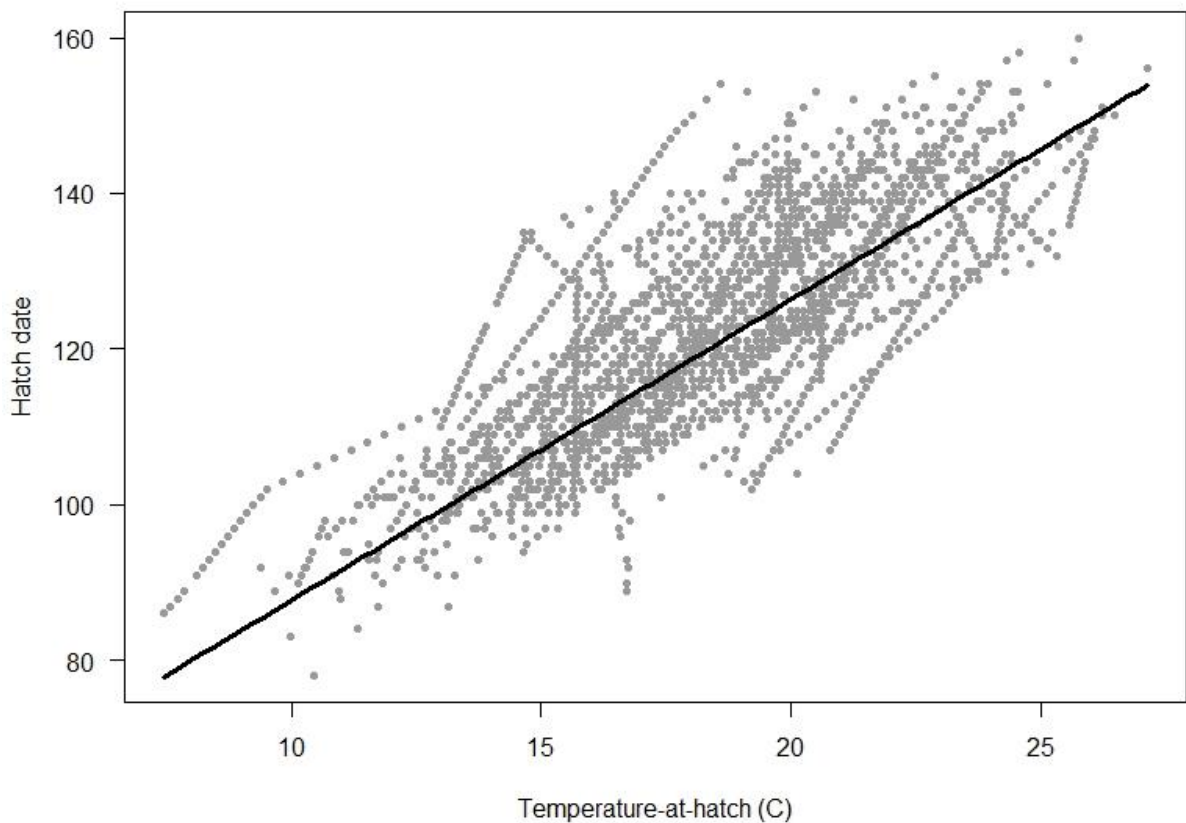
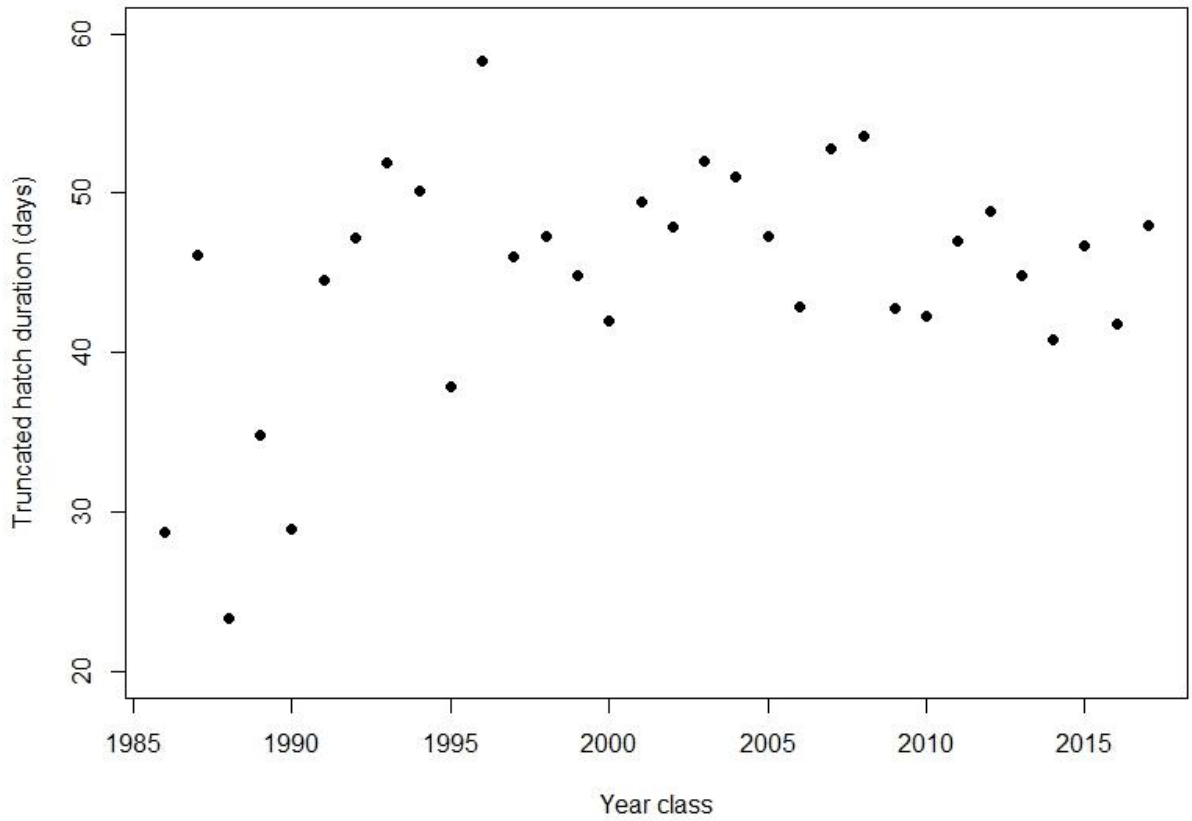


Figure 10. Truncated hatch duration in days (earliest and latest 1% of hatch dates removed) for 32 year classes (1986-2017) of juvenile striped bass in the James and Rappahannock subestuaries of the Chesapeake Bay. Hatch dates were estimated with daily ages estimated from subestuary-specific age-length keys.



CHAPTER 2:
Growth, body condition, and recruitment potential of juvenile striped bass in a declining
population in the Chesapeake Bay

ABSTRACT

Based on the 2018 coast-wide stock assessment, the Atlantic coast striped bass fishery is overfished and overfishing is occurring. In the past, recruitment played a key role in the recovery of the fishery, and thus a contemporary study of recruitment may indicate the ability of the current population to recover. Year classes of juvenile striped bass were characterized using daily growth rates, body condition, and recruitment potential in the James and Rappahannock subestuaries of the Chesapeake Bay. Juvenile striped bass were collected annually by the VIMS seine survey between 2009 and 2017. Length and weight measurements were recorded for the entire time series, whereas otoliths were collected from three year classes associated with low (2016), average (2017), and high (2011) relative abundance of juveniles. Otolith-derived daily ages together with length, weight, and numbers of fish captured (catch) were used to estimate daily growth rate, weight-specific instantaneous growth rates (G , g/day), and instantaneous daily mortality rates (Z , day⁻¹). Length and weight of juvenile striped bass from 2009 to 2017 were used to calculate Fulton's K as a measure of body condition. Daily growth rates and body condition were modeled as functions of year class, subestuary, and environmental variables to identify temporal and spatial similarities in characteristics of juvenile striped bass in the Virginia portion of the Chesapeake Bay. Mean daily growth rates ranged from 0.55 mm/day (95% CI: 0.53-0.59 mm/day) to 0.80 mm/day (95% CI: 0.78-0.84 mm/day), and were significantly greater in the James subestuary than in the Rappahannock subestuary. Body condition also varied between subestuaries, but exhibited the opposite pattern as daily growth rates, such that mean body condition was greater in the Rappahannock than in the James. Mean body condition varied among year classes and ranged from 1.02 (95% CI: 1.01-1.04) to 1.32 (95% CI: 1.28-1.35); mean condition increased from 2009 to 2012, but declined thereafter. Chlorophyll- a and temperature had no effect on mean daily growth rates of juvenile striped bass, but did significantly affect body condition, such that 30-day lagged chlorophyll- a negatively affected mean body condition and 30-day lagged temperature positively affected mean body condition. Unlike daily growth rates and body condition, recruitment potential, estimated by the ratio of G to Z , did not vary among year classes or between subestuaries. Moreover, $G:Z$ was less than one for all year classes within each

subestuary (range: 0.11-0.44), which indicates that more biomass was lost through mortality, emigration, or both than gained through growth. The results of this study show that growth and body condition of juvenile striped bass are inversely related, and that environmental and biotic conditions in the James and Rappahannock subestuaries likely differ. Nevertheless, the annual recruitment potential of juvenile striped bass may not differ between these two subestuaries.

INTRODUCTION

In the United States, adult striped bass support lucrative recreational and commercial fisheries from Maine to South Carolina, with harvest records dating back to the 1600's. The Atlantic striped bass fisheries collapsed in the early 1970's as a result of recruitment overfishing and poor water quality in the nursery habitats (Richards & Rago 1999). Management agencies acted quickly to protect the spawning stock, and the stock recovered in 1995 after several years of strong recruitment and favorable environmental conditions (Richards & Rago 1999). More specifically, regulations successfully protected the 1982 and subsequent year classes of Atlantic coast striped bass, which allowed for reproduction, promoted age diversity of spawners, and achieved eventual recovery of the stock. Although striped bass are more abundant today (1996 to 2019) than they were in the midst of the collapse, the stock is currently overfished, and overfishing is occurring (ASMFC 2019). Moreover, the recent decline in striped bass abundance appeared to begin around 2010 (ASMFC 2019). Because recruitment success contributed to the previous recovery of the fishery, a re-examination of the population characteristics of juvenile striped bass during the recent period of decline may provide insight into the ability of the current population of striped bass to recover.

Recruitment, or the number of larvae that survive to the juvenile stage, is highly variable from year to year and this inter-annual variability is a defining characteristic of many fisheries, including striped bass (Jennings *et al.* 2001). One view of recruitment variability is that it represents a population-level, adaptive response to highly variable environmental conditions (Fogarty 2001). However, recruitment variability can be a concern to fisheries managers because such variability reduces the certainty about

predictions for future productivity of the stock. For example, fisheries supported by short-lived, opportunistic species, such as California Pacific sardine (*Sardinops sagax*) are often characterized by cycles of highly productive year-classes followed by years of poor production and possible collapse (Murphy 1966; Anderson *et al.* 2008). For long-lived fishes such as striped bass, the fishery may rely on a single strong year class, which can lead to collapse if that year class is removed from the population through harvesting, natural mortality, or both. However, the long life span of striped bass, and relatively early maturity, is believed to render the population more resilient to factors that lead to changes in abundance (i.e., the population can adapt to the presence of disturbance; Secor 2000). From a management perspective, it is necessary to acknowledge the role of recruitment variability in recovering stocks, and to adopt strategies that promote resiliency.

Variability in recruitment occurs because recruitment is a consequence of mortality and growth of early-life stages of fishes, and thus, slight changes in these factors can lead to dramatic variability in year-class strength (Miller 2007). The ratio of instantaneous growth rate to instantaneous mortality rate, $G:Z$, can be used to estimate the relative recruitment potential of the population of young fish (Ware 1975; Werner & Gilliam 1984; Houde 1997). Here, G is the weight-specific instantaneous daily growth rate and Z is the instantaneous daily total mortality rate. Year classes exhibit high recruitment potential when the $G:Z$ ratio exceeds one because these year classes gain more biomass than they lose (i.e., growth across individuals in the population exceeds total losses; Houde 1997). The $G:Z$ ratio may be used to assess environmental effects on recruitment potential and identify environmental conditions that are more (or less) suitable for growth and survival of early-life stages of fishes. For example, $G:Z$ ratios of

pinfish and sand trout are negatively related to freshwater discharge in the Suwannee River, such that in years of high discharge, recruitment of pinfish and sand trout is low (Purtlebaugh & Allen 2010). The G:Z ratio may also be used to compare recruitment potential across year classes, such that a year class with a G:Z of 0.8 has a higher recruitment potential than a year class with a G:Z of 0.5 (Houde 1997).

Growth and mortality rates of juvenile fishes may be estimated using length and weight observations along with daily ages derived from otoliths, which are structures responsible for hearing and balance, and which are located within the inner ear of fishes (Barton 2007). Otolith growth occurs incrementally and increments are commonly associated with age in fishes (Campana & Thorrold 2001). In early-life stages of fishes, each increment represents one day. This daily aging technique was validated for juvenile striped bass (Jones & Brother 1987; Secor & Dean 1989; Kline 1990; Douglas 1995), and has been used to estimate growth and mortality rates of early-life stages of striped bass (e.g., Secor & Houde 1995; Vanalderweireldt *et al.* 2019). For example, daily age estimates, length, and catches of the 1991 year class of larval striped bass in the Patuxent River were used to estimate growth (G, g/day) and mortality rates (Z, day⁻¹) for sub-cohorts, or groups of fish within a single year class that hatched close together in time (Secor & Houde 1995). The resulting instantaneous G:Z ratios were greater than 1.0 for three of the six sub-cohorts, and showed that sub-cohorts experienced low mortality when they co-occurred with optimal temperature conditions (16-20°C) during the first 25 days of life (Secor & Houde 1995).

In young fishes, growth rates may be negatively correlated with mortality rates (Houde 1989; Sim-Smith *et al.* 2012), although this size-specific mortality hypothesis

does not have unequivocal support from empirical observations (Litvak & Leggett 1992; Houde 1997; Sogard 1997). Small changes in growth rates of early-life stages can lead to changes in mortality rates because slow-growing fishes are believed to be exposed to predation risk for longer periods of time (Miller *et al.* 1988). Growth and mortality of early-life stages of fishes are affected by a number of environmental factors including water temperature (Jobling 1988; Cowan *et al.* 1993; Houde & Zastrow 1993; Houde 1996; Koster *et al.* 2005) and, for anadromous and estuarine fishes, freshwater flow (Martino & Houde 2003; Hoffman *et al.* 2007; Martino & Houde 2010; Purtlebaugh & Allen 2010). These environmental conditions affect growth and survival because they impact prey abundance and feeding success of young fishes. More specifically, warm water temperatures are associated with increased prey abundances (Logan 1985; Franz & Tanacredi 1992; Rutherford *et al.* 1997) and increased feeding rates in juvenile fishes (Houde 1989; Fonds *et al.* 1992; Lloret *et al.* 2014), both of which influence growth of young fishes (Houde 1989; Rutherford *et al.* 1997; Booth & Alquezar 2002). High freshwater flow is associated with increased growth rates and survival because freshwater discharge introduces terrestrial and upriver nutrients that can increase production and prey availability (Rutherford *et al.* 1997; North & Houde 2003; Purtlebaugh & Allen 2010).

Annual variability in temperature and flow conditions in nursery areas plays a role in shaping recruitment variability in striped bass. For this species, recruitment success is associated with cool water temperatures and high flows in March, April, and May because this combination can prolong the spring phytoplankton bloom, allowing zooplankton abundance to increase and provide high concentrations of food for striped

bass larvae and juveniles (Martino *et al.* 2006). Moreover, high freshwater flow rates promote retention of eggs and larvae in the estuarine turbidity maximum zone through enhanced estuarine gravitational circulation (North & Houde 2003), and this retention ensures that larval striped bass co-occur spatially with their zooplankton prey (Martino *et al.* 2006). However, pulsed high-flow events can increase mortality of larval and early juvenile striped bass through advection or by flushing individuals from the system. Excessive or irregular freshwater discharge may also increase mortality rates of young striped bass by exposing them to water temperatures above or below their optimal range of 15°C to 20°C (Secor & Houde 1995).

Body condition, a proxy for individual health, may also contribute to variations in year-class strength (Balcombe *et al.* 2012; Lloret *et al.* 2014; Schloesser & Fabrizio 2016). Body condition, which reflects energy and lipid content in juvenile fishes (Schloesser & Fabrizio 2016, 2017), is associated with measures of fitness such as growth and swimming performance, and has been correlated with mortality of larval and juvenile fishes (Booth & Beretta 2004). Most juvenile fishes, including striped bass, allocate energy to growth rather than storage, and thus relatively fast (or slow) growth may result in low (or high) body condition (Francis 1997; Hurst & Conover 2003; Chapman *et al.* 2011; Lloret *et al.* 2014). In striped bass, higher body condition indices during the first winter are associated with greater survival of juveniles (Hurst & Conover 2002). Environmental conditions that affect growth can also affect body condition in fishes (Tanner *et al.* 2009; Vasconcelos *et al.* 2009; Morgan *et al.* 2010; Lloret *et al.* 2014). For example, body condition of juvenile Pacific cod (*Gadus macrocephalus*) is greater when water temperatures are warmer (Lloret & Ratz 2000; Ratz & Lloret 2003).

During the end of their first year of life (November to June), body condition of juvenile striped bass (117-200 mm) is affected by environmental factors such as salinity, temperature, and dissolved oxygen (Schloesser & Fabrizio 2019). Body condition of these juveniles also varies among subestuaries (Schloesser & Fabrizio 2017) and among year classes, reflecting annual variation in environmental conditions observed in nursery habitats and, perhaps, density-dependent responses (Schloesser & Fabrizio 2016).

Body condition of juvenile fishes can be ascertained using organosomatic or morphometric indicators (Lloret *et al.* 2014). Body condition values derived from organosomatic indicators require direct measurements of internal organs that are associated with lipid and energy storage. For example, the hepatosomatic index (HSI) is estimated using the weight of the liver, which is an important site for lipid storage in many fish species. One drawback of the organosomatic approach is that the fish must be euthanized. Morphometric indicators require only length and weight measurements, which are generally inexpensive and less invasive than organosomatic indicators. One such morphometric indicator is Fulton's K, which assumes that for fish of the same length, heavier fish are in better body condition (Ricker 1975). For juvenile striped bass, morphometric indicators, such as Fulton's K, can be better indicators of body condition than organosomatic indicators, such as HSI (Schloesser & Fabrizio 2017).

The objective of this study was to evaluate and compare (1) daily growth rates, (2) body condition, and (3) recruitment potential of juvenile striped bass during the first summer of life (June to July) among year classes of varying abundances, and between subestuaries. Because I investigated multiple year classes of varying abundances, the results of this study could be important in ascertaining the factors that influence

recruitment success. Such knowledge may aid in future management of the declining stock of striped bass.

METHODS

To estimate daily growth rates and the elements of the G:Z ratio (weight-specific instantaneous daily growth rate, G , and instantaneous daily mortality rate, Z), otolith ages were obtained from juvenile striped bass from the 2011, 2016, and 2017 year classes. These year classes represented fish from high, low, and average year-class strength (Gallagher *et al.* 2019). I also estimated body condition of multiple year classes in the James and Rappahannock subestuaries of the Chesapeake Bay using weight data recorded by survey scientists. I applied multiple linear regression methods to compare daily growth rates and body condition among year classes and between subestuaries to elucidate patterns in growth and condition of the current population of juvenile striped bass across temporal and spatial scales. I considered temperature, freshwater flow, and chlorophyll-a (as a proxy for food availability) as covariates in each model because environmental variability likely contributed to variation in growth rate and body condition among year classes of juvenile striped bass. To better understand current characteristics of the juvenile striped bass population in the Virginia portion of the Chesapeake Bay, I tested several null hypotheses: (1) daily growth rates, (2) recruitment potential (G:Z ratio), and (3) body condition are similar among year classes and across subestuaries.

Fish sampling & otolith preparation

Length and weight data for estimation of body condition were obtained from nine year-classes (2009-2017) of juvenile striped bass from the James and Rappahannock subestuaries (Figure 1) as described in Chapter 1. To estimate otolith-derived daily ages, the left sagittal otolith was removed from 75 randomly selected juvenile striped bass from

each subestuary (Rappahannock and James) within three year classes (2011, 2016, and 2017), for a total of 450 otoliths. Each otolith was prepared using standard methods previously described (Chapter 1).

Consistency of age determinations

To ensure age determinations were consistent, I randomly selected a subsample of 40 juvenile striped bass otoliths, which represented both subestuaries and all three years, to age multiple times and estimated error, bias, and average percent error (APE) among my readings (Campana 2001). Here, error is defined as the mean magnitude of the deviance (absolute value) between each reading; bias incorporates the positive and negative direction of deviance, which describes the true mean deviance in increment count between readings of the same otolith (Campana *et al.* 1995; Campana 2001). APE provides a measure of precision among increment readings for each otolith (Campana 1995; Campana 2001; Gallagher *et al.* 2018). As described in Chapter 1, aging error ranged from 4.5 to 8 days for each reading, APE across individual otoliths was 5.8% and ranged from 2.0 to 17%, and bias ranged from -2.4 to 2.0 days across all readings. There was a significantly negative age bias between the second and third readings (2.3 days; $p < 0.05$) and between the second and fourth readings (2.0 days; $p = 0.05$), but bias was non-significant in all other reading combinations (Chapter 1). Based on my error, bias, and APE estimates, I concluded that my age determinations did not exhibit a systematic bias (Chapter 1).

Environmental factors

I included water temperature, chlorophyll-a, and freshwater flow as environmental factors in the models of fish growth and body condition. I obtained

temperature and chlorophyll-a observations from water quality monitoring stations sampled by the Chesapeake Bay Program (Figure 2; Water Quality Monitoring Database available at www.chesapeakebay.net/data). I calculated mean biweekly temperature and chlorophyll-a values for each subestuary (James and Rappahannock). I used mean biweekly, subestuary-specific temperature and chlorophyll-a values to linearly interpolate daily temperature and chlorophyll-a values in the James and Rappahannock subestuaries from April to August of each year, from 2009 to 2017; these linearly interpolated values were then used to calculate mean daily temperature and chlorophyll-a concentrations in the 30- and 60-day period prior to collection of fish by the VIMS seine survey. I obtained daily freshwater discharge records from the United States Geological Survey (USGS <http://waterdata.usgs.gov/va/nwis/rt>) and calculated mean freshwater flow during the 30 days and 60 days prior to each specimen's collection in the James and Rappahannock subestuaries of the Chesapeake Bay.

I chose 30-day and 60-day lags from the day each fish was collected because temperature, chlorophyll-a, and freshwater discharge likely affect growth and body condition of fish on the order of one to two months, rather than days or weeks. More specifically, the average age of juvenile striped bass at capture in this study was about 70 days; because striped bass larvae begin to feed 5 to 10 days post-hatch (Secor & Houde 1995), juvenile striped bass in this study experienced, on average, about 60 to 65 days of growth after initial feeding. The 30-day and 60-day mean temperature, chlorophyll-a concentration, and freshwater discharge were used as covariates in the growth and body condition models because both lags could reasonably explain changes in juvenile daily growth rates and body condition. That is, the temperature, chlorophyll-a concentrations,

and freshwater flow a young striped bass is exposed to within the first 30 to 60 days of life carryover to the juvenile period (Conroy *et al.* 2015; Gallagher *et al.* 2018).

Daily growth rates of juvenile striped bass

Daily growth rates of juvenile striped bass were estimated from total length (TL) and otolith-derived ages using:

$$(1) \text{ Daily growth rate} = \frac{\text{Total length} - 3.1\text{mm}}{\text{Age}}$$

where 3.1-mm is the average length at hatch (Mansueti 1958; Mohan *et al.* 2015), and age is the number of daily increments, adjusted for temperature during hatching. I used juvenile fish collected between 21 June and 21 July for this analysis. After 21 July, juvenile striped bass begin to inhabit deeper waters and are less accessible to the gear, and thus, fish collected after 21 July may not be representative of the population of juvenile striped bass present in these nursery areas between June and July.

Mean daily growth rates were compared among three year classes of juvenile striped bass (2011, 2016, and 2017) and between two subestuaries (James and Rappahannock) controlling for the effects of environmental covariates. Temperature, flow, and chlorophyll-a were included in the analyses as covariates because they affect prey abundance, feeding rates, and overall growth and survival of juvenile striped bass (Logan 1985; Franz & Tanacredi 1992; Rutherford *et al.* 1997; North & Houde 2003; Purtlebaugh & Allen 2010). I used least-squares means, adjusted to covariates and estimated from an analysis of covariance (ANCOVA) that modeled daily growth rate as a function of subestuary, year class, and 30-day or 60-day lagged temperature, flow, and chlorophyll-a. The initial statistical model fit to the data using the `lm()` function in R statistical software (R Core Team 2019) was:

(2) *Daily Growth*_{ijk}

$$= \beta_0 + (\textit{Subestuary})_i + (\textit{Year})_j + \beta_1(\textit{Chla}) + \beta_2(\textit{Temp}) + \beta_3(\textit{Flow}) \\ + \varepsilon_{ijk}$$

- where *Daily Growth*_{ijk} = mean daily growth rate of the kth individual in the ith subestuary (i= James or Rappahannock) and the jth year class (j= 2011, 2016, or 2017), assumed to be normally distributed;
- β_0 = intercept, overall mean daily growth rate for juvenile striped bass from 3 year classes (2011, 2016, 2017) in the James and Rappahannock subestuaries;
- (Subestuary)*_j = effect of the ith subestuary (i= James or Rappahannock);
- (Year)*_j = effect of the jth year class (j=2011, 2016, or 2017);
- β_1 = partial regression coefficient accounting for effect of chlorophyll-a concentrations (30-day or 60-day lag) on daily growth rate;
- (Chla)* = chlorophyll-a concentration with a 30-day or 60-day lag measured in $\mu\text{g/L}$;
- β_2 = partial regression coefficient accounting for effect of temperature (30-day or 60-day lag) on daily growth rate;
- (Temp)* = mean daily temperature with a 30-day or 60-day lag measured in $^{\circ}\text{C}$;
- β_3 = partial regression coefficient accounting for effect of flow (30-day or 60-day lag) on daily growth rate;
- (Flow)* = daily discharge with a 30-day or 60-day lag measured in m^3/sec ;
- ε_{ijk} = random unexplained error associated with the kth individual from the ith subestuary and jth year class, assumed to be normally distributed with mean of 0 and variance of σ_{ε}^2 .

All factors in the model were considered fixed effects. The 30-day lag includes environmental conditions on dates between 21 May and 21 June and the 60-day lag includes dates between 21 April and 21 May; the specific values for each fish depended on its collection date. I examined residuals to assess model fit and the assumption of homogeneity of variance. I used the *ols_vif_tol()* command in the *olsrr* package in R to calculate tolerance values for each factor and to identify collinearity issues (tolerance

values less than 0.1 indicate the presence of collinearity). I also examined interaction plots to detect the presence of interactions between independent factors. I used AIC to guide model selection (i.e., lowest AIC indicated the model with the most empirical support from among the models considered; Burnham & Anderson 2002).

Body condition of juvenile striped bass

I used fork length (mm) and wet-weight (g) to estimate Fulton’s K, a measure of body condition, with:

$$(7) K = \left(\frac{W}{L^3}\right) * 10^N$$

where W is wet weight (g), L is fork length (mm), and N is an integer that brings K closer to 1 (Ricker 1975). In my study, N was 5.

To compare mean body condition among nine year classes (2009-2017) of juvenile striped bass and between the James and Rappahannock subestuaries, I used the least-squares means, adjusted for covariates and estimated from the ANCOVA that modeled Fulton’s K as a function of subestuary and year. I also examined partial regression plots to understand the effect of temperature, flow, and chlorophyll-a concentrations on body condition of juvenile striped bass. The statistical model fitted to the data using the `lm()` function in R statistical software (R Core Team 2019) was:

$$(8) \text{Body condition}_{ijk} = \beta_0 + (\text{Subestuary})_i + (\text{Year})_j + \beta_1(\text{Chla}) + \beta_2(\text{Temp}) + \beta_3(\text{Flow}) + \varepsilon_{ijk}$$

where $Body\ condition_{ijk}$ = mean body condition of the k^{th} individual in the i^{th} subestuary (i = James or Rappahannock) and the j^{th} year class (j = 2009-2017), assumed to be normally distributed;

β_0 = intercept, overall mean body condition for juvenile striped bass from 9 year classes (from 2009 to 2017) in the James and Rappahannock subestuaries;

$(Subestuary)_i$ = effect of the i^{th} subestuary (i = James or Rappahannock);

$(Year)_j$ = effect of the j^{th} year class (j =2009 to 2017);

β_1 = partial regression coefficient accounting for effect of chlorophyll-a concentration (30-day or 60-day lag) on body condition;

$(Chla)$ = chlorophyll-a concentration with a 30-day or 60-day lag measured in $\mu\text{g/L}$;

β_2 = partial regression coefficient accounting for effect of mean daily temperature (30-day or 60-day lag) on body condition;

$(Temp)$ = daily temperature with a 30-day or 60-day lag measured in $^{\circ}\text{C}$;

β_3 = partial regression coefficient accounting for effect of flow (30-day or 60-day lag) on body condition;

$(Flow)$ = daily discharge with a 30-day or 60-day lag measured in m^3/sec ;

ε_{ijk} = random unexplained error associated with the k^{th} individual in the i^{th} subestuary and j^{th} year class, assumed to be normally distributed with mean of 0 and variance of σ_{ε}^2 .

All factors in the model were considered fixed effects. As before, I examined residuals to assess model fit and the assumption of homogeneity of variance. I also examined interaction plots to detect the presence of interactions between predictors and covariates. I developed multiple models with temperature, flow, and chlorophyll-a lagged by 30 or 60 days and used Akaike's Information Criterion (AIC) to select the most parsimonious model (Burnham & Anderson 2002).

Preliminary observations of mean body condition across years suggested a period of increasing body condition from 2009 to 2011 or 2012 followed by a period of decreasing body condition. To confirm the presence of such a relationship in body condition of juvenile striped bass through time, I used the *davies.test* function in the segmented package in R. The *davies.test* function tests the null hypothesis that the

difference in slopes of body condition through time equals zero (i.e., the relationship between body condition and time can be explained by a single slope), and allows the user to specify the alternative hypothesis (e.g., two-sided, less than zero, or greater than zero). I used the two-sided alternative hypothesis in my analysis because preliminary observations suggested one positive slope (2009-2011) and one negative slope (2012-2017). To determine the breakpoint at which the slope changed, I used the *segmented* function in the segmented package in R to develop a piece-wise regression with an estimated breakpoint at t . I identified the initial breakpoint as 2011, which is required by the *segmented* function, but ultimately the breakpoint is identified by the model. The model was as follows:

$$(9) Y_k = \beta_0 + \beta_1(\text{Year}) + \varepsilon_k, \quad \text{for Year} \leq t$$

$$Y_k = \beta_0 + \beta_2(\text{Year}) + \varepsilon_k, \quad \text{for Year} > t$$

- where Y_k = mean condition (Fulton's K) of the k^{th} individual, assumed be normally distributed;
- β_0 = intercept, overall mean condition (Fulton's K) for juvenile striped bass in the James and Rappahannock from 2009 to 2017;
- β_1 = regression coefficient accounting for effect of year in segment 1 on Y_k ;
- β_2 = partial regression coefficient accounting for effect of year in segment 2 on Y_k ;
- ε_k = random unexplained error associated with the k^{th} individual, assumed to be normally distributed with mean of 0 and variance of σ_ε^2 .

Recruitment potential of juvenile striped bass

To calculate the annual recruitment potential (G:Z) of three year classes (2011, 2016, and 2017) of juvenile striped bass in the James and Rappahannock subestuaries of the Chesapeake Bay, I estimated weight-specific instantaneous daily growth rates (G,

g/day) and instantaneous daily mortality rates (Z , day^{-1}). Weight-specific instantaneous growth rates are usually given by:

$$(3) W_a = W_0 * e^{GA}$$

where W_a is the wet weight (g) at age a , W_0 is the estimated wet weight at age-0 (i.e., weight-at-hatch), G is the estimated weight-specific instantaneous growth coefficient, and A is the otolith-derived temperature-adjusted age (Houde & Lubbers 1986). This model assumes a multiplicative error structure because there is more variability in weight-at-age as age increases. I examined residuals to assess model fit and to ensure that assumptions were reasonably met. However, model diagnostics indicated poor fit with equation 3. As a result, I modified equation (3) following Kimura (2008):

$$(4) W_{ai} = W_{0i} * e^{G_i A_i}$$

where for the i^{th} individual, W_{ai} is the wet weight at age a , W_{0i} is the estimated wet-weight at age 0, G_i is the weight-specific instantaneous daily growth rate, and A_i is the daily age. Further, W_{0i} and G_i were modeled as linear functions of covariates x_{ij} :

$$\begin{pmatrix} W_{0i} \\ G_i \end{pmatrix} = \begin{pmatrix} \beta_{0W_0} + x_{i1}\beta_{1W_0} + x_{i2}\beta_{2W_0} + x_{i3}\beta_{3W_0} \\ \beta_{0G} + x_{i1}\beta_{1G} + x_{i2}\beta_{2G} + x_{i3}\beta_{3G} \end{pmatrix}$$

where x_{ij} is the j^{th} covariate with coefficients β_{jW_0} and β_{jG} . This formulation allowed me to include year class and subestuary as covariates in the model to better explain variation in W_0 and G .

Ten parameterizations of the exponential growth equation (4) were considered:

(M₁) no covariates for W_0 or G ; (M₂) year class as a covariate for W_0 ; (M₃) year class as a covariate for G ; (M₄) year class as a covariate for W_0 and G ; (M₅) subestuary as a covariate for W_0 ; (M₆) subestuary as a covariate for G ; (M₇) subestuary as a covariate for W_0 and G ; (M₈) year class and subestuary as covariates for W_0 ; (M₉) year class and

subestuary as covariates for G ; and (M_{10}) year class and subestuary as covariates for W_0 and G . The estimates of the β_0 s, represent how much a particular covariate increases or decreases model predictions of year-class-specific and subestuary-specific W_0 and G , relative to the reference levels of the covariates. For the covariates considered, 2011 was set as the year-class reference level and the James subestuary was set as the subestuary reference level. This model was fit with the *nls()* command in R (R Core Team 2019). I compared AIC values to choose the most parsimonious model from among the 10 considered (Burnham & Anderson 2002).

To estimate instantaneous daily mortality rates in July, I used catch curves constructed from daily ages (independent variable) and log-transformed catches (dependent variable). The absolute value of the slope of the descending limb of the catch curve provides an estimate of the instantaneous daily mortality rate, Z . This rate may be estimated using a catch curve if the following assumptions are met: (1) the population is closed and there is no immigration or emigration, (2) instantaneous daily mortality rates are independent of age or length, (3) all fish are equally vulnerable to the gear, and (4) the sample is unbiased (Ogle 2016). I used length data from the VIMS seine survey to estimate daily ages using the subestuary-specific age-length keys developed in Chapter 1. Catches were those from the VIMS seine survey, and ages were grouped by day (i.e., daily bins). To estimate daily Z , I used the *catchCurve()* command in the FSA package in R (Ogle 2016). Discrete daily mortality (A) was estimated for each year class with:

$$(6) A = (1 - e^{-Z}) * 100$$

where A describes percent of fish lost from the population per day.

Finally, the ratio of G (g/day) to Z (d^{-1}) was used to estimate the recruitment potential for each year class within each subestuary. Graphical analysis was used to examine the relationship between $G:Z$ and relative recruitment.

RESULTS

Daily growth rates of juvenile striped bass

The best model from among the 28 models I considered to assess changes in mean daily growth rates of juvenile striped bass included year, subestuary, 60-day-lagged chlorophyll-a concentrations, and 30-day lagged temperature (Table 1). Interaction plots exhibited no interactions among year and either 60-day lagged chlorophyll-a concentrations (Figure 3B), 30-day lagged temperature (Figure 3D), or subestuary (Figure 3E); no interactions among subestuary and 30-day lagged temperature (Figure 3C); and no interactions among 60-day lagged chlorophyll-a concentrations and 30-day temperature (Figure 3F). However, the interaction plot for subestuary and 60-day lagged chlorophyll-a showed that 60-day lagged chlorophyll-a positively affected daily growth rates of fish from the James subestuary, but had no effect on daily growth rates of fish from the Rappahannock subestuary (Figure 3A). More importantly, subestuary, 60-day lagged chlorophyll-a, and the interaction between subestuary and 60-day lagged chlorophyll-a were associated with tolerance values less than 0.1, indicating collinearity (Table 2). To address collinearity observed in the model, I centered the 60-day lagged chlorophyll-a observations by subtracting the mean from each observation, however, mean-centering of the chlorophyll-a values did not address the issue of collinearity, and graphical inspection suggested that chlorophyll-a was statistically confounded with subestuary. As a result, chlorophyll-a was removed from the model, and the next most parsimonious model was selected. The final ANCOVA included year and subestuary. The histogram of residuals (Figure 4A) exhibited a relatively normal, bell-shaped distribution of residuals, which further supported the use of this model for these data.

However, I observed some deviations from the expected line at the upper end of the Q-Q plot (large positive residuals; Figure 4B). The large positive residuals are likely the result of the small number of juvenile striped bass that exhibited a relatively large length at a young age. For example, I observed a few fish less than 90 days old that were greater than 70 mm (TL). The relationship between fitted and residual values (Figure 4C) indicated equal distribution of residuals around zero, and supported the assumption of homogeneity of variance. The plot of the predicted versus observed values (Figure 4D) exhibited equal distribution of residuals around the one-to-one line, indicating that the model could be used to make reasonable predictions about daily growth rates of juvenile striped bass.

On average, mean daily growth rates of juvenile striped bass were significantly greater in the James subestuary than in the Rappahannock subestuary ($F = 70.09$, $p < 0.01$). Mean daily growth rates, adjusted for temperature, were 0.737 mm/day (95% CI: 0.720-0.754 mm/day) in the James and 0.640 mm/day (95% CI: 0.623-0.658 mm/day) in the Rappahannock subestuary. Year class was also a significant factor in explaining the variation in daily growth rates of juvenile striped bass ($F = 17.63$, $p < 0.01$). The mean daily growth rates, adjusted for temperature, ranged from 0.60 mm/day (95% CI: 0.57-0.62 mm/day) for the 2011 year class in the Rappahannock subestuary to 0.78 mm/day (95% CI: 0.75-0.80 mm/day) for the 2017 year class in the James subestuary (Figure 5). In contrast, 30-day lagged temperature was not a significant factor in explaining variation in mean daily growth rates ($F = 0.004$, $p = 0.95$).

Body condition of juvenile striped bass

The model I selected to explain changes in mean body condition (Fulton's K) of juvenile striped bass included year, subestuary, 30-day-lagged chlorophyll-a concentrations, 30-day lagged flow, and 30-day-lagged temperature (Table 3). I found no evidence for collinearity among the independent factors (all tolerance values were greater than 0.1; Table 4), and no apparent interactions between factors (Figure 6). The histogram of residuals (Figure 7A) and the Q-Q plot (Figure 7B) indicated that the assumption of normality was reasonable, and the fitted versus residuals plot (Figure 7C) showed that the assumption of homogeneity of variance was reasonably met.

Mean body condition of juvenile striped bass differed significantly between subestuaries ($F = 50.06$, $p < 0.01$), such that, in most years, mean condition was greater in the Rappahannock than in the James subestuary. Mean body condition of juvenile striped bass varied among year classes ($F = 178.5$, $p < 0.01$). Estimated mean body condition, adjusted for chlorophyll-a, temperature, and flow, ranged from 1.02 (95% CI: 1.01-1.03) for the 2017 year class in the James subestuary to 1.32 (95% CI: 1.29-1.36) for the 2012 year class in the Rappahannock subestuary (Figure 8). Temperature, flow, and chlorophyll-a were also significant factors in the model ($F_{\text{Temp}} = 151.7$, $p_{\text{Temp}} < 0.01$; $F_{\text{Flow}} = 18.56$, $p_{\text{Flow}} < 0.01$; $F_{\text{Chl-a}} = 91.62$, $p_{\text{Chl-a}} < 0.01$). Temperature, lagged by 30 days, had a positive effect on mean body condition, such that, mean body condition increased by 0.021 (95% CI: 0.018 – 0.024) units for every degree ($^{\circ}\text{C}$) increase in temperature (Figure 9). Chlorophyll-a, lagged by 30 days, had a negative effect on mean body condition, where mean body condition decreased by 0.009 (95% CI: 0.007 – 0.011) units for every $\mu\text{L/g}$ increase in chlorophyll-a (Figure 10). Flow, lagged by 30 days, had a

positive effect on mean body condition, where mean body condition increased by 0.00010 (95% CI: 0.00005 – 0.00014) units for every m^3/sec increase in freshwater flow discharge (Figure 11).

I found two significantly different slopes describing the relationship of body condition of juvenile striped bass across years, such that body condition increased from 2009 to 2011 and declined thereafter (breakpoint = 2012; $p < 0.01$ Davie's test). The model estimate for the first slope (2009 to 2011) was 0.027 (95% CI: 0.016 – 0.036), indicating that body condition increased by 0.03 units each year until 2011. The model estimate for the second slope (2012 to 2017) was -0.043 (95% CI: -0.040 – 0.045), indicating that body condition decreased annually by 0.04 units beginning in 2012 (Figure 12).

Recruitment potential of juvenile striped bass

Based on AIC, the most parsimonious exponential growth model for juvenile striped bass aged 36 to 90 days old included both year class and subestuary as covariates for W_0 and G (Table 5). Diagnostic plots showed that the assumptions of normality and homogeneity of variance were reasonable (Figure 13). The estimate of weight at age-0 (or weight at hatch), W_0 , was significantly different among year classes and between subestuaries, ranging from 0.07 g for the 2011 year class in the James subestuary to 0.30 g for the 2017 year class in the Rappahannock subestuary (Figure 14). Similarly, the estimate of weight-specific instantaneous daily growth rate, G , also varied among year classes and between subestuaries, ranging from 0.01 g/day for the 2016 year class in the Rappahannock subestuary to 0.04 g/day for the 2011 and 2017 year classes in the James

subestuary (Table 6; Figure 14). Further, the model-based parameter estimates of W_0 were significantly greater for fish from the Rappahannock subestuary than from the James subestuary, and by nature of the exponential growth equation, the parameter estimates of G for year classes of juvenile striped bass in the Rappahannock subestuary were significantly less than those in the James subestuary (Table 5).

The descending limb of the catch curve encompassed fish aged 79 to 100 days for all year classes, except for the 2011 and 2016 year classes from the James subestuary, which encompassed fish aged 72 to 100 days (Figure 17). The estimated daily Z values ranged from 0.09 day^{-1} for the 2011 year class in the James subestuary and the 2016 year class in the Rappahannock subestuary, to 0.19 day^{-1} for the 2017 year class in the James subestuary (Table 6); discrete mortality (A) estimates ranged from $8.8\% \text{ day}^{-1}$ for the 2016 year class in the Rappahannock subestuary to $17\% \text{ day}^{-1}$ for the 2017 year class in the James subestuary (Figure 15).

The resulting $G:Z$ values for the month of July for each year class within each subestuary were less than 1, and ranged from 0.11 for the 2016 year class in the Rappahannock subestuary to 0.44 for the 2011 year class in the James subestuary (Table 6). Graphical examination indicated no linear relationship between $G:Z$ and relative abundance of juvenile striped bass.

DISCUSSION

Daily growth rates and body condition (Fulton's K) of juvenile striped bass during their first summer in Chesapeake Bay varied among year classes and between subestuaries, and recruitment potential was less than one for all year classes within each subestuary. Further, daily growth rates and body condition of juvenile striped bass appeared to exhibit opposing patterns whereby growth rate was high when body condition was low, and vice versa. The observed variability in daily growth rate and body condition supported my hypothesis that spatially and temporally varying environmental conditions result in spatially and temporally varying growth and body condition of juvenile striped bass.

For a given year class, daily growth rates of juvenile striped bass in the James subestuary were significantly greater than those observed in the Rappahannock subestuary, which was unexpected because juvenile striped bass exhibit counter-gradient growth along the Atlantic coast (Conover *et al.* 1997). That is, young striped bass at northern latitudes exhibit faster growth rates than young striped bass from southern latitudes. For example, juvenile striped bass in New York exhibit faster growth rates than young striped bass in North Carolina (Conover *et al.* 1997). Because the Rappahannock subestuary is north of the James subestuary, I expected to observe faster growth rates in juvenile striped bass residing in the Rappahannock subestuary. Perhaps the counter-gradient pattern observed by Conover and colleagues (1997) was not observed in my study because subestuaries or rivers within a restricted geographic region, such as the subestuaries of the Chesapeake Bay, are much closer to one another than subestuaries and rivers across the eastern seaboard, such as those in New York and North Carolina. In

contrast to the results of my study, the 1986 and 1987 year classes of juvenile striped bass exhibited similar growth rates in the James and Rappahannock (Kline 1990). However, growth rates for the 1986 and 1987 year classes were estimated for juveniles collected between 1 July and 30 August, a period of collection that only partially overlaps with the time period that juvenile striped bass were collected in my study (22 June to 21 July); such sampling differences may explain the observed discrepancy in subestuary-specific growth rates between my study and Kline (1990). Moreover, environmental conditions in nursery areas have changed in the James and Rappahannock subestuaries since 1987 (Preston 2004; Gallagher *et al.* 2019). Perhaps rising water temperatures and increased precipitation (Ding & Elmore 2015; Rice & Jastram 2015) have affected the James and Rappahannock subestuaries unequally, and resulted in environmental conditions that promote faster growth of juvenile striped bass in the James subestuary. Alternatively, the difference in estimated growth rates between my study and Kline (1990) may reflect changes in growth rates in late summer. That is, growth rates may vary between subestuaries early in the summer (this study) but converge as the summer progresses (Kline 1990 study). Future studies should consider growth rates of juvenile striped bass in the James and Rappahannock subestuaries at progressive stages throughout the summer to identify subestuary-specific growth dynamics. Moreover, an estimate of subestuary-specific daily growth rates throughout the first year of life may help to understand the importance of each subestuary as nursery habitat for young juvenile striped bass.

Between early-June and mid-July, juvenile striped bass grew at significantly faster rates in 2016 and 2017 than they did in 2011. The 2011 year class, which exhibited the slowest daily growth rates on average, is associated with the highest relative

abundance of juvenile striped bass in the Virginia portion of the Chesapeake Bay since 1967 (Gallagher *et al.* 2019). This year class exhibited strong recruitment in the Maryland portion of the Chesapeake Bay, as well (Durell & Weedon 2017). The pattern of daily growth rates among year classes of varying relative abundance observed in my study provides further evidence for density-dependent growth in juvenile striped bass, as reported by Martino & Houde (2012). Juvenile striped bass exhibit density-dependent growth when resources are limited, and under these conditions, slow growth could result in size-dependent mortality due to predation or to a lack of adequate energy reserves necessary for survival during the first winter (Martino & Houde 2012).

Body condition of juvenile striped bass varied among the nine year classes investigated in this study (2009-2017), which is consistent with the variability in body condition observed among year classes in older, larger (117-200 mm FL) juvenile striped bass in the Chesapeake Bay (Schloesser & Fabrizio 2016). In my study, the largest difference of 0.26 units in mean body condition occurred between the 2017 year class (1.04) and the 2012 year class (1.30). This difference implied that a 55-mm juvenile striped bass from the 2017 year class would weigh 1.73 g on average, but 2.16 g on average in 2012. Assuming size-selective mortality, this observed variability may affect overall recruitment of juvenile striped bass because, in this example, holding all other factors constant (e.g., food availability), a 55-mm juvenile striped bass from the 2012 year class is more likely to survive than a 55-mm juvenile striped bass from the 2017 year class. There were also significant differences in body condition among subestuaries, such that, juvenile striped bass in the Rappahannock subestuary exhibited significantly greater body condition than juveniles in the James subestuary, which further supported the idea

that differences in environmental conditions in the James and Rappahannock subestuaries affect overall body condition and growth of juveniles in these subestuaries. Note, the observed pattern of body condition among subestuaries is reversed for daily growth rates in this study, where growth rates were significantly greater in juveniles from the James subestuary than juveniles in the Rappahannock subestuary.

Mean body condition for juvenile striped bass increased from 2009 to 2012, but decreased thereafter. This suggested that factors that affect body condition of juvenile striped bass may be different in recent years compared with earlier years. The pattern observed in body condition of juvenile striped bass during 2009 to 2017 may represent a response to large-scale climactic patterns, such as the North Atlantic Oscillation (NAO). The NAO index, modeled by the National Weather Service, was low during 2009 to 2011 and high during 2014 to 2017 (Climate prediction center; https://www.cpc.ncep.noaa.gov/products/precip/CWlink/pna/nao_index.html). Notably, the NAO index follows a similar pattern to the body condition pattern observed in my study, where fish collected between 2009 and 2011 were characterized by increasing body condition (low NAO index) and fish collected between 2014 and 2017 were characterized by decreasing body condition (high NAO index). However, because large-scale climatic patterns occur over decadal or greater time scales, it is necessary to observe metrics such as body condition over a long period of time to infer associations with these climate patterns. More specifically, future studies should measure body condition of juvenile striped bass for more than nine years, and investigate relationships between body condition and the NAO index.

The recent decline in mean body condition does not necessarily provide evidence for an unhealthy population of juvenile striped bass, but does suggest a progressive change in the population, perhaps as a result of changing environmental conditions in nursery habitats on which juvenile striped bass rely. As climate change continues, environmental conditions are expected to be increasingly variable (Najjar *et al.* 2010), which may reduce the value of nursery habitats in the James and Rappahannock subestuaries and potentially lead to lower recruitment. In support of this hypothesis is the observation that summer water temperature was more variable during 2013 to 2017, when mean body condition decreased, than it was during 2009 to 2012, when mean body condition increased (Water Quality Monitoring Database available at www.chesapeakebay.net/data). To better understand how the declining pattern of body condition may affect recruitment, future studies should investigate the relationship between body condition and recruitment strength. More specifically, year classes that exhibit low body condition on average, in mid-June to mid-July, may not be properly equipped to survive their first winter. The effect of low mean body condition on average winter survival may affect juvenile abundance, such that fewer striped bass may enter the fishery than predicted. An inaccurate estimate of the abundance of juvenile striped bass within a year class could result in poor management decisions because the recruiting cohort may be smaller than anticipated.

Freshwater flow had a significant positive effect on body condition of juvenile striped bass in the James and Rappahannock subestuaries. However, upon further examination I found that, although the effect of freshwater flow was statistically significant, flow may not have had a biologically relevant effect on body condition. More

specifically, the estimated effect of freshwater flow was an increase in one unit of body condition for every 0.0001 m³/sec increase in flow, which implies that an increase in mean body condition of 0.04 units would be expected with an increase in freshwater flow to 400 m³/sec. In this example, 400 m³/sec was one of the greatest flow rates observed in my study (range = 0.29 – 435 m³/sec). The relatively small effect size of freshwater flow during mid-May to mid-June did not appear to appreciably affect body condition of juvenile striped bass. However, recent evidence suggests that condition of older juvenile striped bass (117 – 200 mm FL) increases with increasing distance downriver (Schloesser & Fabrizio 2019), which may explain the negligible effect of freshwater flow on body condition of juvenile striped bass observed in my study because my samples were collected from upriver sites and exhibited a relatively narrow range of body condition indices. Future studies are necessary to understand the effect of freshwater flow on body condition of juvenile striped bass across multiple spatial scales.

Surprisingly, chlorophyll-a concentration had a significant negative effect on body condition of juvenile striped bass in the James and Rappahannock subestuaries. In my study, chlorophyll-a concentration was used as a proxy for zooplankton (prey) abundance. I would have expected to see a positive effect of chlorophyll-a on body condition of juvenile striped bass because high prey abundance typically yields fish in good body condition (Jorgensen 1992; Shulman *et al.* 2005; Lloret *et al.* 2014). However, the quality or composition of prey is also important for body condition in fishes (Rose & O'Driscoll 2002; Ferraton *et al.* 2007; Sherwood *et al.* 2007; Lloret *et al.* 2014; Latour *et al.* 2017), and quality of prey cannot be ascertained with proxies such as chlorophyll-a concentrations. If zooplankton abundance is high (i.e., high chlorophyll-a), but the

abundance of optimal prey, *Bosmina longirostris* or *Eurytemora affinis* (Martino & Houde 2010), is low, striped bass may not gain the necessary nutrients for growth, and body condition may decline. Another explanation for the negative relationship is that chlorophyll-a directly represents phytoplankton abundance, and thus the negative relationship between chlorophyll-a and body condition was a consequence of top-down control: juvenile striped bass consume zooplankton, which consume phytoplankton. Perhaps the higher concentrations of chlorophyll-a, and thus phytoplankton abundance, occurred because the abundance of zooplankton was low. The low abundance of zooplankton, and thus limited prey resources, may have resulted in juvenile striped bass with lower body condition. Alternatively, the 30-day lag used for this covariate may not have adequately represented the effect of chlorophyll-a concentration on body condition of juvenile striped bass.

Water temperatures in the James and Rappahannock subestuaries from 2009 to 2017 had a significant positive effect on body condition of juvenile striped bass in mid-June to mid-July. However, the opposite pattern was observed during the first winter, such that high temperatures negatively affected body condition (Schloesser & Fabrizio 2019). The negative relationship between body condition and temperature during the winter reflected the temperature-dependent energy allocation strategy of this species (Schloesser & Fabrizio 2019); during winter, when temperatures are relatively lower, juvenile fish allocate energy to growth in length rather than to lipid storage (Hurst & Conover 2002; Schloesser & Fabrizio 2016). Notably, juvenile striped bass feeding is limited to periods of time when temperatures are above 10⁰C (Hurst & Conover 2001), which may occur rarely during the winter, but would not be limited during the summer in

the Chesapeake Bay. Therefore, temperature effects on energy allocation of juvenile fish are not likely to be the same in summer as they are in winter. Further, the higher summer temperatures drive increased prey abundances and overall feeding rates (Houde 1989; Fonds *et al.* 1992; Lloret *et al.* 2014); this is more so than in winter when only sporadic warm temperatures ($> 10^{\circ}\text{C}$) may be observed.

Growth and body condition of juvenile fishes can be used as indicators of habitat quality (Houde 1989; Lloret *et al.* 2014; Van Beveren *et al.* 2016; Schloesser & Fabrizio 2019) and can provide an indication of the overall health of the juvenile population (Miller 2007; Lloret *et al.* 2014). Although I did not make direct comparisons between body condition and growth rates of individuals, the results of my study showed opposite patterns of growth in length and body condition for the three year classes (2011, 2016, and 2017). That is, the 2011 year class exhibited high mean body condition and slow mean daily growth rate, the 2016 year class exhibited moderate mean body condition and mean daily growth rate, and the 2017 year class exhibited low mean body condition and fast mean daily growth rate. Further, daily growth rates were significantly higher and body condition was significantly lower in the James than they were in the Rappahannock subestuary. These findings suggest that juvenile striped bass allocated energy to increases in body length rather than increases in weight during the early period of their first summer (i.e. late-June to mid-July). This observed pattern in body condition and growth of juvenile striped bass is common among juvenile fishes, such that body condition is high during periods of slow growth and declines during periods of fast growth (Francis 1997; Sim-Smith *et al.* 2013; Schloesser & Fabrizio 2016). Future studies should directly

compare growth rates and body condition indices to quantify the observed relationship found in this study.

The pattern of growth in length of juvenile striped bass observed in the James and Rappahannock subestuaries was also observed in the results from the exponential model of growth in weight. This model indicated that, although juvenile striped bass in the James subestuary were associated with smaller weights at hatch (W_0) than those in the Rappahannock, juvenile striped bass from the James subestuary grew at a faster rate than those in the Rappahannock subestuary. For example, an 80-day old juvenile striped bass from the 2011 year class weighed, on average, 1.61 g in the James subestuary, but only 1.25 g in the Rappahannock subestuary. Notably, juvenile striped bass from the Rappahannock subestuary began life larger than those in the James subestuary, but the presence (or absence) of some factor (e.g., food availability, food quality, predators) resulted in slower overall growth in the Rappahannock subestuary. To better understand the pattern in growth rates (and body condition) between subestuaries, future studies should seek to identify differences in physical and biological factors between the James and Rappahannock subestuary that could potentially affect growth of juvenile striped bass.

There did not appear to be a relationship between recruitment potential (G:Z) and the recruitment index expressed as relative juvenile abundance for the three year classes and two subestuaries investigated in my study, although a larger number of year classes is required to address this relationship. I expected the G:Z ratio to reflect the same variability in recruitment potential as the variability exhibited in the recruitment index for juvenile striped bass in the Virginia portion of the Chesapeake Bay, but the G:Z ratios

measured in mid-June to mid-July did not vary significantly across year classes or among subestuaries. Moreover, G:Z ratios were less than 1.0 for all year classes (2011, 2016, and 2017) within each subestuary, which indicated that in mid-June to mid-July populations of juvenile striped bass lost more biomass through apparent mortality than they gained through growth. A G:Z ratio less than 1.0 during an early life stage is expected, but I did not expect the 2011 year class, which is associated with the highest relative abundance of juvenile striped bass since 1967 (Gallagher *et al.* 2019), to exhibit a G:Z ratio less than 1.0. Perhaps the G:Z estimates in this study did not follow the same pattern as the juvenile recruitment index because the stage during which the G:Z ratios were estimated (juveniles between 22 and 89 mm) is not the stage when daily Z is highest, and thus this metric may not have provided the best representation of the overall biomass dynamics for juvenile striped bass. G:Z was proposed as a measure of recruitment for the larval stage (Houde & Rutherford 1992), and correlations between the G:Z ratio at the larval stage and the juvenile recruitment index have been observed for juvenile striped bass in Maryland (Rutherford *et al.* 1997). However, no studies have estimated G:Z values for older juveniles (22-89 mm) in mid-June to mid-July, or compared the G:Z ratio at the juvenile stage to the juvenile recruitment index. Both G and Z estimates for juveniles are marked by high uncertainty, and thus future studies should continue to focus on larval stages, especially considering the high mortality rates during the larval stage. Conceivably, the juvenile sizes and ages investigated in this study may not have truly exhibited annual variation in G:Z, but G:Z estimates for more than three year classes are necessary to address this hypothesis. The G:Z ratio, or recruitment potential, may not be the best method to understand recruitment in juvenile striped bass,

although my observations cannot be used to confirm that G:Z ratios are (more or) less accurate than recruitment indices. However, using G:Z ratios to understand recruitment of juvenile striped bass requires otolith-derived daily ages, which is more time consuming than estimation of a recruitment index based on abundance of juveniles.

Although my study suggested that G:Z may not be the best metric to estimate recruitment at the juvenile stage, my study did show that growth and body condition of juvenile striped bass were inversely related and that mean body condition of juvenile striped bass decreased since 2012. Moreover, the inverse relationship between growth and body condition of juvenile striped bass was true on both temporal (annual) and spatial (subestuaries) scales, indicating that an unmeasured factor (e.g., prey quality) or combination of factors (e.g., prey availability and predator avoidance) acting in nursery habitats favor growth in length over growth in weight (lipid gain). Factors that favor growth or body condition of juvenile striped bass vary, but are likely closely associated with environmental or biotic conditions in the nursery habitats. Notably, environmental conditions in nursery habitats have shifted in the Chesapeake Bay during the previous 30 years as a result of climate change (Preston 2004). Currently, year-class strength of juvenile striped bass is estimated at the juvenile stage in the summer because the abundance of a year class at the juvenile stage is correlated with the abundance of that year class when it recruits to the fishery (Goodyear 1985); however, I note that this correlation was established about 30 years ago, prior to shifts in environmental conditions resulting from climate change (Preston 2004). Perhaps the use of additional metrics such as growth rates and body condition could allow managers to more fully characterize year classes and perhaps allow for more informed predictions about future recruitment to the

fishery. Ultimately, recruitment success was crucial in the recovery of the fishery in 1995, and should be considered again, as managers seek to return the current population to sustainable levels, especially as environmental conditions in nursery habitats continue to change.

LITERATURE CITED

- Anderson CNK, Hsieh C, Sanding SA, Hewitt R, Hollowed A, Beddington J, May RM, Sugihara G. 2008. Why fishing magnifies fluctuations in fish abundance. *Nature*. 452: 835-839
- Atlantic States Marine Fisheries Commission (ASMFC). 2019. Summary of the 2019 benchmark stock assessment of Atlantic striped bass. ASMFC, Arlington, Virginia
- Balcombe SR, Lobegeiger JS, Marshall SM, Marshall JC, Ly D, Jones DN. 2012. Fish body condition and recruitment success reflect antecedent flows in an Australian dryland river. *Fisheries Sci.* 78: 841-847
- Barton M. 2007. Bond's biology of fishes. 3rd Edition, Belmont, California
- Booth D, Alquezar R. 2002. Food supplementation increases larval growth, condition and survival of *Acanthochromis polyacanthus*. *J. Fish Biol.* 60: 1126-1133
- Booth DJ, Beretta GA. 2004. Influence of recruit condition on food competition and predation risk in a coral reef fish. *Oecologia*. 140: 289-294
- Booth DJ, Hixon MA. 1999. Food ration and condition affect early survival of the coral reef damselfish, *Stegastes partitus*. *Oecologia*. 121: 364-368
- Burnham KP, Anderson DR. 2002. Model selection and inference: a practical information theoretic approach. 2nd Edition, Springer-Verlag, New York.
- Campana SE. 2001. Accuracy, precision and quality control in age determinations, including a review of the use and abuse of age validation methods. *J. Fish Biol.* 59: 197-242

- Campana SE, Annand MC, McMillan JI. 1995. Graphical and statistical methods for determining the consistency of age determinations. *T. Am. Fish. Soc.* 124: 131-138
- Campana SE, Thorrold SR. 2001. Otoliths, increments, and elements: keys to a comprehensive understanding of fish populations? *Can. J. Fish. Aquat. Sci.* 58: 30-38
- Chapman EW, Jorgensen C, Lutcavage ME. 2011. Atlantic bluefin tuna (*Thunnus thynnus*): a state dependent energy allocation model for growth, maturation, and reproductive investment. *Can. J. Fish. Aquat. Sci.* 68: 1934-1951
- Conover DO, Brown JJ, Ehtisham A. 1997. Countergradient variation in growth of young striped bass (*Morone saxatilis*) from different latitudes. *Can. J. Fish. Aquat. Sci.* 54: 2401-2409
- Conroy CW, Piccoli PM, Secor DH. 2015. Carryover effects of early growth and river flow on partial migration in striped bass *Morone saxatilis*. *Mar.Ecol. Prog. Ser.* 541: 179-194
- Cowan Jr. JH, Rose KA, Rutherford ES, Houde ED. 1993. Individual-based model of young-of-the-year striped bass population dynamics. II. Factors affecting recruitment in the Potomac River, Maryland. *T. Am. Fish. Soc.* 122: 439-458
- Ding H, Elmore AJ. 2015. Spatio-temporal patterns in water surface temperature from Landsat time series data in the Chesapeake Bay, USA. *Remote Sens. Environ.* 168: 335-348

- Douglas SG. 1995. Validation of daily increment formation on otoliths with applications to wild striped bass (*Morone saxatilis*) at the northern limit of its range. MS Thesis. Acadia University, Nova Scotia.
- Durell EQ, Weedon C. 2017. Striped bass seine survey juvenile index web page. dnr.maryland.gov/fisheries/Pages/juvenile-index.aspx. Maryland Department of Natural Resources, Fisheries Service
- Ferraton F, Harmelin-Vivien M, Mellon-Duval C, Souplet A. 2007. Spatio-temporal variation in diet may affect condition and abundance of juvenile European hake in the Gulf of Lions (NW Mediterranean). *Mar. Ecol. Prog. Ser.* 337: 197-208
- Fogarty MJ, Myers RA, Bowen KG. 2001. Recruitment of cod and haddock in the North Atlantic: a comparative analysis. *ICES J. Mar. Sci.* 58: 952-961
- Fonds M, Cronie R, Vethaak AD, Van der Puyl P. 1992. Metabolism, food consumption, and growth of plaice (*Pleuronectes platessa*) and flounder (*Platichthys flesus*) in relation to fish size and temperature. *Neth. J. Sea Res.* 29: 127-143
- Francis MP. 1997. Condition cycles in juvenile *Pagrus auratus*. *J. Fish Biol.* 51: 583-600
- Franz DR, Tanacredi JT. 1992. Secondary production of the amphipod *Amplisca abdita* Mills and its importance in the diet of juvenile winter flounder (*Pleuronectes americanus*) in Jamaica Bay, New York. *Estuaries.* 15: 193-203
- Gallagher BK, Fabrizio MC, Tuckey TD. 2019. Estimation of juvenile striped bass relative abundance in the Virginia portion of the Chesapeake Bay. Annual Progress Report: 2018-2019. Virginia Institute of Marine Science, William & Mary.

- Gallagher BK, Piccoli PM, Secor DH. 2018. Ecological carryover effects associated with partial migration in white perch (*Morone Americana*) within the Hudson River Estuary. *Estuar. Coast. Mar. Sci.* 200: 277-288
- Goodyear CP. 1985. Relationships between reported commercial landings and abundance of young striped bass in Chesapeake Bay, Maryland. *T. Am. Fish. Soc.* 114: 92-96
- Hoffman JC, Bronk BA, Olney JE. 2007. Contribution of allochthonous carbon to American shad production in the Mattaponi River, Virginia, using stable isotopes. *Estuar. Coasts.* 30: 1034-1048
- Houde ED. 1989. Comparative growth, mortality, and energetic of marine fish larvae: temperature and implied latitudinal effects. *Fish B-NOAA.* 87: 471-495
- Houde ED. 1996. Evaluating stage-specific survival during the early life of fish. In: Proceedings of an international workshop: Survival Strategies in Early Life Stages of Marine Resources. AA Balkema Publishers, Brookfield, VT
- Houde ED. 1997. Patterns and trends in larval-stage growth and mortality of teleost fish. *J. Fish Biol.* 51: 52-83
- Houde ED, Lubbers L. 1986. Survival and growth of striped bass, *Morone saxatilis*, and *Morone* hybrid larvae: Laboratory and pond enclosure experiments. *Fish-B NOAA.* 84: 905-914
- Houde ED, Rutherford ES. 1992. Egg production, spawning biomass and factors influencing recruitment of striped bass in the Potomac River and the upper Chesapeake Bay. Final Report to Maryland Department of Natural Resources, Annapolis, Contract no: CB89-001-003

- Houde ED, Zastrow CE. 1993. Ecosystem- and taxon-specific dynamic and energetic properties of larval fish assemblages. *B. Mar. Sci.* 53: 290-335
- Hurst TP, Conover DO. 2001. Diet and consumption rates of overwintering YOY striped bass, *Morone saxatilis*, in the Hudson River. *Fish. Bull.* 99: 545-553
- Hurst TP, Conover DO. 2002. Effects of temperature and salinity on survival of young-of-the-year Hudson River striped bass (*Morone saxatilis*): implications for optimal overwintering habitats. *Can. J. Fish. Aquat. Sci.* 59: 787-795
- Hurst TP, Conover DO. 2003. Seasonal and interannual variation in the allometry of energy allocation in juvenile striped bass. *Ecology.* 84: 3360-3369
- Jennings S, Kaiser MJ, Reynolds JD. 2001. Marine Fisheries Ecology. Blackwell Publishing company, Oxford, UK
- Jobling M. 1988. A review of physiology and nutritional energetic cod, *Gadus morhua* L., with particular reference to growth under farmed conditions. *Aquaculture.* 70: 1-19
- Jones C, Brother EB. 1987. Validation of the otolith increment aging technique for striped bass, *Morone saxatilis*, larvae reared under suboptimal feeding conditions. *Fish B-NOAA.* 85: 171-178
- Jorgensen T. 1992. Long-term changes in growth of north-east Arctic cod (*Gadus morhua*) and some environmental influences. *ICES J. Mar. Sci.* 49: 263-27
- Kimura DK. 2008. Extending the von Bertalanffy growth model using explanatory variables. *Can. J. Fish. Aquat. Sci.* 65: 1879-1891

- Kline L. 1990. Population dynamics of young-of-the-year striped bass, *Morone saxatilis*, populations, based on daily increments. PhD Dissertation. William & Mary, Virginia
- Koster FW, Mollmann C, Hinrichsen H, Wieland K, Tomkiewicz J, Kraus G, Voss R, Makarchouk A, MacKenzie BR, St. John MA, Schnack D, Rohlf N, Linkowski T, Beyer JE. 2005. Baltic cod recruitment – the impact of climate variability on key processes. *ICES J. Mar. Sci.* 62: 1408-1425
- Latour RJ, Gartland J, Bonzek CF. 2017. Spatiotemporal trends and drivers of fish condition in Chesapeake Bay. *Mar. Ecol. Prog. Ser.* 579: 1-17
- Litvak MK, Leggett WC. 1992. Age and size-selective predation on larval fishes: the bigger-is-better hypothesis revisited. *Mar. Ecol. Prog. Ser.* 81: 13-24
- Lloret J, Shulman G, Love RM. 2014. Condition and health indicators of exploited marine fishes. John Wiley, Chichester, UK
- Lloret J, Ratz HJ. 2000. Condition of cod (*Gadus morhua*) off Greenland during 1982-1998. *Fish. Res.* 48: 79-86
- Logan DT. 1985. Environmental variation and striped bass population dynamics: A size dependent mortality model. *Estuaries.* 8: 28-38
- Mansueti RJ. 1958. Eggs, larvae, and young of the striped bass *Roccus saxatilis*. Solomons, MD, Maryland Department of Research and Education. 112: 35
- Martino EJ, Houde ED. 2003. Linking ETM physics, zooplankton prey, and fish early-life histories to striped bass *Morone saxatilis*, and white perch *M. americana* recruitment. *Mar. Ecol. Prog. Ser.* 260: 219-236

- Martino EJ, Houde ED. 2010. Recruitment of striped bass in Chesapeake Bay: spatial and temporal environmental variability and availability of zooplankton prey. *Mar. Ecol. Prog. Ser.* 409: 213-228
- Martino EJ, Houde ED. 2012. Density-dependent regulation of year-class strength in age-0 juvenile striped bass (*Morone saxatilis*). *Can. J. Fish. Aquat. Sci.* 60: 430-446
- Martino EJ, North EW, Houde ED. 2006. Biophysical controls and survival of striped bass larvae in the Chesapeake Bay estuarine turbidity maximum. International Council for the Exploration of the Sea (ICES) 2006 Conference Proceedings. Session G.
- Miller TJ. 2007. Contributions of individual-based coupled physical-biological models to understand recruitment of marine fish populations. *Mar. Ecol. Prog. Ser.* 347: 127-138
- Miller TJ, Crowder LB, Rice JA, Marschall EA. 1988. Larval size and recruitment mechanisms in fishes: toward conceptual framework. *Can. J. Fish. Aquat. Sci.* 45: 1657-1670
- Mohan JA, Halden NM, Rulifson RA. 2015. Habitat use of juvenile striped bass *Morone saxatilis* (Actinopterygii: Moronidae) in rivers spanning a salinity gradient across a shallow wind-driven estuary. *Environ. Biol. Fish.* 98: 1105-1116
- Morgan MJ, Rideout RM, Colbourne EB. 2010. Impact of environmental temperature on Atlantic cod *Gadus morhua* energy allocation to growth, condition and reproduction. *Mar. Ecol. Prog. Ser.* 404: 185-195
- Murphy GI. 1966. Population biology of the Pacific sardine (*Sardinops caerulea*). *Proc. Calif. Acad. Sci.* Fourth Series, 34: 1-84

- Najjar RG, Pyke CR, Adams MB, Breitburg D, Hershner C, Kemp M, Howarth R, Muholland MR, Paolisso M, Secor D, Sellner K, Wardrop D, Wood R. 2010. Potential climate-change impacts on the Chesapeake Bay. *Estuar. Coast Shelf S.* 86: 1-20
- North EW, Houde ED. 2003. Linking ETM physics, zooplankton prey, and fish early-life histories to striped bass *Morone saxatilis* and white perch *M. americana* recruitment. *Mar. Ecol. Prog. Ser.* 260: 219-236
- Ogle DH. 2016. Introductory fisheries analysis with R. Boca Raton, FL-CRC Press.
- Preston BL. 2004. Observed winter warming of the Chesapeake Bay estuary (1949-2002): implications for ecosystem management. *Environ. Manage.* 34: 125-139
- Purtlebaugh CH, Allen MS. 2010. Relative abundance, growth, and mortality of five age-0 estuarine fishes in relation to discharge of the Suwannee River, Florida. *T. Am. Fish. Soc.* 139: 1233-1246
- Ratz HJ, Lloret J. 2003. Variation in fish condition between Atlantic cod (*Gadus morhua*) stocks, the effect on their productivity and management implications. *Fish. Res.* 60: 369-380
- R Core Team. 2019. R: A language and environment for statistical computing. R foundation for statistical computing, Vienna, Austria
- Rice KC, Jastram JD. 2015. Rising air and stream-water temperatures in Chesapeake Bay region, USA. *Climatic Change.* 128: 127-138
- Richards RA, Rago PJ. 1999. A case history of effective fishery management: Chesapeake Bay striped bass. *N. Am. J. Fish. Manage.* 19: 356-375

- Ricker EW. 1975. Computation and interpretation of biological statistics of fish populations. *Can. J. Fish. Aquat. Sci.* 191: 1-382.
- Rose GA, O'Driscoll RL. 2002. Capelin are good for cod: can the northern stock rebuilt without them? *ICES J. Mar. Sci.* 59: 1018-1026
- Rutherford ES, Houde ED, Nyman RM. 1997. Relationship of larval-stage growth and mortality to recruitment of striped bass, *Morone saxatilis*, in Chesapeake Bay. *Estuaries*. 20: 174-198
- Schloesser RW, Fabrizio MC. 2016. Temporal dynamics of condition for estuarine fishes in their nursery habitats. *Mar. Ecol. Prog. Ser.* 557: 207-219
- Schloesser RW, Fabrizio MC. 2017. Condition indices as surrogates of energy density and lipid content in juveniles of three fish species. *T. Am. Fish. Soc.* 146: 1058-1069
- Schloesser RW, Fabrizio MC. 2019. Nursery habitat quality assessed by the condition of juvenile fishes: not all estuarine areas are equal. *Estuar. Coasts*. 42: 548-566
- Secor DH, Dean JM. 1989. Somatic growth effects on the otolith-fish size relationship in young pond-reared striped bass, *Morone saxatilis* (Walbaum). *Can. J. Fish. Aquat. Sci.* 46: 113-121
- Secor DH, Houde ED. 1995. Temperature effects on the timing of striped bass egg production, larval viability, and recruitment potential in the Patuxent River (Chesapeake Bay). *Estuaries*. 18: 527-544
- Secor DH. 2000. Longevity and resilience of Chesapeake Bay striped bass. *ICES J. Mar. Sci.* 57: 808-815

- Shelton AO, Mangel M. 2011. Fluctuations in fish populations and the magnifying effects of fishing. *PNAS*. 108: 7075-7080
- Sherwood GD, Rideout RM, Fudge SB, Rose, GA. 2007. Influence of diet on growth, condition and reproductive capacity in Newfoundland and Labrador cod (*Gadus morhua*): insights from stable carbon isotopes ($\delta^{13}\text{C}$). *Deep-Sea Res. Pt. II* 54: 2794-2809
- Shulman GE, Nikolsky VN, Yuneva TV, Minyuk GS, Shchepkin VY, Shchepkina AM, Ivleva EV, Ynev OA, Dobrovlov IS, Bingel F, Kideys AE. 2005. Fat content in Black Sea sprat as an indicator of fish food supply and ecosystem condition. *Mar. Ecol. Prog. Ser.* 293: 201-212
- Sim-Smith CJ, Jeffs AG, Radford CA. 2012. Variation in the growth of larval and juvenile snapper, *Chrysophrys auratus* (Sparidae). *Mar. Freshwater Res.* 63: 1231-1243
- Sogard SM. 1997. Size-selective mortality in the juvenile stage of teleost fishes: a review. *Bull. Mar. Sci.* 60: 1129-1157
- Tanner SE, Fonseca VF, Cabral HN. 2009. Condition of 0-group and adult pouting, *Trisopterus luscus* L., along the Portuguese coast: evidence of habitat quality and latitudinal trends. *J. Appl. Ichthyol.* 25: 387-393
- Vanalderweireldt L, Winkler G, Mingelbier M, Sirois P. 2019. Early growth, mortality, and partial migration of striped bass (*Morone saxatilis*) larvae and juveniles in the St. Lawrence estuary, Canada. *ICES J. Mar. Sci.* 116: 1-12

- Van Beveren E, Klein M, Serrao EA, Goncalves EJ, Borges R. 2016. Early life history of larvae and early juvenile Atlantic horse mackerel *Trachurus trachurus* off the Portuguese west coast. *Fish. Res.* 183: 111-118
- Vasconcelos RP, Reis-Santos P, Fonseca V, Ruano M, Tanner S, Costa MJ, Cabral HN. 2009. Juvenile fish condition in estuarine nurseries along the Portuguese coast. *Estuar. Coast. Shelf. S.* 82: 128-138
- Walter JF, Austin HM. 2003. Diet composition of large striped bass (*Morone saxatilis*) in Chesapeake Bay. *Fish. Bull.* 101: 414-423
- Walter JF, Overton AS, Ferry KH, Mather ME. 2003. Atlantic coast feeding habits of striped bass: a synthesis supporting a coast-wide understanding of trophic biology. *Fish. Manag. Ecol.* 10: 349-360
- Ware DM. 1975. Relation between egg size, growth and natural mortality of larval fish. *Can. J. Fish. Aquat. Sci.* 32: 2503-2512
- Werner RG, Gilliam JF. 1984. The ontogenetic niche and species interactions in size-structured populations. *Annu. Rev. Ecol. Syst.* 15: 393-425

Table 1. Models considered to describe daily growth of three year classes (2011, 2016, and 2017) of juvenile striped bass in the James and Rappahannock subestuaries of the Chesapeake Bay (N = 450). AIC and Δ AIC are presented for the final model (shaded), the model with the lowest AIC (bold), and alternate models. Symbols in the model are: the model intercept (β_0), partial regression coefficients (β_{1-5}) for year class (*Year*), subestuary (*Subestuary*), chlorophyll-a (*Chla_{30 day lag}* or *Chla_{60 day lag}*), temperature (*Temp_{30 day lag}* or *Temp_{60 day lag}*), and freshwater flow (*Flow_{30 day lag}* or *Flow_{60 day lag}*). The asterisk (*) in the model notation indicates the inclusion of subestuary, chlorophyll-a, and the interaction between subestuary and chlorophyll-a in the model.

Model	-2log(L)	AIC	Δ AIC
$Y = \beta_0 + \beta_1(\textit{Year})_i + \varepsilon_i$	67.23	-537.86	72.57
$Y = \beta_0 + \beta_2(\textit{Subestuary})_i + \varepsilon_i$	95.04	-570.27	40.16
$Y = \beta_0 + \beta_1(\textit{Year})_i + \beta_2(\textit{Subestuary})_i + \varepsilon_i$	60.15	-601.49	8.94
$Y = \beta_0 + \beta_1(\textit{Year})_i + \beta_2(\textit{Subestuary})_i * \beta_3(\textit{Chla}_{30 \textit{ day lag}}) + \varepsilon_i$	43.21	-604.93	5.50
$Y = \beta_0 + \beta_1(\textit{Year})_i + \beta_2(\textit{Subestuary})_i * \beta_3(\textit{Chla}_{60 \textit{ day lag}}) + \varepsilon_i$	43.54	-609.54	0.89
$Y = \beta_0 + \beta_1(\textit{Year})_i + \beta_2(\textit{Subestuary})_i + \beta_3(\textit{Temp}_{30 \textit{ day lag}}) + \varepsilon_i$	49.96	-599.49	10.94
$Y = \beta_0 + \beta_1(\textit{Year})_i + \beta_2(\textit{Subestuary})_i + \beta_3(\textit{Temp}_{60 \textit{ day lag}}) + \varepsilon_i$	49.99	-599.91	10.52
$Y = \beta_0 + \beta_1(\textit{Year})_i + \beta_2(\textit{Subestuary})_i + \beta_3(\textit{Flow}_{30 \textit{ day lag}}) + \varepsilon_i$	49.96	-599.82	10.61
$Y = \beta_0 + \beta_1(\textit{Year})_i + \beta_2(\textit{Subestuary})_i + \beta_3(\textit{Flow}_{60 \textit{ day lag}}) + \varepsilon_i$	49.96	-599.49	10.94
$Y = \beta_0 + \beta_1(\textit{Year})_i + \beta_2(\textit{Subestuary})_i * \beta_3(\textit{Chla}_{30 \textit{ day lag}}) + \beta_4(\textit{Temp}_{30 \textit{ day lag}}) + \varepsilon_i$	37.71	-603.43	7.00

$Y = \beta_0 + \beta_1(\text{Year})_i + \beta_2(\text{Subestuary})_i * \beta_3(\text{Chla}_{30 \text{ day lag}}) + \beta_4(\text{Temp}_{60 \text{ day lag}}) + \varepsilon_i$	37.68	-602.93	7.50
$Y = \beta_0 + \beta_1(\text{Year})_i + \beta_2(\text{Subestuary})_i * \beta_3(\text{Chla}_{60 \text{ day lag}}) + \beta_4(\text{Temp}_{30 \text{ day lag}}) + \varepsilon_i$	38.15	-610.43	0.000
$Y = \beta_0 + \beta_1(\text{Year})_i + \beta_2(\text{Subestuary})_i * \beta_3(\text{Chla}_{60 \text{ day lag}}) + \beta_4(\text{Temp}_{60 \text{ day lag}}) + \varepsilon_i$	38.06	-608.97	1.46
$Y = \beta_0 + \beta_1(\text{Year})_i + \beta_2(\text{Subestuary})_i * \beta_3(\text{Chla}_{30 \text{ day lag}}) + \beta_4(\text{Flow}_{30 \text{ day lag}}) + \varepsilon_i$	37.68	-602.93	7.50
$Y = \beta_0 + \beta_1(\text{Year})_i + \beta_2(\text{Subestuary})_i * \beta_3(\text{Chla}_{60 \text{ day lag}}) + \beta_4(\text{Flow}_{30 \text{ day lag}}) + \varepsilon_i$	37.97	-607.56	2.87
$Y = \beta_0 + \beta_1(\text{Year})_i + \beta_2(\text{Subestuary})_i * \beta_3(\text{Chla}_{30 \text{ day lag}}) + \beta_4(\text{Flow}_{60 \text{ day lag}}) + \varepsilon_i$	37.69	-603.00	7.43
$Y = \beta_0 + \beta_1(\text{Year})_i + \beta_2(\text{Subestuary})_i * \beta_3(\text{Chla}_{60 \text{ day lag}}) + \beta_4(\text{Flow}_{60 \text{ day lag}}) + \varepsilon_i$	37.97	-607.59	2.84
$Y = \beta_0 + \beta_1(\text{Year})_i + \beta_2(\text{Subestuary})_i + \beta_3(\text{Temp}_{30 \text{ day lag}}) + \beta_4(\text{Flow}_{30 \text{ day lag}}) + \varepsilon_i$	42.70	-597.82	12.61
$Y = \beta_0 + \beta_1(\text{Year})_i + \beta_2(\text{Subestuary})_i + \beta_3(\text{Temp}_{60 \text{ day lag}}) + \beta_4(\text{Flow}_{30 \text{ day lag}}) + \varepsilon_i$	42.75	-598.46	11.97
$Y = \beta_0 + \beta_1(\text{Year})_i + \beta_2(\text{Subestuary})_i + \beta_3(\text{Temp}_{30 \text{ day lag}}) + \beta_4(\text{Flow}_{60 \text{ day lag}}) + \varepsilon_i$	42.68	-597.49	12.94
$Y = \beta_0 + \beta_1(\text{Year})_i + \beta_2(\text{Subestuary})_i + \beta_3(\text{Temp}_{60 \text{ day lag}}) + \beta_4(\text{Flow}_{60 \text{ day lag}}) + \varepsilon_i$	42.71	-597.91	12.52
$Y = \beta_0 + \beta_1(\text{Year})_i + \beta_2(\text{Subestuary})_i * \beta_3(\text{Chla}_{30 \text{ day lag}}) + \beta_4(\text{Temp}_{30 \text{ day lag}}) + \beta_5(\text{Flow}_{30 \text{ day lag}}) + \varepsilon_i$	33.42	-601.47	8.96
$Y = \beta_0 + \beta_1(\text{Year})_i + \beta_2(\text{Subestuary})_i * \beta_3(\text{Chla}_{30 \text{ day lag}}) + \beta_4(\text{Temp}_{30 \text{ day lag}}) + \beta_5(\text{Flow}_{60 \text{ day lag}}) + \varepsilon_i$	33.39	-601.58	8.85
$Y = \beta_0 + \beta_1(\text{Year})_i + \beta_2(\text{Subestuary})_i * \beta_3(\text{Chla}_{30 \text{ day lag}}) + \beta_4(\text{Temp}_{60 \text{ day lag}}) + \beta_5(\text{Flow}_{30 \text{ day lag}}) + \varepsilon_i$	33.39	-600.93	9.50
$Y = \beta_0 + \beta_1(\text{Year})_i + \beta_2(\text{Subestuary})_i * \beta_3(\text{Chla}_{30 \text{ day lag}}) + \beta_4(\text{Temp}_{60 \text{ day lag}}) + \beta_5(\text{Flow}_{60 \text{ day lag}}) + \varepsilon_i$	33.81	-601.00	9.43
$Y = \beta_0 + \beta_1(\text{Year})_i + \beta_2(\text{Subestuary})_i * \beta_3(\text{Chla}_{60 \text{ day lag}}) + \beta_4(\text{Temp}_{30 \text{ day lag}}) + \beta_5(\text{Flow}_{30 \text{ day lag}}) + \varepsilon_i$	33.82	-608.62	1.68
$Y = \beta_0 + \beta_1(\text{Year})_i + \beta_2(\text{Subestuary})_i * \beta_3(\text{Chla}_{60 \text{ day lag}}) + \beta_4(\text{Temp}_{30 \text{ day lag}}) + \beta_5(\text{Flow}_{60 \text{ day lag}}) + \varepsilon_i$	33.72	-608.76	1.67
$Y = \beta_0 + \beta_1(\text{Year})_i + \beta_2(\text{Subestuary})_i * \beta_3(\text{Chla}_{60 \text{ day lag}}) + \beta_4(\text{Temp}_{60 \text{ day lag}}) + \beta_5(\text{Flow}_{30 \text{ day lag}}) + \varepsilon_i$	33.72	-607.04	3.39
$Y = \beta_0 + \beta_1(\text{Year})_i + \beta_2(\text{Subestuary})_i * \beta_3(\text{Chla}_{60 \text{ day lag}}) + \beta_4(\text{Temp}_{60 \text{ day lag}}) + \beta_5(\text{Flow}_{60 \text{ day lag}}) + \varepsilon_i$	33.73	-607.19	3.24

Table 2. Tolerance values for effects in the ANCOVA model of mean daily growth rate as a function of year class (2011, 2016, and 2017), subestuary (James or Rappahannock), 60-day lagged chlorophyll-a (covariate), and 30-day lagged temperature. Tolerance values for the effect of “Year: 2011” and “Subestuary: James” were not calculated because these effects are included in the intercept of the ANCOVA. Tolerance values less than 0.1 indicate collinearity among variables. To address collinearity, chlorophyll-a data were centered by subtracting the mean chlorophyll-a, which yielded new tolerance values less than 0.1.

Effect	Tolerance	Tolerance (centered Chl-a)
Year: 2016	0.23	0.23
Year: 2017	0.21	0.21
Subestuary: Rappahannock	0.01	0.15
Chlorophyll-a	0.02	0.02
Temperature	0.34	0.40
Subestuary * Chlorophyll-a	0.004	0.03

Table 3. Models considered to describe body condition (Fulton’s K) of nine year classes (2009-2017) of juvenile striped bass in the James and Rappahannock subestuaries of the Chesapeake Bay. AIC and Δ AIC are presented for each model; the model with the lowest AIC is indicated in bold. Symbols in the model are: the model intercept (β_0), partial regression coefficients (β_{1-5}) for year class (*Year*), subestuary (*Subestuary*), chlorophyll-a (*Chla_{30 day lag}* or *Chla_{60 day lag}*), temperature (*Temp_{30 day lag}* or *Temp_{60 day lag}*), and freshwater flow (*Flow_{30 day lag}* or *Flow_{60 day lag}*).

Model	-2log(L)	AIC	Δ AIC
$Y = \beta_0 + \beta_1(\textit{Year})_i + \varepsilon_i$	414.2	-8283.2	256.7
$Y = \beta_0 + \beta_2(\textit{Subestuary})_i + \varepsilon_i$	1065.6	-6393.7	2146.2
$Y = \beta_0 + \beta_1(\textit{Year})_i + \beta_2(\textit{Subestuary})_i + \varepsilon_i$	379.3	-8343.5	196.4
$Y = \beta_0 + \beta_1(\textit{Year})_i + \beta_2(\textit{Subestuary})_i + \beta_3(\textit{Chla}_{30 \text{ day lag}}) + \varepsilon_i$	349.7	-8392.5	147.4
$Y = \beta_0 + \beta_1(\textit{Year})_i + \beta_2(\textit{Subestuary})_i + \beta_3(\textit{Chla}_{60 \text{ day lag}}) + \varepsilon_i$	347.6	-8343.5	196.4
$Y = \beta_0 + \beta_1(\textit{Year})_i + \beta_2(\textit{Subestuary})_i + \beta_3(\textit{Temp}_{30 \text{ day lag}}) + \varepsilon_i$	351.6	-8437.7	102.2
$Y = \beta_0 + \beta_1(\textit{Year})_i + \beta_2(\textit{Subestuary})_i + \beta_3(\textit{Temp}_{60 \text{ day lag}}) + \varepsilon_i$	351.1	-8426.8	113.1
$Y = \beta_0 + \beta_1(\textit{Year})_i + \beta_2(\textit{Subestuary})_i + \beta_3(\textit{Flow}_{30 \text{ day lag}}) + \varepsilon_i$	347.6	-8342.2	197.7
$Y = \beta_0 + \beta_1(\textit{Year})_i + \beta_2(\textit{Subestuary})_i + \beta_3(\textit{Flow}_{60 \text{ day lag}}) + \varepsilon_i$	347.8	-8347.1	192.8
$Y = \beta_0 + \beta_1(\textit{Year})_i + \beta_2(\textit{Subestuary})_i + \beta_3(\textit{Chla}_{30 \text{ day lag}}) + \beta_4(\textit{Temp}_{30 \text{ day lag}}) + \varepsilon_i$	327.8	-8523.3	16.60
$Y = \beta_0 + \beta_1(\textit{Year})_i + \beta_2(\textit{Subestuary})_i + \beta_3(\textit{Chla}_{30 \text{ day lag}}) + \beta_4(\textit{Temp}_{60 \text{ day lag}}) + \varepsilon_i$	326.8	-8495.5	44.40

$Y = \beta_0 + \beta_1(\text{Year})_i + \beta_2(\text{Subestuary})_i + \beta_3(\text{Chla}_{60 \text{ day lag}}) + \beta_4(\text{Temp}_{30 \text{ day lag}}) + \varepsilon_i$	324.5	-8459.4	80.50
$Y = \beta_0 + \beta_1(\text{Year})_i + \beta_2(\text{Subestuary})_i + \beta_3(\text{Chla}_{60 \text{ day lag}}) + \beta_4(\text{Temp}_{60 \text{ day lag}}) + \varepsilon_i$	324.9	-8447.8	92.10
$Y = \beta_0 + \beta_1(\text{Year})_i + \beta_2(\text{Subestuary})_i + \beta_3(\text{Chla}_{30 \text{ day lag}}) + \beta_4(\text{Flow}_{30 \text{ day lag}}) + \varepsilon_i$	322.7	-8391.0	148.9
$Y = \beta_0 + \beta_1(\text{Year})_i + \beta_2(\text{Subestuary})_i + \beta_3(\text{Chla}_{60 \text{ day lag}}) + \beta_4(\text{Flow}_{30 \text{ day lag}}) + \varepsilon_i$	320.9	-8342.4	197.5
$Y = \beta_0 + \beta_1(\text{Year})_i + \beta_2(\text{Subestuary})_i + \beta_3(\text{Chla}_{30 \text{ day lag}}) + \beta_4(\text{Flow}_{60 \text{ day lag}}) + \varepsilon_i$	322.8	-8393.8	146.1
$Y = \beta_0 + \beta_1(\text{Year})_i + \beta_2(\text{Subestuary})_i + \beta_3(\text{Chla}_{60 \text{ day lag}}) + \beta_4(\text{Flow}_{60 \text{ day lag}}) + \varepsilon_i$	321.1	-8347.4	192.5
$Y = \beta_0 + \beta_1(\text{Year})_i + \beta_2(\text{Subestuary})_i + \beta_3(\text{Temp}_{30 \text{ day lag}}) + \beta_4(\text{Flow}_{30 \text{ day lag}}) + \varepsilon_i$	325.0	-8450.5	89.40
$Y = \beta_0 + \beta_1(\text{Year})_i + \beta_2(\text{Subestuary})_i + \beta_3(\text{Temp}_{60 \text{ day lag}}) + \beta_4(\text{Flow}_{30 \text{ day lag}}) + \varepsilon_i$	324.5	-8437.0	102.9
$Y = \beta_0 + \beta_1(\text{Year})_i + \beta_2(\text{Subestuary})_i + \beta_3(\text{Temp}_{30 \text{ day lag}}) + \beta_4(\text{Flow}_{60 \text{ day lag}}) + \varepsilon_i$	325.1	-8453.6	86.30
$Y = \beta_0 + \beta_1(\text{Year})_i + \beta_2(\text{Subestuary})_i + \beta_3(\text{Temp}_{60 \text{ day lag}}) + \beta_4(\text{Flow}_{60 \text{ day lag}}) + \varepsilon_i$	324.6	-8447.8	92.10
$Y = \beta_0 + \beta_1(\text{Year})_i + \beta_2(\text{Subestuary})_i + \beta_3(\text{Chla}_{30 \text{ day lag}}) + \beta_4(\text{Temp}_{30 \text{ day lag}}) + \beta_5(\text{Flow}_{30 \text{ day lag}}) + \varepsilon_i$	305.0	-8539.9	0.000
$Y = \beta_0 + \beta_1(\text{Year})_i + \beta_2(\text{Subestuary})_i + \beta_3(\text{Chla}_{30 \text{ day lag}}) + \beta_4(\text{Temp}_{30 \text{ day lag}}) + \beta_5(\text{Flow}_{60 \text{ day lag}}) + \varepsilon_i$	304.9	-8536.1	3.800
$Y = \beta_0 + \beta_1(\text{Year})_i + \beta_2(\text{Subestuary})_i + \beta_3(\text{Chla}_{30 \text{ day lag}}) + \beta_4(\text{Temp}_{60 \text{ day lag}}) + \beta_5(\text{Flow}_{30 \text{ day lag}}) + \varepsilon_i$	303.8	-8507.0	32.90
$Y = \beta_0 + \beta_1(\text{Year})_i + \beta_2(\text{Subestuary})_i + \beta_3(\text{Chla}_{30 \text{ day lag}}) + \beta_4(\text{Temp}_{60 \text{ day lag}}) + \beta_5(\text{Flow}_{60 \text{ day lag}}) + \varepsilon_i$	303.8	-8504.9	35.00
$Y = \beta_0 + \beta_1(\text{Year})_i + \beta_2(\text{Subestuary})_i + \beta_3(\text{Chla}_{60 \text{ day lag}}) + \beta_4(\text{Temp}_{30 \text{ day lag}}) + \beta_5(\text{Flow}_{30 \text{ day lag}}) + \varepsilon_i$	302.7	-8475.4	64.50
$Y = \beta_0 + \beta_1(\text{Year})_i + \beta_2(\text{Subestuary})_i + \beta_3(\text{Chla}_{60 \text{ day lag}}) + \beta_4(\text{Temp}_{30 \text{ day lag}}) + \beta_5(\text{Flow}_{60 \text{ day lag}}) + \varepsilon_i$	302.8	-8478.7	61.20
$Y = \beta_0 + \beta_1(\text{Year})_i + \beta_2(\text{Subestuary})_i + \beta_3(\text{Chla}_{60 \text{ day lag}}) + \beta_4(\text{Temp}_{60 \text{ day lag}}) + \beta_5(\text{Flow}_{30 \text{ day lag}}) + \varepsilon_i$	302.2	-8460.6	79.30
$Y = \beta_0 + \beta_1(\text{Year})_i + \beta_2(\text{Subestuary})_i + \beta_3(\text{Chla}_{60 \text{ day lag}}) + \beta_4(\text{Temp}_{60 \text{ day lag}}) + \beta_5(\text{Flow}_{60 \text{ day lag}}) + \varepsilon_i$	302.3	-8463.2	76.70

Table 4. Tolerance effects for variables in the ANCOVA model of mean body condition (Fulton’s K) as a function of year class (2009-2017), subestuary (James or Rappahannock), and 30-day lagged chlorophyll-a, temperature, and flow (covariates). Tolerance values for the “Year: 2009” and “Subestuary: James” effects were not calculated because these effects are included in the intercept of the ANCOVA. Tolerance values less than 0.1 indicate collinearity among variables. There is no collinearity present among these variables.

Effect	Tolerance
Year: 2010	0.45
Year: 2011	0.33
Year: 2012	0.83
Year: 2013	0.30
Year: 2014	0.32
Year: 2015	0.25
Year: 2016	0.20
Year: 2017	0.12
Subestuary: Rappahannock	0.23
Temperature	0.32
Chlorophyll-a	0.18
Flow	0.60

Table 5. Residual sum-of-squares (RSS), Akaike’s Information Criterion (AIC), and Δ AIC for models M_1 - M_{10} fitted to juvenile striped bass weight-at-age data collected from the 2011, 2016, and 2017 year classes within the James and Rappahannock subestuaries of the Chesapeake Bay.

Model	Covariates	Effect on	RSS	No. of Parameters	AIC	ΔAIC
M_1	None		149.7	3	797.2	96.9
M_2	Year class	β_{W_0}	138.5	5	465.2	64.8
M_3	Year class	β_G	139.7	5	769.1	68.8
M_4	Year class	β_{W_0}, β_G	135.3	7	758.4	58.1
M_5	Subestuary	β_{W_0}	133.2	4	745.2	44.9
M_6	Subestuary	β_G	131.9	4	740.6	40.2
M_7	Subestuary	β_{W_0}, β_G	131.2	5	740.2	39.9
M_8	Year class, subestuary	β_{W_0}	124.7	6	718.7	18.3
M_9	Year class, subestuary	β_G	122.3	6	709.6	9.3
M_{10}	Year class, subestuary	β_{W_0}, β_G	118.3	9	700.3	0.0

Table 6. Estimates and 95% confidence intervals (in parentheses) of weight-specific instantaneous growth rates (G, g/day), instantaneous daily mortality rates (Z, day⁻¹), and recruitment potential (G:Z) for juvenile striped bass from the James and Rappahannock subestuaries. The juvenile recruitment index values were provided by the VIMS seine survey (Gallagher *et al.* 2018).

Subestuary	Year class	G	Z	G:Z	Juvenile recruitment index (VIMS seine survey)
James	2011	0.04	0.09 (0.07-0.12)	0.44	10.64
	2016	0.03	0.12 (0.08-0.17)	0.25	5.48
	2017	0.04	0.19 (0.07-0.30)	0.21	5.57
Rappahannock	2011	0.02	0.13 (0.06-0.20)	0.15	10.72
	2016	0.01	0.09 (0.04-0.14)	0.11	3.71
	2017	0.02	0.12 (0.06-0.18)	0.22	5.44

Figure 1. Location of VIMS seine survey sites from which juvenile striped bass were collected from the 2009 to 2017 year classes in the James and Rappahannock subestuaries of the Chesapeake Bay.

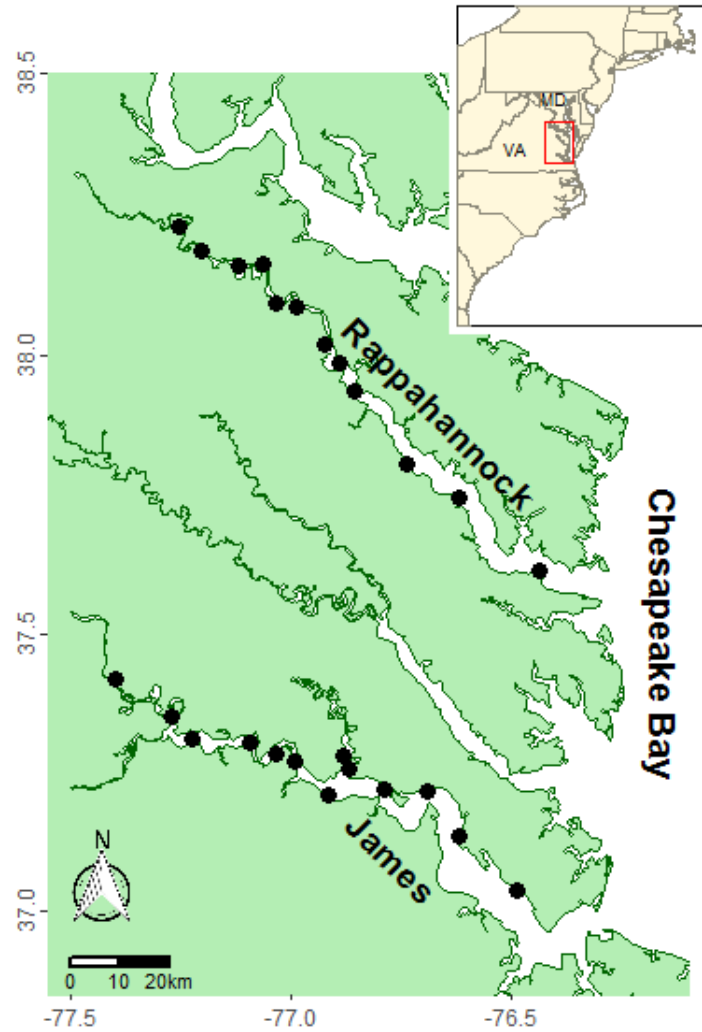


Figure 2. Location of temperature stations (TF = tidal fresh zone, RET = riverine-estuarine transition zone, LE = lower estuarine zone) monitored by the Chesapeake Bay Program. Daily temperature values were linearly interpolated from approximately biweekly observations at each site. Daily chlorophyll-a values were also linearly interpolated using approximately biweekly observations collected at each site.

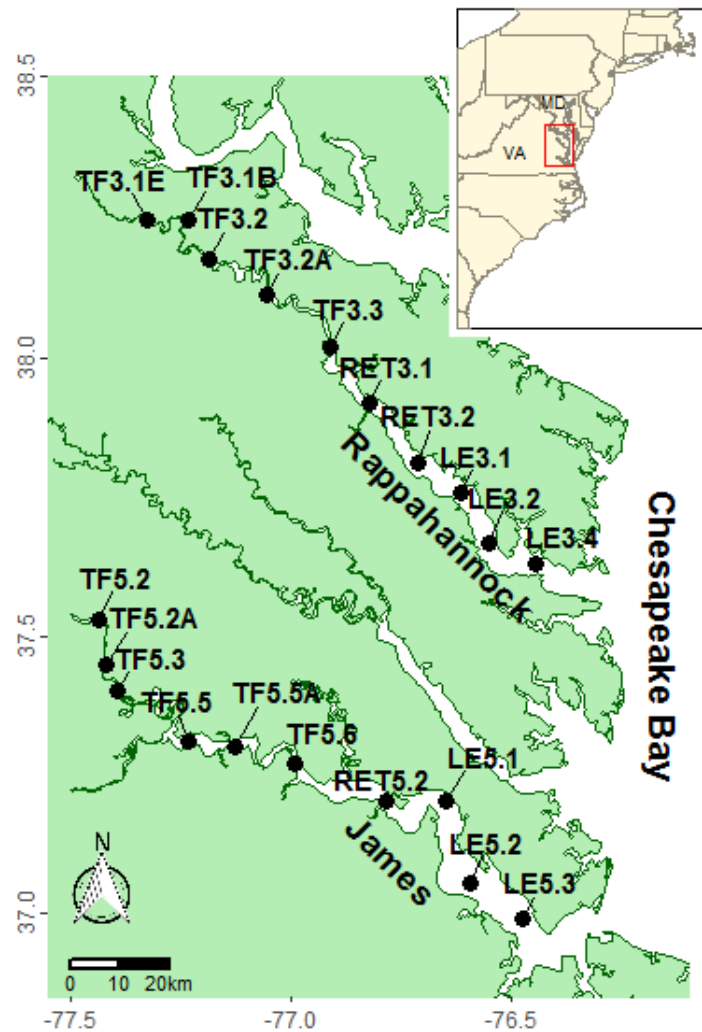
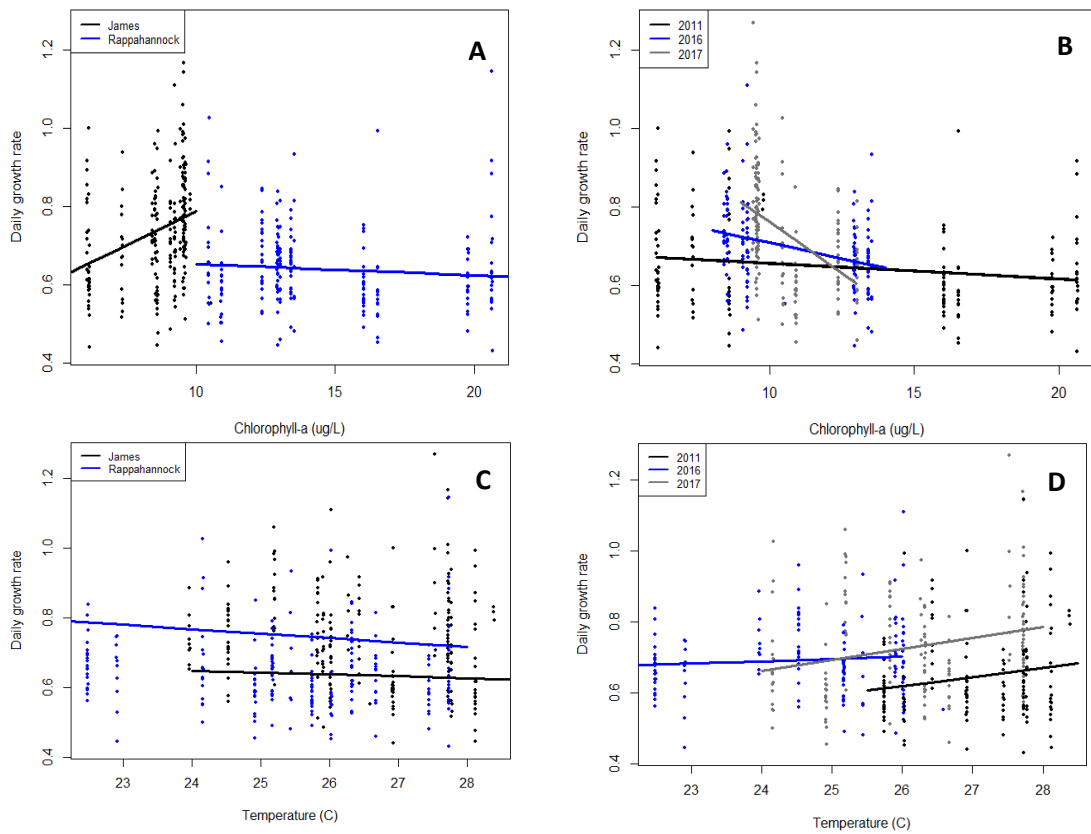
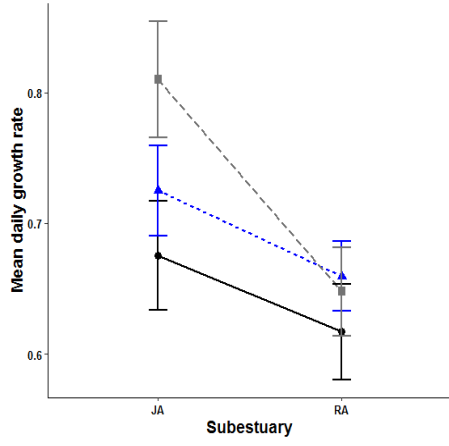


Figure 3. Interaction plots for year, subestuary, 60-day lagged chlorophyll-a, and 30-day lagged temperature for the model of daily growth rates for the 2011, 2016, and 2017 year classes of juvenile striped bass in the James (JA) and Rappahannock (RA) subestuaries of the Chesapeake Bay. Panels A-D show the interaction between the categorical factors (subestuary and year class) and the continuous covariates (60-day lagged chlorophyll-a and 30-day lagged temperature). The points represent the observed chlorophyll-a (A and B) and temperature (C and D) associated with daily growth rates, and the solid lines represent the effect of the covariate on daily growth rate for each categorical variable. For example, in panel A, chlorophyll-a has a positive effect on daily growth rate in the James (black), but a negative effect on daily growth rate of fish in the Rappahannock subestuary (blue). Panel E shows the interaction plot between subestuary and year class. Panel F shows the interaction plot between the two covariates, where 60-day lagged chlorophyll-a is grouped into three bins (0.0-9.4 $\mu\text{g/L}$, N = 147; 9.5-12.4 $\mu\text{g/L}$, N = 132; 12.5-21.0 $\mu\text{g/L}$, N = 150) and 30-day lagged temperature is grouped into two bins (black: 22.0-25.0°C, N = 196; blue: 25.0-30.0°C, N = 233). The vertical bars on the points in panels E and F represent the 95% confidence interval. Generally, interactions are indicated when lines intersect and, for panels E and F, if lines intersect and confidence intervals do not overlap. There were no appreciable interactions between temperature and subestuary (C), subestuary and year class (E), and chlorophyll-a and temperature (F). Although it appeared that interactions occurred between chlorophyll-a and year class (B) and temperature and year class (D) because the lines for each group

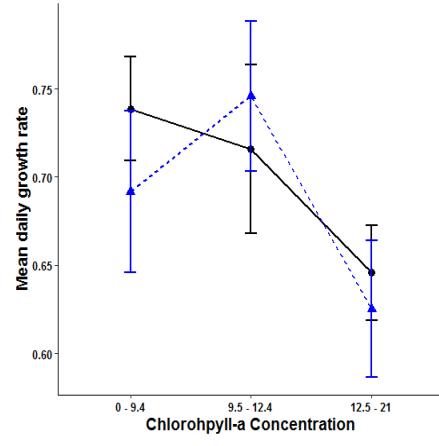
intersect, the variability in the observed points is high, which suggests that an interaction cannot be determined. The interaction plot showing subestuary and chlorophyll-a concentrations (A) shows an interaction between subestuary and 60-day lagged chlorophyll-a, such that there is an effect of 60-day lagged chlorophyll-a on daily growth rates of fish in the James, but not in the Rappahannock subestuary.





E

Year
 ● 2011
 ▲ 2016
 ■ 2017



F

Temp
 ● 22 - 25
 ▲ 26 - 30

Figure 4. Diagnostic plots for the analysis of covariance where daily growth rate was a function of year class (2011, 2016, and 2017) and subestuary (James or Rappahannock).

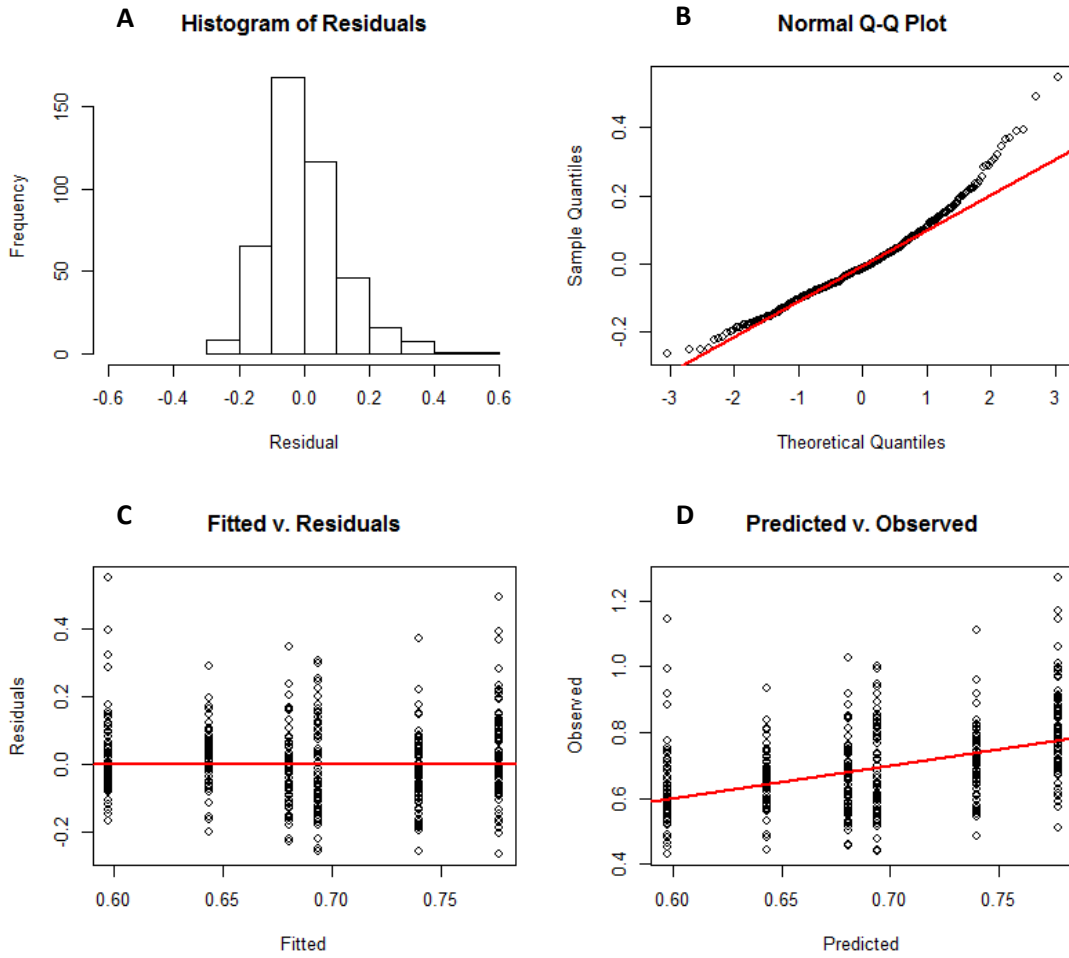


Figure 5. Estimated least-squares (LS) mean daily growth rates for 3 year classes of juvenile striped bass in the James (black dots) and the Rappahannock (gray dots) subestuaries. These LS means are derived from an ANCOVA in which daily growth rate is a function of year class and subestuary. The vertical bars indicate the 95% confidence intervals.

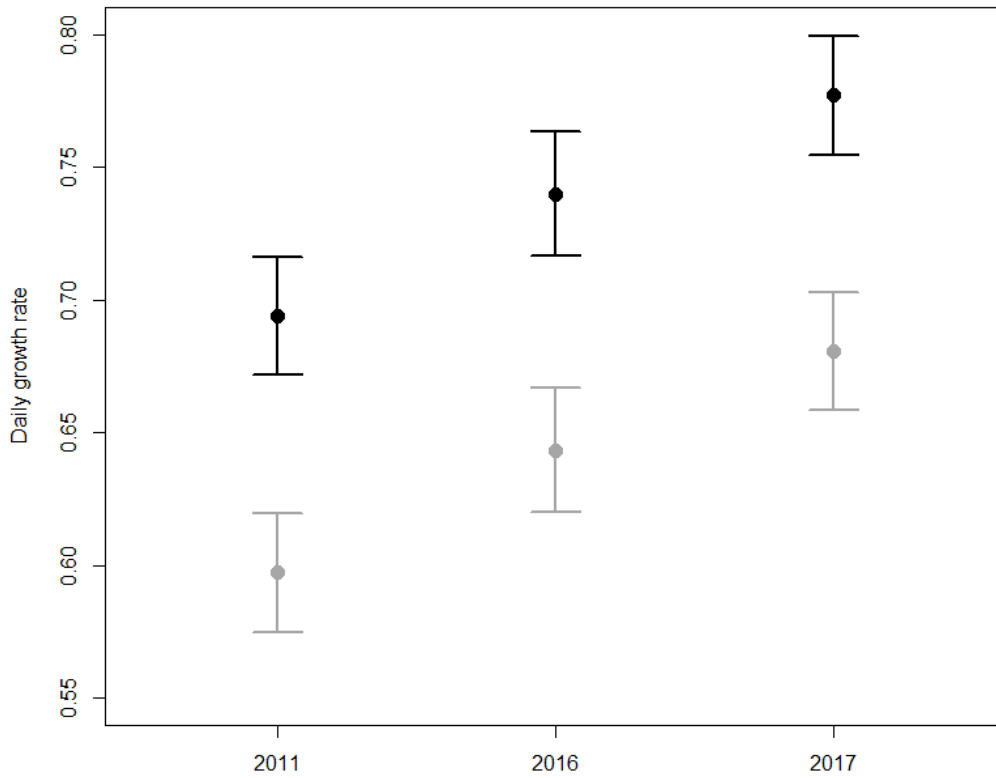
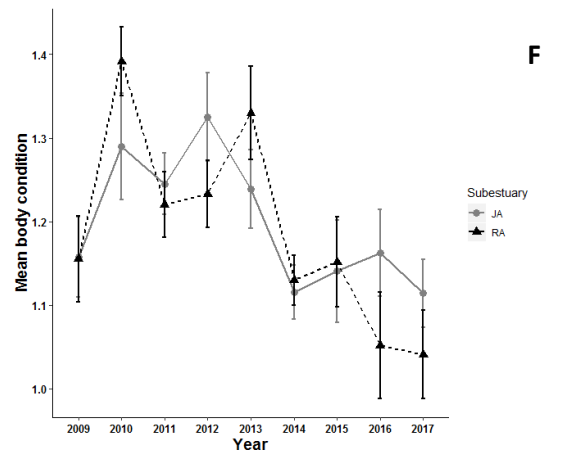
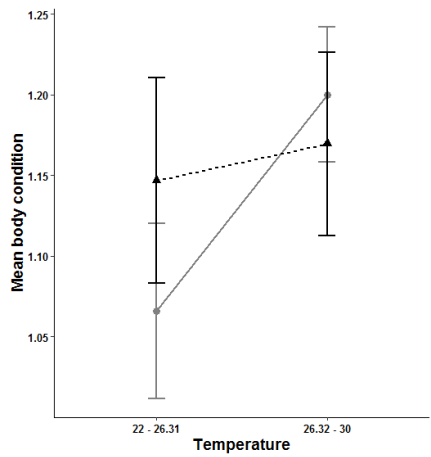
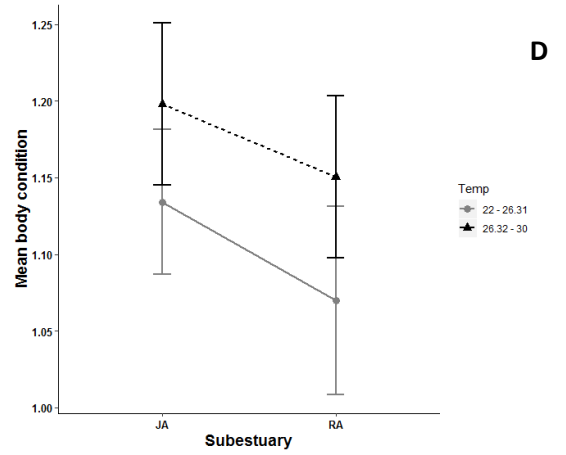
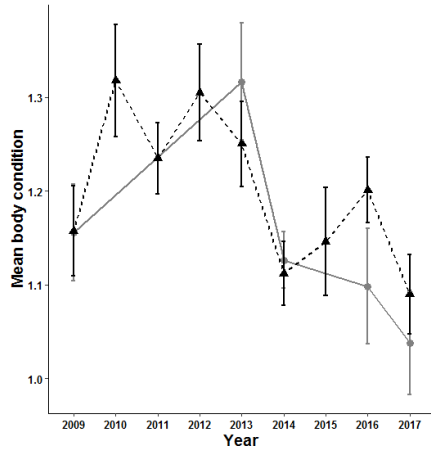
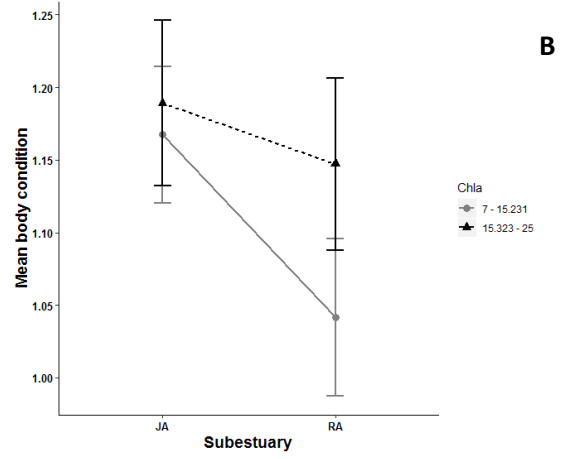
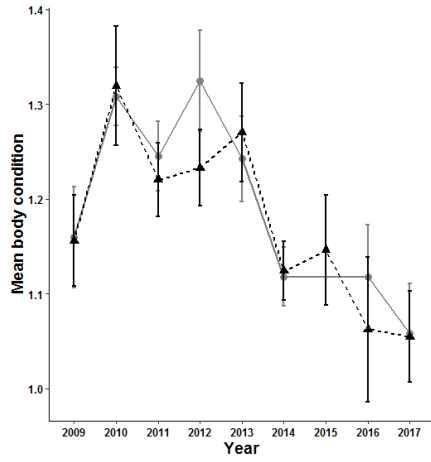


Figure 6. Interaction plots for year, subestuary, 30-day lagged chlorophyll-a, 30-day lagged temperature, and 30-day lagged flow for nine year classes (2009-2017) of juvenile striped bass in the James (JA) and Rappahannock (RA) subestuaries of the Chesapeake Bay. The vertical bars represent the 95% confidence interval. An interaction is indicated when the lines in the figures intersect. If the confidence intervals overlap there is not a significant interaction between factors. There is no interaction observed for year and chlorophyll-a concentrations (A), subestuary and chlorophyll-a concentrations (B), year and temperature (C), subestuary and temperature (D), or year and subestuary (F). The interaction plot of temperature and chlorophyll-a (E) depicts an intersection for the lines corresponding to low (7-15.231 $\mu\text{g/L}$; black) and high (15.323-25 $\mu\text{g/L}$; gray) concentrations of chlorophyll-a; however, the confidence intervals around the mean response for high and low concentrations of chlorophyll-a overlap for low (22.00-26.31°C) and high (26.32-30.00°C) temperature, which indicated a lack of interaction between the two factors. A similar pattern can be observed in the interaction plots for year and flow (G), subestuary and flow (H), chlorophyll and flow (I), and temperature and flow (J).



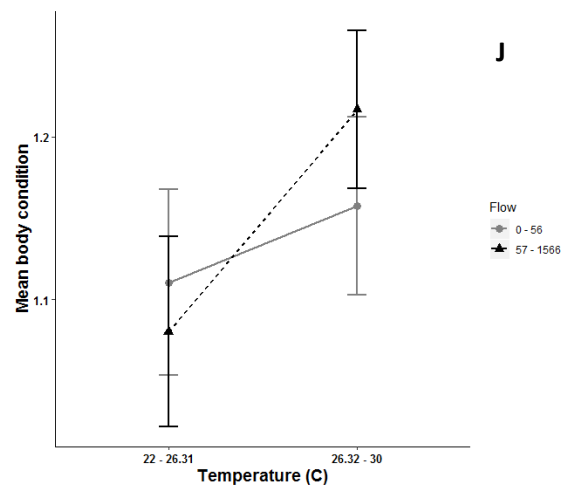
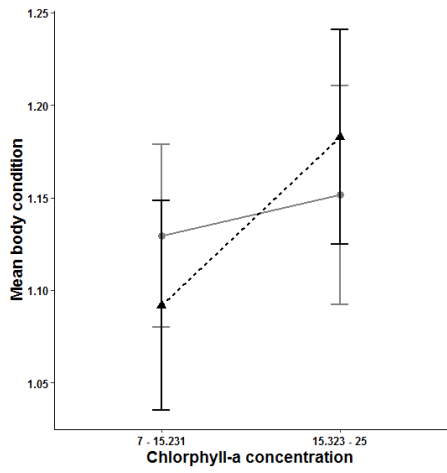
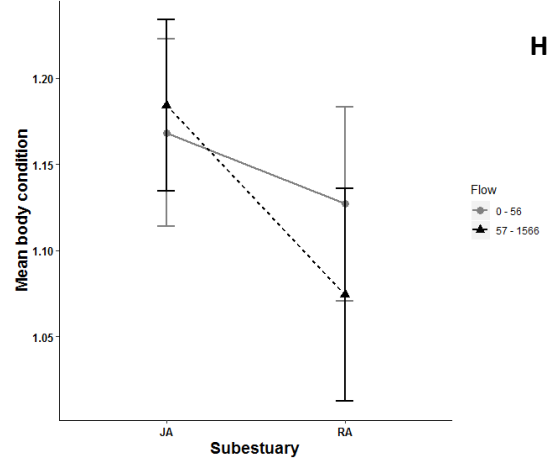
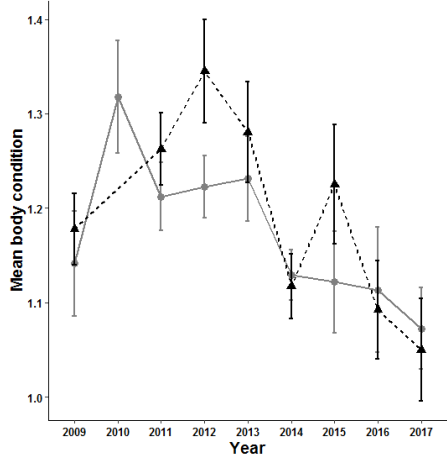


Figure 7. Diagnostic plots for the ANCOVA where body condition (Fulton's K) was a function of year class (2011, 2016, and 2017), subestuary (James and Rappahannock), 30-day lagged temperature, chlorophyll-a, and flow.

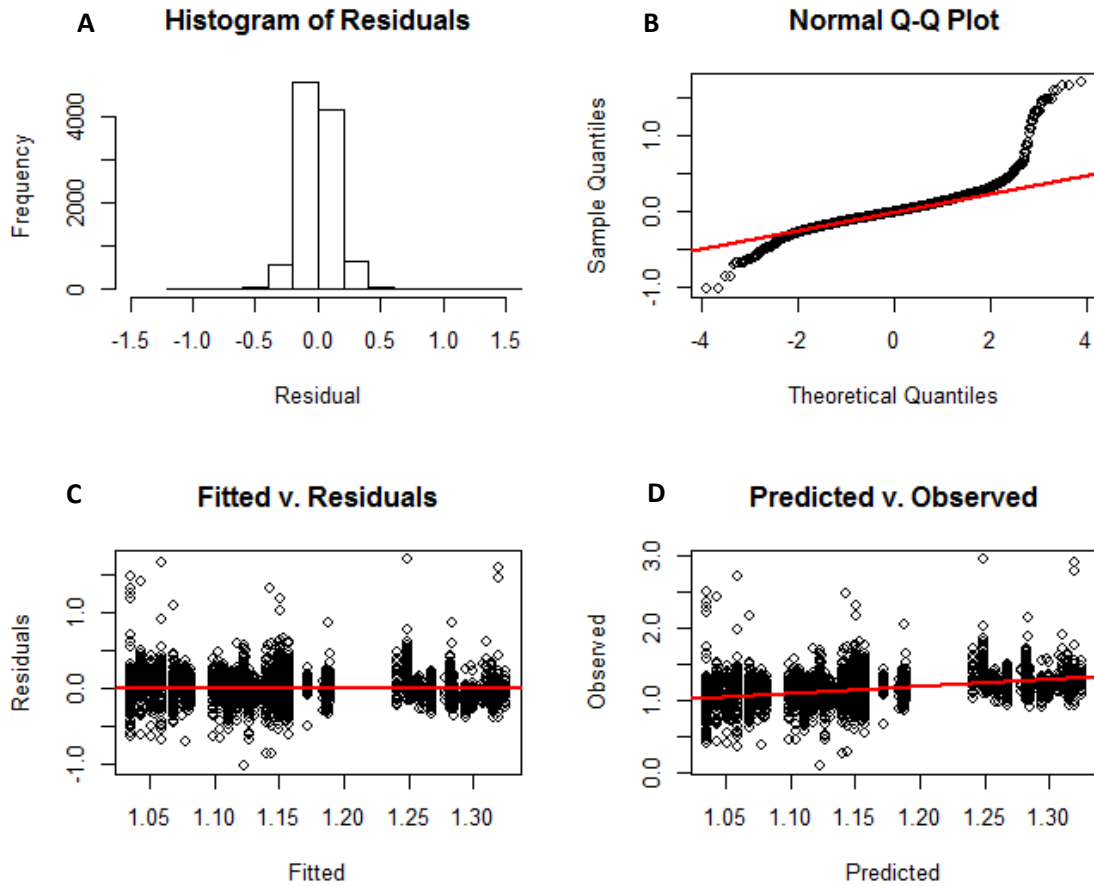


Figure 8. Estimated least-square means for body condition, adjusted for the effects of temperature chlorophyll-a and flow, for nine year classes of juvenile striped bass in the James (black) and Rappahannock (gray) subestuaries. These least-square means were estimated from the ANCOVA in which body condition (Fulton's K) was a function of year class, subestuary, 30-day lagged temperature, 30-day lagged chlorophyll-a, and 30-day lagged flow.

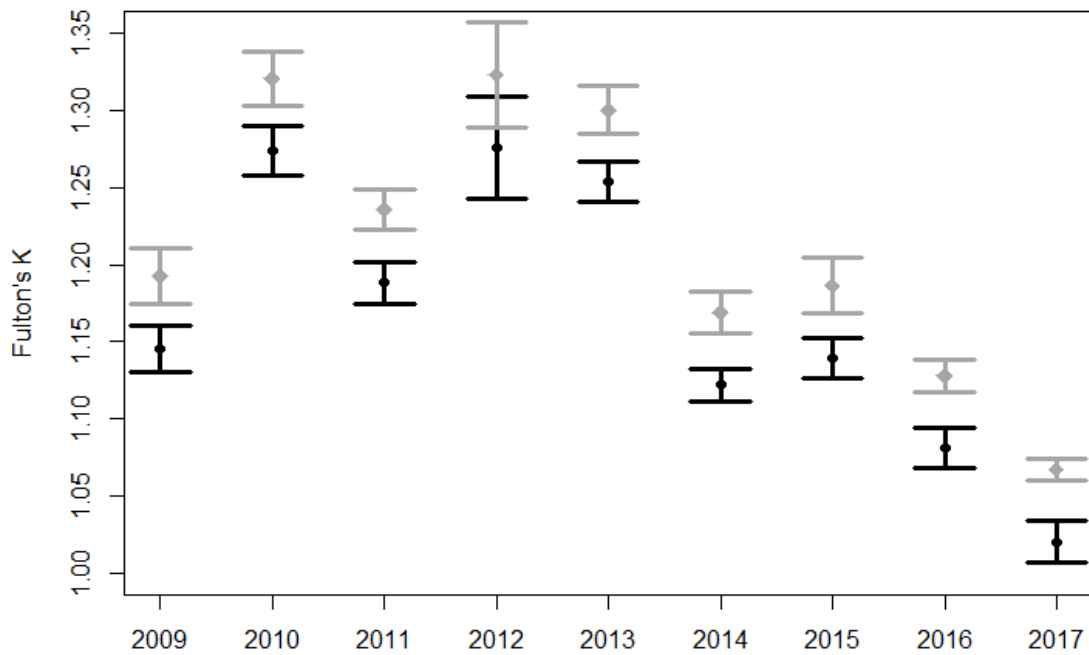


Figure 9. The partial regression plot showing the effect of 30-day lagged temperature, holding all other factors constant, on mean body condition (Fulton's K) of juvenile striped bass, from the ANCOVA in which body condition is a function of year class, subestuary, and 30-day lagged temperature, chlorophyll-a, and flow. For every one degree increase in temperature, mean body condition increased by 0.021 (95% CI: 0.018 – 0.024) units. The dashed red lines represent the 95% confidence interval.

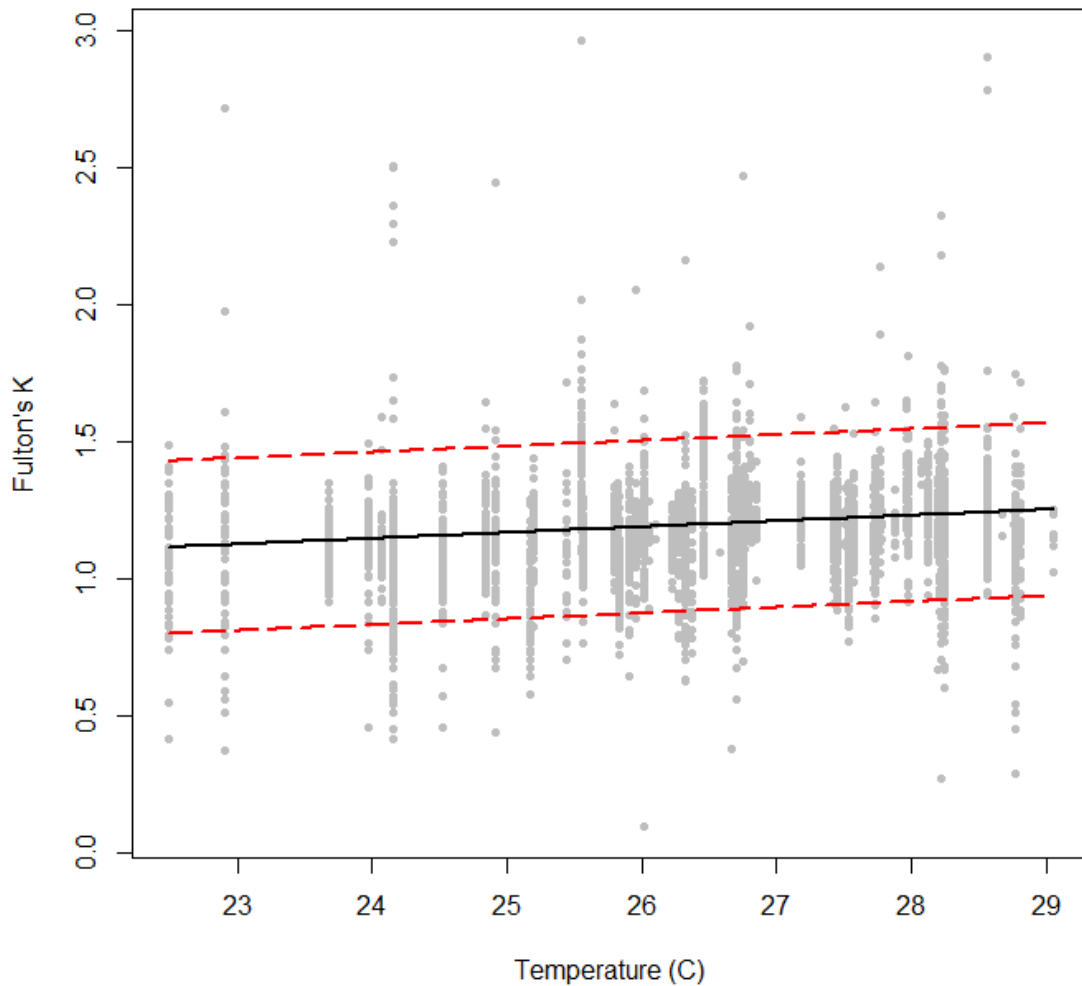


Figure 10. The partial regression plot showing the effect of 30-day lagged chlorophyll-a, holding all other factors constant, on mean body condition (Fulton's K) of juvenile striped bass, from the ANCOVA in which body condition is a function of year class, subestuary, and 30-day lagged temperature, chlorophyll-a, and flow. For every one $\mu\text{L/g}$ increase in chlorophyll-a, mean body condition decreased by 0.009 (95% CI: 0.007 – 0.011) units. The dashed red lines represent the 95% confidence interval.

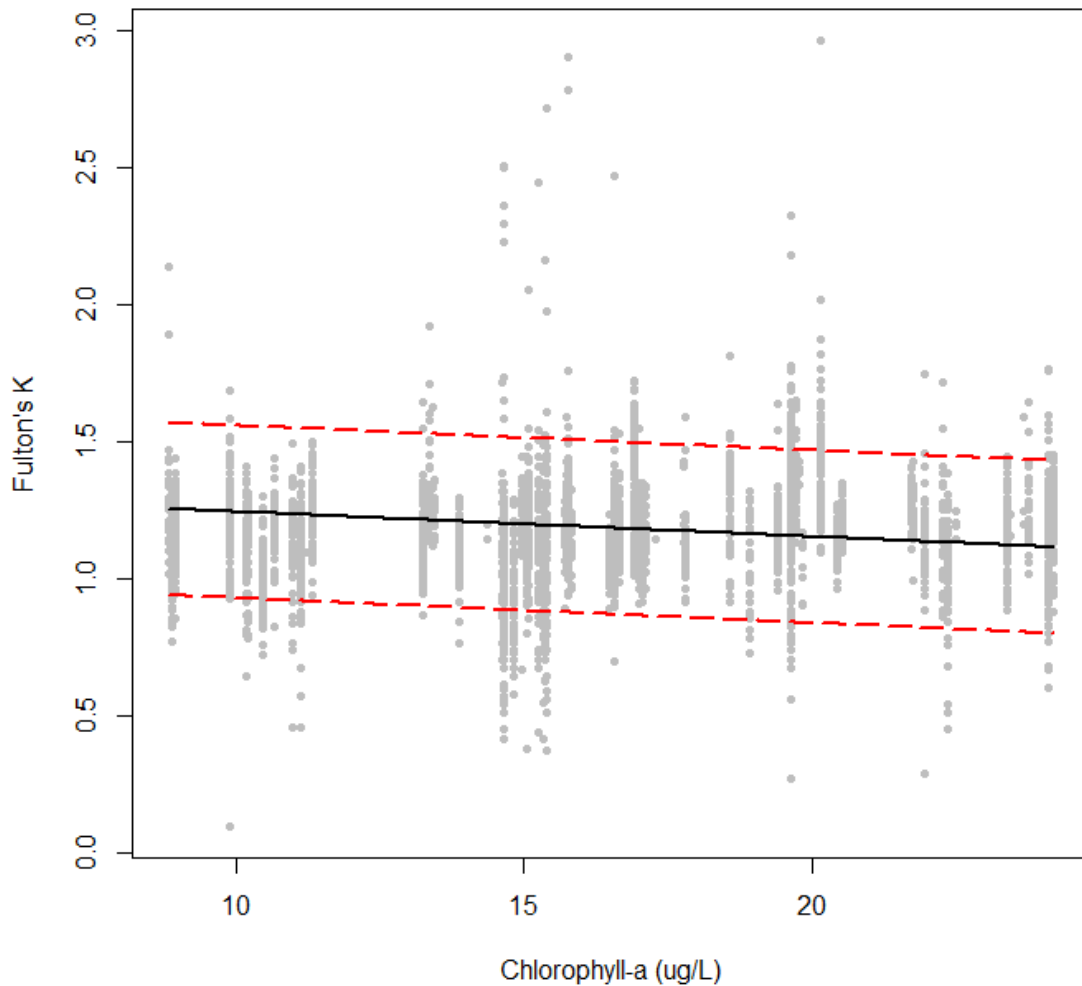


Figure 11. The partial regression plot showing the effect of 30-day lagged flow, holding all other factors constant, on mean body condition (Fulton's K) of juvenile striped bass, from the ANCOVA in which body condition is a function of year class, subestuary, and 30-day lagged temperature, chlorophyll-a, and flow. For every one m³/sec increase in flow, mean body condition increased by 0.00010 (95% CI: 0.00005 – 0.00014) units. The dashed red lines represent the 95% confidence interval.

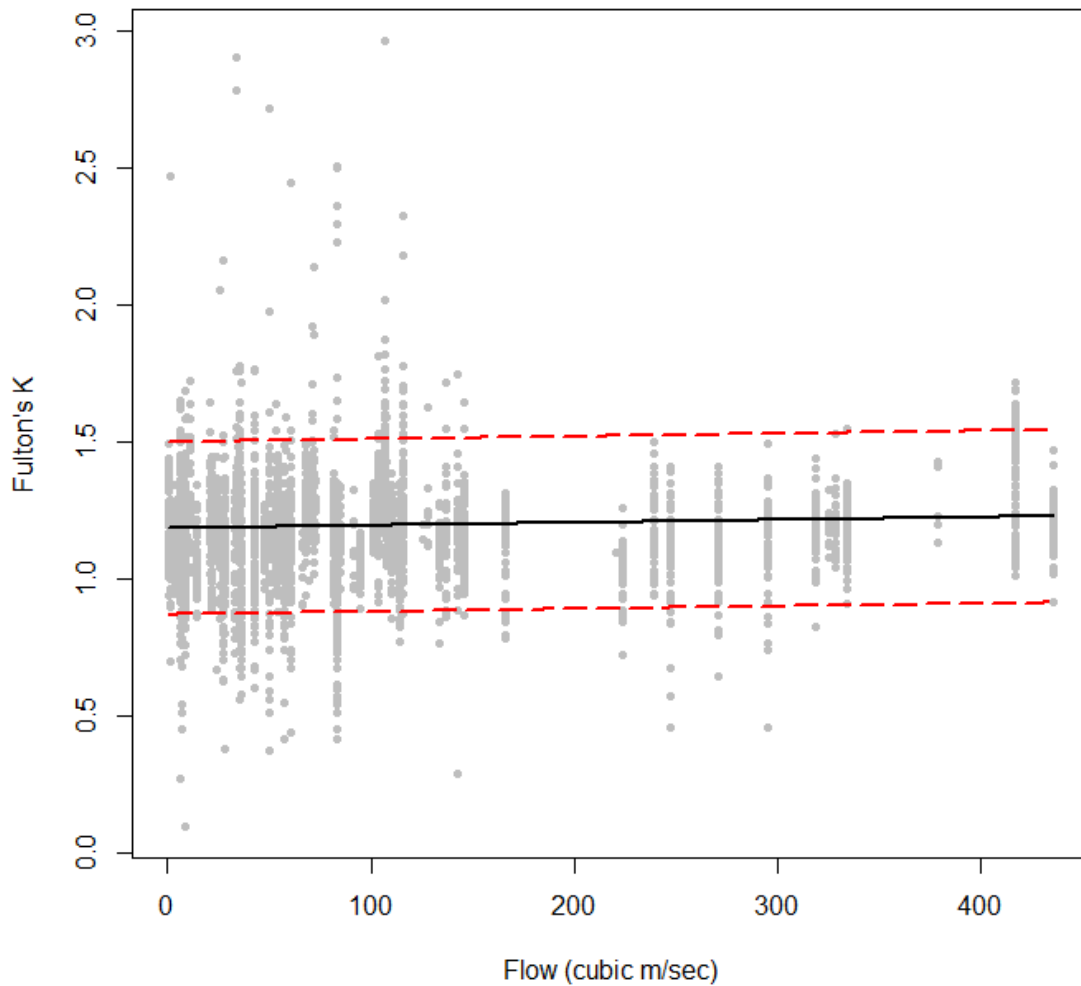


Figure 12. Mean body condition of juvenile striped bass in the James and Rappahannock subestuaries from 2009 to 2017. Body condition (Fulton's K) was modeled as a function of year, and the estimated breakpoint occurred in 2011. The solid line represents the effect of year on body condition from 2009 to 2012, and the dotted line represents the effect of year on body condition from 2012 to 2017. The red circle represents the breakpoint, or point at which the effect of year on body condition changes. The gray shading represent the 95% confidence interval.

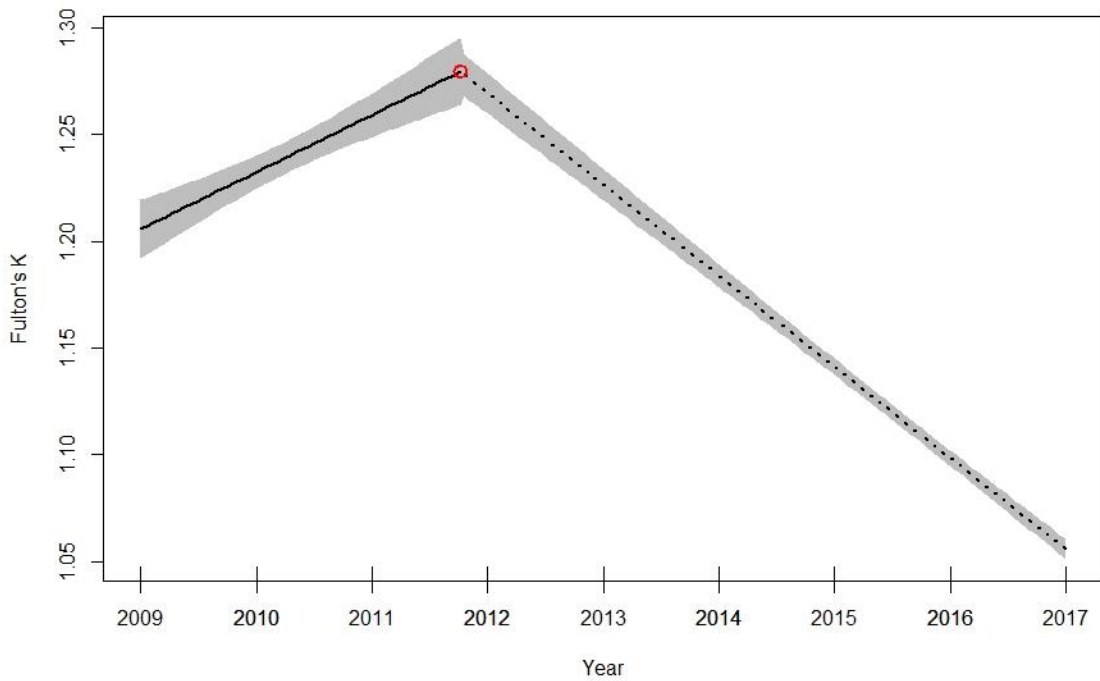


Figure 13. Diagnostic plots for the exponential growth model where known weights and otolith-derived daily ages of the 2011, 2016, and 2017 year classes of juvenile striped bass within the James and Rappahannock subestuaries were used to estimate weight-specific instantaneous growth rates (G) and weight at hatch (W_0). Panel A showed that the assumption of normality is met and panel B showed that the assumption of homogeneity of variance was reasonable.

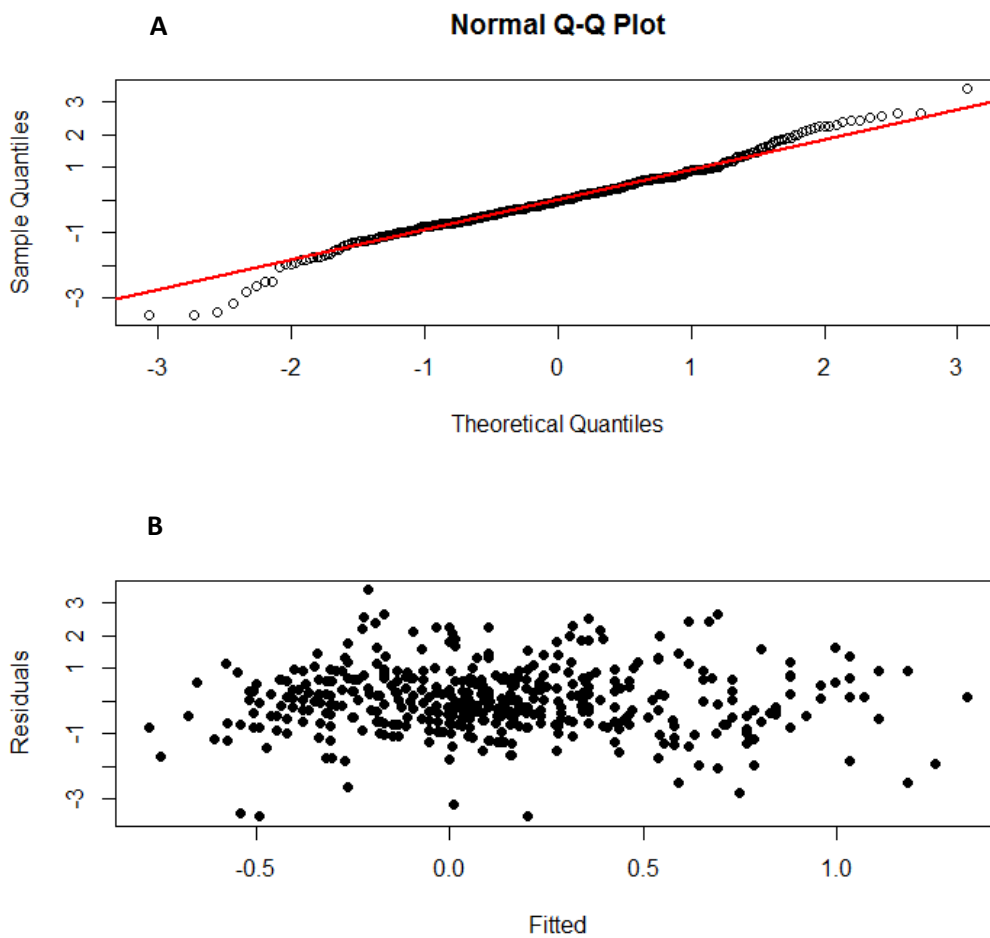


Figure 14. Observed weight-at-age (dots) and predicted exponential growth curves from model M_{10} for juvenile striped bass from the 2011 (black), 2016 (blue), and 2017 (gray) year classes within the (A) James and (B) Rappahannock subestuaries of the Chesapeake Bay.

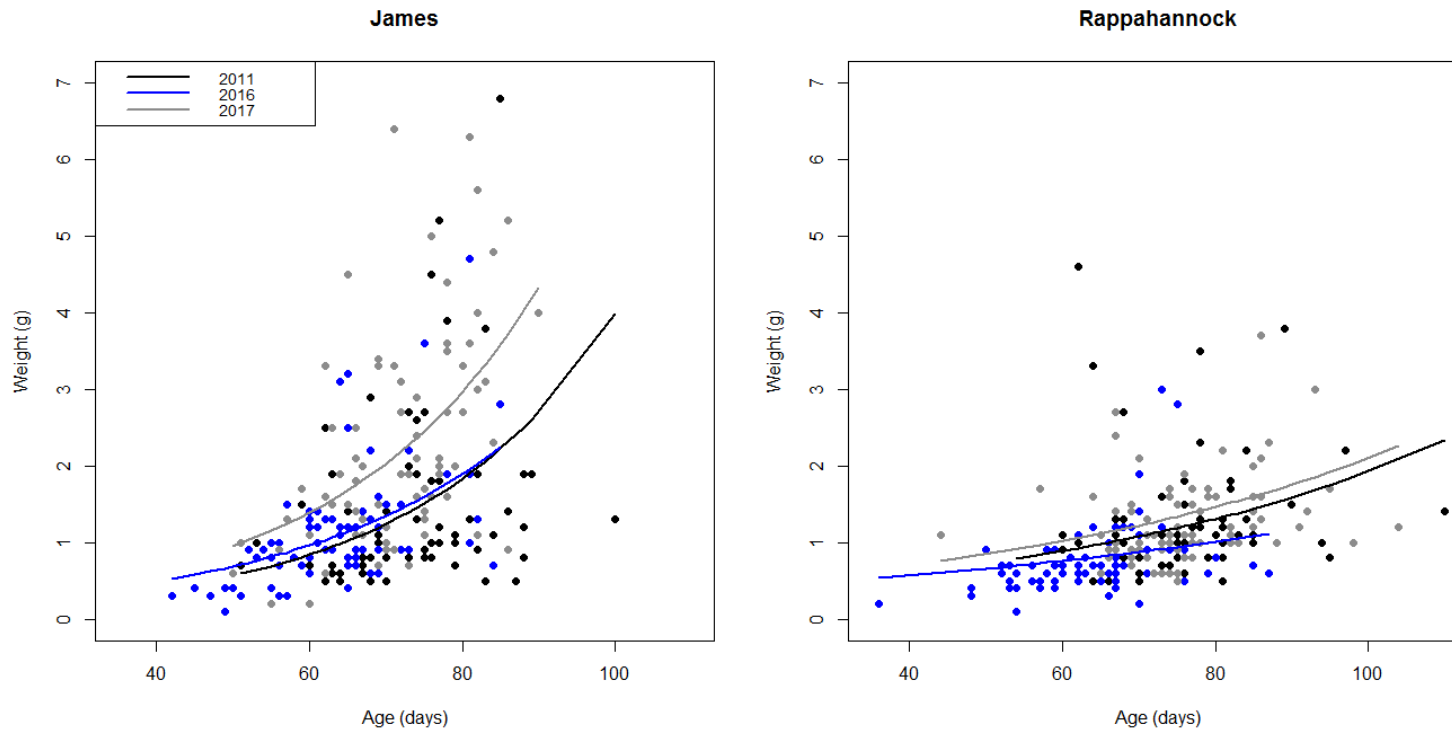
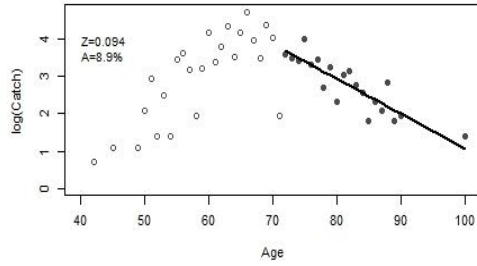


Figure 15. The catch curves used to estimate daily Z values for the 2011 (A), 2016 (C), and 2017 (E) year classes in the James subestuary and the 2011 (B), 2016 (D), and 2017 (F) year classes in the Rappahannock subestuary. The points represent log-transformed catch at each daily age. The solid points represent the juvenile striped bass that were fully recruited to the gear. Daily Z values were estimated using the slope of the black line. Z (instantaneous daily mortality rate) and A (discrete daily mortality rate calculated as $1 - e^{-Z}$) for each year class within each subestuary are indicated on each plot.

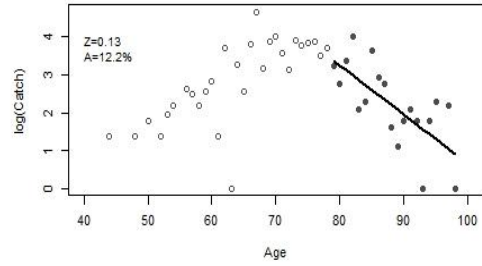
JAMES

2011

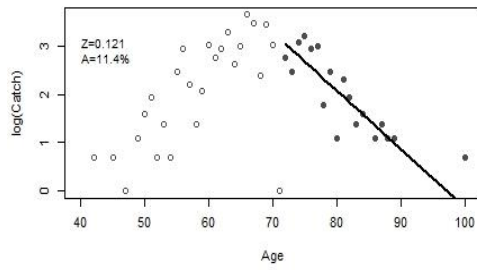


RAPPAHANNOCK

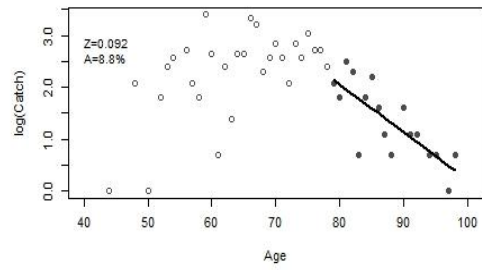
2011



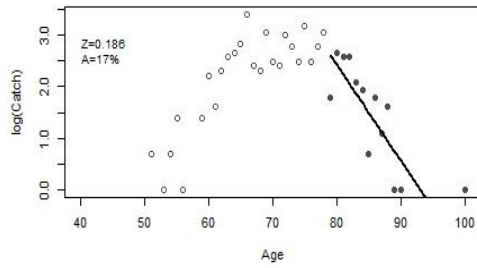
2016



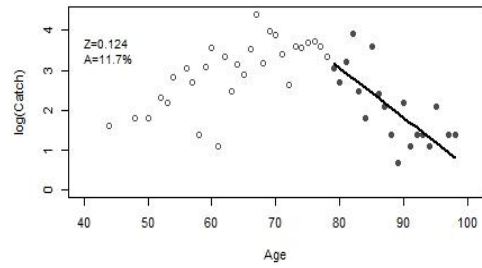
2016



2017



2017



CONCLUSIONS

In this thesis I evaluated and compared characteristics of juvenile striped bass across pre-recovery (1986 to 1994) and post-recovery (1995 to 2017) periods in the James and Rappahannock of the Chesapeake Bay. To characterize recruitment of juvenile striped bass during a period of recent population decline I further examined characteristics of year classes within the post-recovery period. Hatch timing, mortality, growth rates, and body condition of juvenile striped bass were measured, as well as effects of temperature, freshwater flow, and chlorophyll-a concentrations on these measurements, which can be used to characterize incoming year classes of juvenile striped bass and perhaps predict their potential contribution to the striped bass fishery. Further, managers may use the information reported in this thesis to better guide regulations aimed at returning the current striped bass fishery to sustainable levels.

In Chapter 1, daily ages were projected for 32 year classes of juvenile striped bass within the James and Rappahannock subestuaries with subestuary-specific age-length keys. Together with catch data, projected daily ages were used to estimate instantaneous daily mortality rates and hatch-date distributions for each year class. Because environmental conditions in the Chesapeake Bay have changed, I expected to observe significantly different mortality rates between the pre-recovery period and the post-recovery period. However, I observed relatively constant juvenile mortality rates between the two periods, as well as, among the 32 year classes and across the James and Rappahannock subestuaries. Mortality rates stabilize by the juvenile stage, and thus, instantaneous daily mortality rates

at an earlier life stage (e.g., larval) would likely be higher and show more variability, and thus may provide a better indication of differences in survival of young striped bass across year classes. If, however, mortality rates are in fact constant across the 32 year classes assessed in this study, then perhaps hatch timing shifted in such a way that the same proportion of young striped bass still encounter favorable (or unfavorable) environmental conditions today as compared to those in the pre-recovery period. Mean hatch dates are significantly earlier today than they were prior to 1995. Further, the first, last, median, and peak hatch dates shifted earlier as well, suggesting that entire hatch-date distribution, not just mean hatch date, shifts earlier as the years progress, which indicates a potential shift in adult spawning. The positive correlation between temperature during hatching and mean hatch date is likely associated with timing. That is, striped bass hatch from late-March to early-June, as waters warm from spring into summer. Note that as temperatures warm, waters within the Chesapeake Bay reach higher temperatures earlier, and thus, hatch dates can be expected to shift earlier. Further, because hatching and spawning are closely associated these results indicate that spawning may occur earlier today than it did prior to 1995, which supports the earlier spawning migrations observed by Peer and Miller (2014).

In Chapter 2, otolith-derived daily ages were estimated for juvenile striped bass from three year classes associated with high (2011), low (2016), and average (2017) recruitment strength in the James and Rappahannock subestuaries. Together with lengths, weights, and catch data (VIMS seine survey), daily ages

were used to estimate the ratio of weight-specific instantaneous growth rate and instantaneous mortality rate, recruitment potential (G:Z), and daily growth rates. Recruitment potential was less than one for all year classes and within both subestuaries, indicating that these year classes of juvenile striped bass lost more biomass through mortality than they gained through weight-specific growth. However, because recruitment potential did not mirror the variability observed in the recruitment index, I concluded that recruitment potential measured during the juvenile stage may not be the best metric to assess recruitment of juvenile striped bass. Further, there is an observed relationship between recruitment potential of larval striped bass and abundance at the juvenile stage, but there is no such published observation for recruitment potential measured at the juvenile stage. Unlike, recruitment potential, daily growth rates did vary among year classes, and were significantly greater in the James subestuary than in the Rappahannock subestuary. Body condition of juvenile striped bass exhibited a reversed pattern compared to daily growth rates, such that body condition was significantly greater for fish in the Rappahannock subestuary than for fish in the James subestuary. Further, mean body condition was higher for fish in year classes associated with slower growth rates, a pattern that is commonly observed in juvenile fishes (Francis 1997; Sim-Smith *et al.* 2013; Schloesser & Fabrizio 2016). I also observed a pattern in body condition, such that body condition of juvenile striped bass increased from 2009 to 2012, and declined thereafter. Note that this study was conducted using fish from mid-June to mid-July, and thus the patterns in daily growth rates and body condition for these fishes may be indicative of the

state in which juvenile striped bass enter winter, which is a period characterized by low survival. The condition in which juvenile striped bass enter the winter may have implications for recruitment, in particular, larger fish that exhibit better condition are likely to survive and recruit to the fishery.

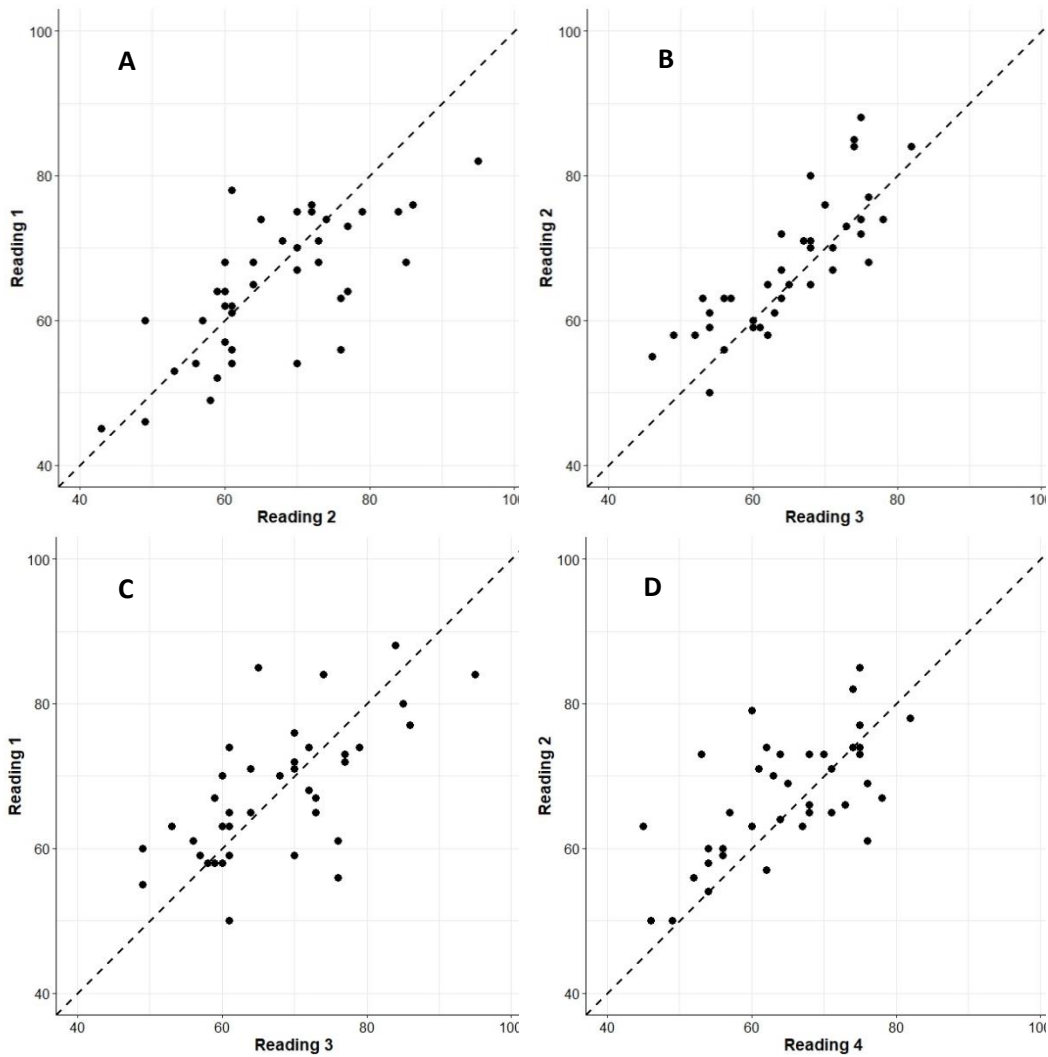
Although instantaneous daily mortality at the juvenile stage is constant across 32 year classes, mean hatch dates have shifted earlier today than prior to 1995, and may continue to do so if temperatures continue to rise as projected (Najjar *et al.* 2010). A shift in hatch dates indicates earlier spawning, and thus managers may consider shifting season closures, reducing maximum size limits to encourage older, more productive females to spawn before being harvested. Recently, and in response to the overfished status of striped bass, managers in Virginia reduced bag limits for the recreational fishery to protect the spawning stock biomass. They have also decreased the maximum size limits to ensure that more, older females have the opportunity to spawn because a greater abundance of older females is associated with stronger year classes of offspring. Adjusted bag limits and size limits are necessary first steps to return the fishery to sustainability, but the earlier shift in hatch-date distributions and implied earlier shift in spawning migration may warrant future regulatory action. Further, the current population of striped bass exhibit fast mean daily growth rates when mean body condition is low, and mean body condition of juvenile striped bass has decreased since 2012. The decline in mean body condition may be indicative of faster mean daily growth rates, which may result in stronger year classes because larger juvenile fish are more likely to survive. Alternatively, a declining mean

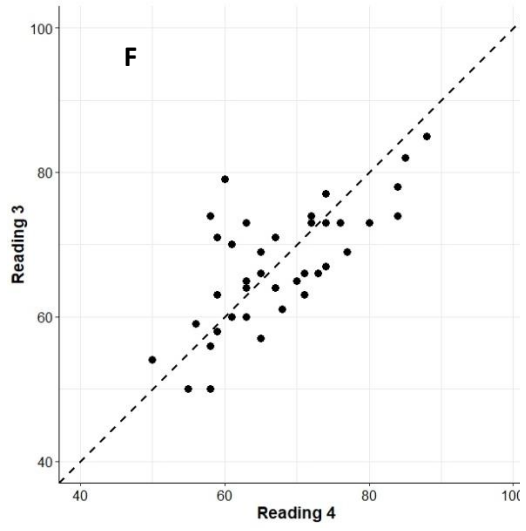
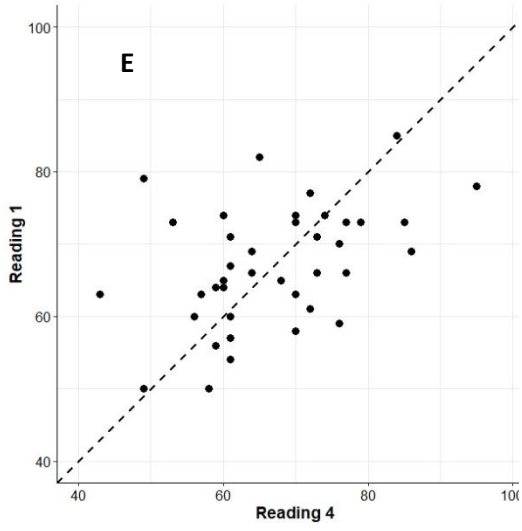
body condition may suggest a change in the quality of nursery habitats, and thus close monitoring of nursery habitats within the Chesapeake Bay may be necessary. Ultimately, the current population of striped bass is in flux, and information supplied from this study about characteristics of juvenile striped bass may prove useful in developing strategies to return the stock to sustainable levels.

LITERATURE CITED

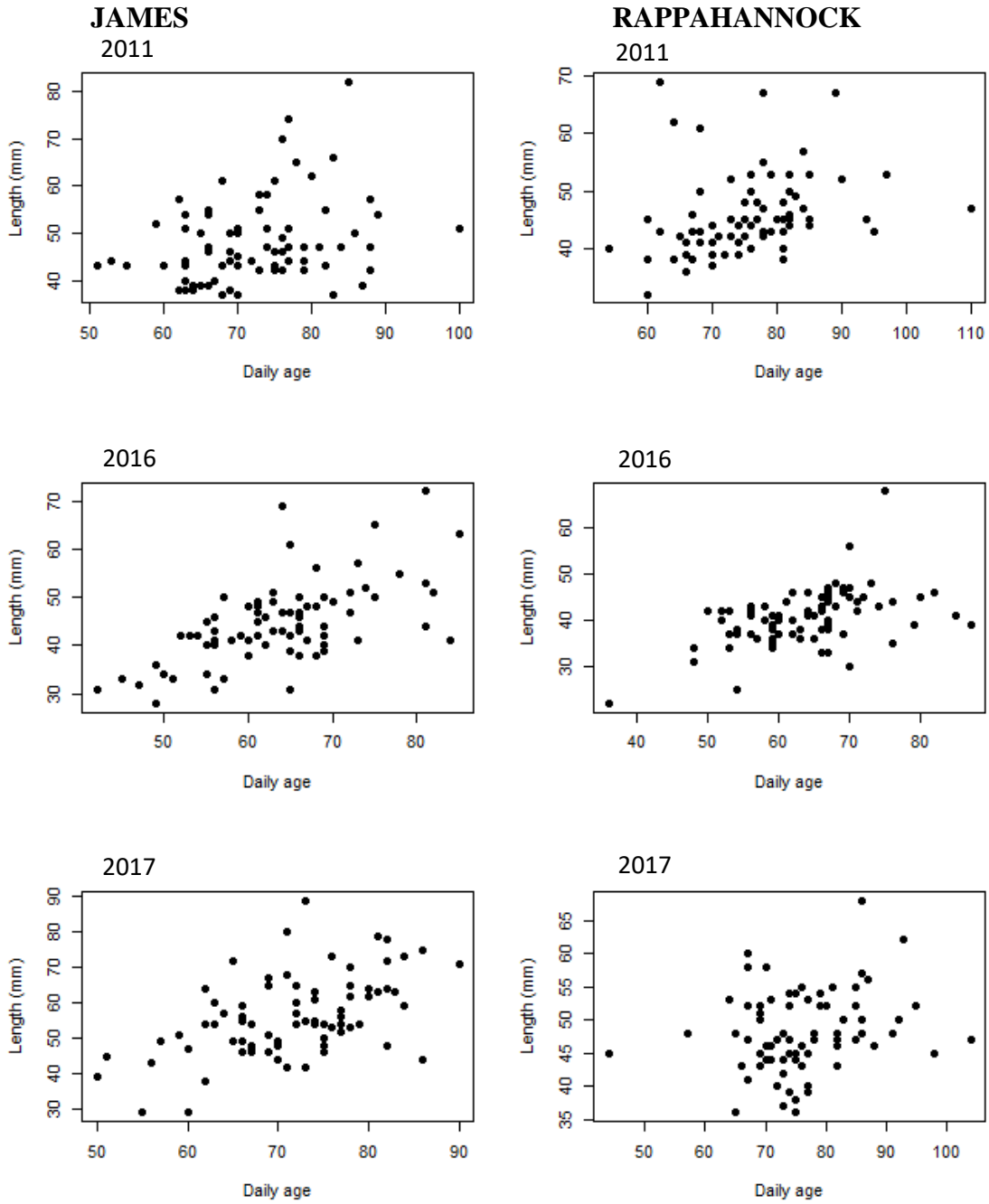
- Francis MP. 1997. Condition cycles in juvenile *Pagrus auratus*. *J. Fish Biol.* 51: 583-600
- Najjar RG, Pyke CR, Adams MB, Breitburg D, Hershner C, Kemp M, Howarth R, Muholland MR, Paolisso M, Secor D, Sellner K, Wardrop D, Wood R. 2010. Potential climate-change impacts on the Chesapeake Bay. *Estuar. Coast Shelf S.* 86: 1-20
- Peer AC, Miller TJ. 2014. Climate change, migration phenology, and fisheries management interact with unanticipated consequences. *N. Am. J. Fish. Manage.* 34: 94-110
- Sim-Smith CJ, Jeffs AG, Radford CA. 2012. Variation in the growth of larval and juvenile snapper, *Chrysophrys auratus* (Sparidae). *Mar. Freshwater Res.* 63: 1231-1243
- Schloesser RW, Fabrizio MC. 2016. Temporal dynamics of condition for estuarine fishes in their nursery habitats. *Mar. Ecol. Prog. Ser.* 557: 207-219

APPENDIX A. Consistency between increment counts from each otolith reading; the black dots represent increment counts from Readings 1 and 2 (A), Readings 2 and 3 (B), Readings 1 and 3 (C), Readings 2 and 4 (D), Readings 1 and 4 (E), and Readings 3 and 4 (F). The dashed line represents a one-to-one line (intercept = 0, slope = 1). The closer the dots are to the dashed line the more consistent are the increment counts between readings.





APPENDIX B. The daily age-at-length relationship for juvenile striped bass from the 2011, 2016, and 2017 year classes within the James and Rappahannock subestuaries of the Chesapeake Bay. Daily ages were estimated from otoliths.



VITA

Olivia Marie Phillips

Born in Ottawa, Ontario, Canada on 18 July 1993. Graduated from Wakefield High School in Raleigh, North Carolina in 2011. Earned B.S. in Biological Science with a concentration in Ecology, Evolution and Conservation and a minor in French language from North Carolina State University in 2015. Entered the Master of Science program at the School of Marine Science, Virginia Institute of Marine Science, at the College of William & Mary in 2015.